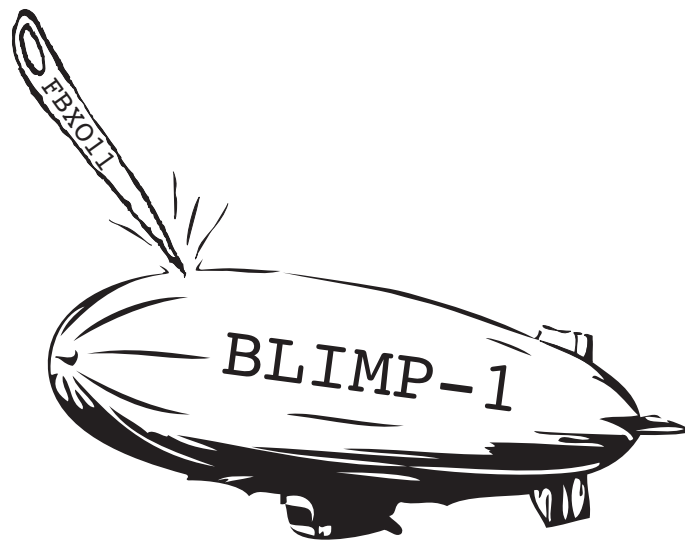


**Coordination of Developmental Timing and Maturation  
by the F-box Protein DRE-1/FBXO11**

*by Moritz Horn*



**Coordination of Developmental Timing and Maturation  
by the F-box Protein DRE-1/FBXO11**

Inaugural-Dissertation  
zur  
Erlangung des Doktorgrades  
der Mathematisch-Naturwissenschaftlichen Fakultät  
der Universität zu Köln



vorgelegt von  
**Moritz Horn**  
aus Düren

Köln, im Mai 2014

Gutachter: Prof. Dr. Adam Antebi  
Prof. Dr. Thorsten Hoppe

Tag der mündlichen Prüfung: 30. Juni 2014

The work described in this dissertation was conducted from November 2010 until May 2014 under the supervision of Prof. Dr. Adam Antebi at the Max Planck Institute for Biology of Ageing, Joseph-Stelzmann-Straße 9b, D-50931, Cologne, Germany. Part of this work was conducted in collaboration with Dr. Lukas Cermak from the laboratory of Prof. Dr. Michele Pagano, Howard Hughes Medical Institute, Department of Pathology, NYU Cancer Institute, New York University School of Medicine, 522 First Avenue, SRB 1107, New York, NY 10016, USA.

Die in dieser Dissertation beschriebenen Arbeiten wurden zwischen November 2010 und Mai 2014 unter der Leitung von Prof. Dr. Adam Antebi am Max-Planck-Institut für Biologie des Alterns, Joseph-Stelzmann-Straße 9b, D-50931, Köln, Deutschland, durchgeführt. Teile dieser Arbeit wurden in Zusammenarbeit mit Dr. Lukas Cermak vom Labor von Professor Dr. Michele Pagano, Howard Hughes Medical Institute, Department of Pathology, NYU Cancer Institute, New York University School of Medicine, 522 First Avenue, SRB 1107, New York, NY 10016, USA, durchgeführt.

Parts of this work have been published:

Teile dieser Arbeit wurden bereits veröffentlicht:

**Horn M**, Geisen C, Cermak L, Becker B, Nakamura S, Klein C, Pagano M and Antebi A (2014). *Dev Cell* 28, 697-710.

*DRE-1/FBXO11 Dependent Degradation of BLMP-1/BLIMP-1 Governs C. elegans Developmental Timing and Maturation*

Rossi M, Duan S, Jeong Y-T, **Horn M**, Saraf A, Florens L, Washburn MP, Antebi A, and Pagano M. (2013). *Mol Cell* 49, 1159–1166.

*Regulation of the CRL4(Cdt2) ubiquitin ligase and cell-cycle exit by the SCF(Fbxo11) ubiquitin ligase*

# Table of Contents

Table of Contents .....	IV
Acknowledgements .....	VII
Abbreviations .....	VIII
Summary .....	XIII
Zusammenfassung .....	XV
<b>Chapter 1 – Introduction .....</b>	<b>1</b>
<b>1.1 Temporal Control of <i>C. elegans</i> Development.....</b>	<b>2</b>
1.1.1 The Concept of Heterochrony .....	2
1.1.2 <i>C. elegans</i> Life Plan .....	3
1.1.3 Dauer Diapause Signaling .....	4
1.1.4 <i>C. elegans</i> Landmarks of Developmental Time .....	5
1.1.4.1 Molt Cycle .....	5
1.1.4.2 Tissue- and Stage-Specific Developmental Programs .....	6
1.1.5 Heterochronic Genes .....	8
1.1.6 Seam Cell Heterochronic Circuitry .....	8
1.1.7 Additional Layers of Seam Cell Fate Coordination - a Link Between Developmental Timing, the Molt Cycle and Environmental Cues .....	11
1.1.7.1 Additional Modulators of the Second microRNA Switch (L2-to-L3 Transition): .....	11
1.1.7.2 Additional Modulators of the Third microRNA Switch (Larval-to-Adult Transition): .....	12
1.1.8 Gonadal Heterochronic Circuitry .....	15
1.1.9 Dauer Diapause - a Reset of Developmental Timing .....	16
1.1.10 Heterochronic Genes – Parallels in Higher Organisms .....	16
<b>1.2 Ubiquitin-Mediated Proteolysis .....</b>	<b>20</b>
1.2.1 Ubiquitin Proteasome System (UPS) .....	20
1.2.2 Specificity of the Canonical UPS Pathway – E3-Ubiquitin Ligases .....	22
1.2.3 SCF E3-Ubiquitin Ligase Complexes .....	23
1.2.4 F-box Proteins – the Key to Substrate Recognition .....	24
1.2.5 F-box Protein-Substrate Pair Identification .....	27
<b>1.3 DRE-1/FBXO11 – Connecting Selective Degradation to Developmental Timing Control.....</b>	<b>28</b>

1.3.1	DRE-1 .....	28
1.3.2	FBXO11 .....	29
<b>1.4</b>	<b>Aim of Thesis .....</b>	<b>30</b>
 <b>Chapter 2 – Results .....</b>		<b>32</b>
<b>2.1</b>	<b>CDT2 – a Cell Cycle Regulator Targeted by DRE-1/FBXO11 .....</b>	<b>33</b>
2.1.1	Identification of CDT2 as FBXO11 Substrate by the Pagano Laboratory .....	33
2.1.2	<i>dre-1</i> and <i>cdt-2</i> Genetically Interact in <i>C. elegans</i> .....	34
<b>2.2</b>	<b>BLMP-1/BLIMP-1 - a Novel DRE-1/FBXO11 Target .....</b>	<b>37</b>
2.2.1	<i>blmp-1</i> and <i>nhr-25</i> Suppress <i>dre-1</i> Epidermal Heterochrony .....	37
2.2.2	<i>blmp-1</i> Suppresses <i>dre-1</i> Gonadal Heterochrony .....	39
2.2.3	<i>blmp-1</i> Works at a Late Step in the Seam Cell Heterochronic Circuit .....	41
2.2.4	<i>dre-1/blmp-1</i> Regulate <i>C. elegans</i> Life History .....	45
2.2.5	BLMP-1 Overexpression Enhances <i>dre-1</i> Phenotypes .....	47
2.2.6	The SCF <sup>DRE-1</sup> Complex Degrades BLMP-1 via the Proteasome .....	48
2.2.7	BLMP-1 is Dynamically Regulated in a Tissue-Specific Manner .....	52
2.2.8	Screen for DRE-1/BLMP-1 Upstream Regulators .....	54
2.2.9	<i>blmp-1</i> Expression Profiles – Seeking for Downstream Effectors .....	55
2.2.10	The DRE-1/BLMP-1 Interaction is Conserved to Mammals .....	57
 <b>Chapter 3 – Discussion.....</b>		<b>62</b>
<b>3.1</b>	<b>DRE-1 Substrates in <i>C. elegans</i> .....</b>	<b>63</b>
<b>3.2</b>	<b>The DRE-1/BLMP-1 Module Coordinates <i>C. elegans</i> Life History.....</b>	<b>64</b>
<b>3.3</b>	<b>Evolutionary Conserved Functions of DRE-1/BLMP-1 .....</b>	<b>66</b>
 <b>Chapter 4 – Significance and Future Perspectives.....</b>		<b>71</b>
<b>4.1</b>	<b>Significance .....</b>	<b>72</b>
<b>4.2</b>	<b>Future Perspectives .....</b>	<b>72</b>
4.2.1	Characterization of the FBXO11-Substrate Interaction Site .....	72
4.2.2	Investigation of Upstream Regulators .....	73
4.2.3	Further Identification of Downstream Effectors .....	75

4.2.4	Explore FBXO11 and BLIMP-1 Function During Tissue Maturation .....	77
4.2.5	Identification of Additional DRE-1/FBXO11 Substrates .....	78
4.2.6	Biological Control of Developmental Timing .....	80
<b>Chapter 5 – Material and Methods .....</b>		<b>80</b>
<b>5.1</b>	<b>Nematology and Genetics .....</b>	<b>82</b>
5.1.1	Worm Maintenance .....	82
5.1.2	Genotyping - PCR .....	82
5.1.3	<i>C. elegans</i> Strains .....	83
5.1.4	UV Integration.....	83
5.1.5	RNAi Depletion and Drug Treatment .....	83
5.1.6	Worm Synchronization .....	84
5.1.7	Microscopy and Phenotype Analysis .....	84
5.1.8	Dauer Assays, Laser Microsurgery and Lifespan Analysis .....	84
<b>5.2</b>	<b>Molecular Biology .....</b>	<b>85</b>
5.2.1	RNA Isolation and qRT-PCR.....	85
5.2.2	RNA-Sequencing and Data Analysis .....	86
5.2.3	Plasmid Construction and Molecular Cloning .....	87
<b>5.3</b>	<b>Biochemistry .....</b>	<b>87</b>
5.3.1	Antibodies .....	87
5.3.2	<i>C. elegans</i> Biochemistry .....	88
5.3.3	Cell Culture and IP Experiments.....	88
5.3.4	Gene Silencing by shRNAs.....	88
5.3.5	<i>In Vitro</i> Ubiquitination .....	89
<b>5.4</b>	<b>Statistical Analysis .....</b>	<b>89</b>
<b>Chapter 6 – References .....</b>		<b>90</b>
<b>Chapter 7 – Appendix .....</b>		<b>107</b>
	Contributions.....	116
	Erklärung.....	117
	Curriculum Vitae.....	118

## Acknowledgements

First of all I would like to thank Prof. Dr. Adam Antebi for giving me the opportunity to perform my Ph.D. in his laboratory. Every step of the way, he provided invaluable support and advice, which helped me develop the skills necessary for a successful scientific career. Adam, I really enjoyed the time in your lab.

I would like to thank all the present and past members of the A-team (Antebi lab) for creating a collaborative, fun, and intellectually stimulating lab environment. Special thanks go to Dr. Nicole Fielenbach who identified *dre-1* about 10 years ago and thereby established the basis of my Ph.D. project. Also I want to thank Dr. Christoph Geisen for all the hours he spent cloning fantastic constructs including all positive and negative controls imaginable. Moreover I am grateful for his intellectual contribution to the project, as well as his continuous support, both on a professional and on a personal level. Also I want to mention my colleagues Dr. Anne-Francoise Ruaud and Dr. Martin Denzel who introduced me to the handling of animals that are just about 1 mm in size. Further I thank the additional people who decisively contributed to the publication of this work: Dr. Lukas Cermak, Dr. Shuhei Nakamura, Dr. Corinna Klein, Dr. Ben Becker and Prof. Dr. Michele Pagano.

Moreover I want to thank my colleagues Ben, Martin, Christoph, Özlem, and Rebecca who became friends during the past years and who essentially contributed to the great atmosphere in the lab. I hope we will keep the contact alive in the future.

I am grateful to Prof. Dr. Thorsten Hoppe and Prof. Dr. Björn Schumacher who always gave helpful advice during my Ph.D. committee meetings. Moreover I want to thank Prof. Dr. Thorsten Hoppe and Prof. Dr. Günther Schwarz for evaluating my work, as well as Dr. André Franz for writing the protocol.

Special thanks go to my best friends in lovely Birgel (+ suburbs) who always kept me motivated during long-lasting soccer sessions and splendid kayak trips and who still pretty successfully manage to avoid calling me a nerd.

Finally, I want to thank my parents, my brother and my family-in-law for always believing in me and supporting me whenever I needed it most. Paramount, my deepest thanks go to my lovely family Tina and Anton, who had to spend many evenings without me to make this work possible, but who still provided me with unconditional love and encouragement.

## Abbreviations

(l)	liquid
°C	degree Celsius
A/Ala	alanine
AIN	ALG interacting protein
AJM	adherence junction marker
ALG	argonaute-like gene
ALK	anaplastic lymphoma kinase
AMA	amanitin resistant
ANOVA	analysis of variance
APC	adenomatous polyposis coli-2
APL	amyloid precursor-like
ARD	adult reproductive diapause
BAR	$\beta$ -catenin/armadillo related
BCL	B cell lymphoma
BED	BED-type zinc finger putative transcription factor
BLIMP	B lymphocyte-induced maturation protein
BLMP	B lymphocyte-induced maturation protein homolog
BTB	broad complex, tramtrack, bric-a-brac
<i>C. elegans</i>	<i>Caenorhabditis elegans</i>
C/Cys	cysteine
CAND1	Cullin-associated Nedd8-dissociated protein
CASH	carbohydrate binding and sugar hydrolysis
CDK	cyclin-dependent kinase
cDNA	complementary DNA
CDT	cdc10-dependent transcript
CED	cell death abnormality
CEP	<i>C. elegans</i> p53-like protein
cGMP	cyclic guanosine monophosphate
ChIP	chromatin immunoprecipitation
CHX	cycloheximide
CKI	CDK inhibitor
cm	centimeter
COL	collagen
COP	constitutively photomorphogenic
CRL	Cullin-ring-ligase
CRY	cryptochrome
CT	cycle threshold
CUL	Cullin
CYP	cytochrome P450
D/Asp	aspartate
DA	dafachronic acid
Daf	abnormal dauer formation
Daf-c	dauer formation constitutive
Daf-d	dauer formation defective
DBD	DNA binding domain

DCAF	DDB1 and CUL4-associated factor
DCR	dicer related
DDB	DNA damage binding protein
DHR	drosophila nuclear hormone receptor
DIC	differential interference contrast
DIN	<i>daf-12</i> interacting protein
DMSO	dimethylsulfoxide
DN	dominant negative
DNA	deoxyribonucleic acid
DRE	<i>daf-12</i> redundant
dsRNA	double-stranded RNA
dte	distal tip cell
DUB	deubiquitinating enzyme
E1	ubiquitin-activating enzyme
E2	ubiquitin-conjugating enzyme
E3	ubiquitin ligase
E4	ubiquitin ligase (specific for ubiquitin chain elongation)
EDTA	ethylenediaminetetraacetic acid
EGR	epidermal growth factor
EMS	ethylmethylsulfate
ENU	N-ethyl-N-nitrosourea
et al.	<i>et alii / et aliae</i> , and others
F/H	FLAG/HA
F/Phe	phenylalanine
FBXL	F-box and leu-rich repeat protein
FBXO	F-box only protein
FBXW	F-box and WD40-repeat containing protein
FOXA	forkhead box protein A
FOXO	forkhead box protein O
FPKM	fragments per kilobase of exon per million fragments mapped
FSN	F-box synaptic protein
FTZ-F	fushi tarazu transcription factor
FXR	farnesoid X receptor
G/Gly	glycine
GFP	green fluorescent protein
GLP	abnormal germ line proliferation
GO	gene ontology
h/hr	hour
HBL	hunchback like
HECT	homologous to the E6-AP carboxyl terminus
HEK	human embryonic kidney
HNF	hepatocyte nuclear factor
IGF	insulin-like growth factor
InsR	insulin receptor
IP	immunoprecipitation
IPTG	isopropyl- $\beta$ -D-thiogalactopyranosid
K/Lys	lysine

KIN	protein kinase
L/Leu	leucine
LB	lysogene broth
LBD	ligand binding domain
LEF	lymphoid enhancer binding factor
LET	lethal
<i>let-7s</i>	<i>let-7</i> sisters/ <i>let-7</i> microRNA family members <i>mir-48</i> , <i>-84</i> , <i>-241</i>
LF	loss of function
LIN	abnormal cell lineage
LXR	liver X receptor
MAB	male abnormal
MEC	mechanosensory abnormality
MFB	MAFBx protein homolog
mig	gonadal migration defect
min	minute
<i>mir</i>	microRNA
ml	milliliter
mM	millimolar
mRNA	messenger RNA
ms	mouse
N2	wild type <i>C. elegans</i>
NAB	NGFI-A binding protein
NAS	nematode astacin protease
ng	nanogram
NGM	nematode growth medium
NHL	NCL-1, HT2A, LIN-41
NHR	nuclear hormone receptor
nM	nanomolar
NP-40	octylphenoxypolyethoxyethanol
NYU	New York University
OCT	octamer-binding transcription factor
OE	overexpression
OP50	<i>Escherichia coli</i> strain OP50
ORF	open reading frame
p27	kip1/CDK inhibitor
PAS	per arnt sim
PCG	polycomb-group
PCNA	proliferating cell nuclear antigen
PER	period
PHA	defective pharynx development
PIAS	protein inhibitors of activated STAT
POP	posterior pharynx defect
PTR	patched related family
PUP	poly (U) polymerase
Q/Gln	glutamine
qRT-PCR	quantitative real-time polymerase chain reaction
RAF	rapidly accelerated fibrosarcoma (a protein kinase family)

rb	rabbit
RBX	RING-box protein
RFLP	restriction fragment length polymorphism
RING	really interesting new gene
RNA	ribonucleic acid
RNAi	RNA interference
RPN	proteasome regulatory particle, non-ATPase-like
RRF	RNA-dependent RNA polymerase family
RXR	retinoid x receptor
s	second
S phase	DNA synthesis phase
S/Ser	serine
SCD	suppressor of constitutive dauer formation
SCF	Skp, Cullin, F-box containing complex
SCM	seam cell marker
SDS	sodiumdodecylsulfate
SDS-PAGE	sodium dodecylsulfate polyacrylamide gel electrophoresis
SEL	suppressor/enhancer of <i>lin-12</i>
SET	Su(var)3-9, enhancer-of-zeste and trithorax/ methyltransferase domain
SF	steroidogenic factor
shRNA	short hairpin RNA
SIC	<i>Saccharomyces cerevisiae</i> ; CDK inhibitor p40
siRNA	small interfering RNA
SKP	S phase kinase-associated protein
SKPT	S phase kinase-associated protein-2 homolog
SKR	SKP related
SMAD	mothers against decapentaplegic homolog
SNP	single nucleotide polymorphism
SOCS	suppressor of cytokine signaling
SOP	suppressor of <i>pal-1</i>
SOX	sex-determining region Y-box
SRS	substrate-recognition subunit
SUB	substrate
SUMO	small ubiquitin-like modifier
T/Thr	threonine
TCF	transcription factor
TGF	transforming growth factor
TIM	timeless
TRIM	tripartite motif containing
Tris	tris-hydroxymethylaminomethane
ts	temperature-sensitive
UNC	uncoordinated
UPS	ubiquitin proteasome system
UTR	untranslated region
UV	ultraviolet light
v/v	volume/volume
V/Val	valine

VDR	vitamin D receptor
W/Trp	tryptophane
w/v	weight/volume
WRM	worm armadillo
WRT	warthog (hedgehog-like family)
WT	wild type
Zn/ZnF	zinc/zinc finger
ZnF-UBR	putative zinc finger in N-recognin (N-end rule pathway)
$\beta$ -TRCP	$\beta$ -transducin repeat containing protein
$\mu$ g	microgram
$\mu$ l	microliter
$\mu$ m	micrometer
$\mu$ M	micromolar

## Summary

Spatiotemporal control of cellular events is key to developmental progression in all organisms. Accordingly the abundance of regulatory proteins must be tightly controlled in a highly time- and tissue-specific manner. Pioneering work in the small roundworm *Caenorhabditis elegans* (*C. elegans*) has uncovered a network of genes, termed the heterochronic loci, which govern temporal coordination of developmental processes. Importantly this heterochronic network is remarkably conserved across species. There are currently over 30 identified heterochronic loci, which encode various transcriptional, translational and post-translational regulators including the first discovered microRNAs *lin-4* and *let-7*.

In 2007 our laboratory discovered a novel heterochronic gene, *dre-1*, which specifies late larval development in the *C. elegans* epidermis and gonad. Interestingly *dre-1* encodes a highly conserved F-box protein; F-box proteins typically function as substrate recognition components of SCF E3-ubiquitin ligase complexes, thus conferring substrate specificity to the ubiquitin proteasome system (UPS). The initial analysis of DRE-1 and its mammalian homolog FBXO11 revealed their interaction with SCF complex components, suggesting conservation also on the functional level. Mutation of *C. elegans dre-1* leads to a diverse array of developmental alterations including precocious terminal differentiation of epidermal blast cells, molting defects and alterations in gonadal outgrowth. Likewise, haploinsufficiency of *Fbxo11* has been linked to craniofacial malformations such as cleft palates, as well as otitis media, an inflammation of the middle ear, in both mice and men. Furthermore, FBXO11 was recently shown to function as a tumor suppressor in lymphoid malignancies by controlling turnover of the oncoprotein BCL6. However, the DRE-1/FBXO11 substrate(s) coordinating developmental progression still remain to be elucidated. Thus the central questions of my thesis are: what are the substrates of DRE-1/FBXO11 in the heterochronic circuit, and how do they illuminate developmental timing events?

In an effort to identify novel substrates of the SCF<sup>DRE-1/FBXO11</sup> E3-ubiquitin ligase complex involved in developmental timing, I pursued an RNAi-based suppressor approach in *C. elegans*. I reasoned that client substrates should aberrantly accumulate in *dre-1* mutants and cause developmental alterations across tissues. If so, then knockdown of such substrates would ameliorate related phenotypes. Here, I identified the highly conserved zinc-finger transcriptional repressor BLMP-1 as a new substrate of the SCF<sup>DRE-1</sup> complex. Several lines of evidence reveal that BLMP-1 is a substrate of the SCF<sup>DRE-1</sup> complex in developmental timing

circuits. First, *blmp-1* loss of function strongly suppressed *dre-1* heterochronic phenotypes in epidermis and gonad and *blmp-1* mutation itself exhibited developmental timing defects opposite to *dre-1*. *blmp-1* also opposed *dre-1* for other life history traits such as entry into the dauer diapause and adult longevity. Second, BLMP-1 protein was strikingly elevated upon depletion of *dre-1* and other SCF complex components, as well as by inhibition of the proteasome. Moreover, BLMP-1 was regulated in a time- and tissue-specific manner by *dre-1*, consistent with corresponding phenotypes. Third, DRE-1 and BLMP-1 physically interacted *in vivo* in *C. elegans* and *in vitro* in a cell-based system. Importantly the role of DRE-1 in regulating BLMP-1 stability is evolutionary conserved, as direct protein interaction and degradation function was also observed for the human counterparts FBXO11 and BLIMP-1.

In addition to *blmp-1*, I also investigated genetic interactions of *dre-1* and *cdt-2* in *C. elegans*, since CDT2 was recently identified as a FBXO11 substrate in mammalian systems. I found *cdt-2* to genetically interact with *dre-1* for specific processes in the epidermis. In particular gaps in an adult-specific cuticular structure occurring in *dre-1* mutants could arise from elevated CDT-2 levels and a subsequent failure of cell cycle exit of epidermal blast cells, which synthesize these structures. My findings are in line with mammalian studies that established CDT2, which itself is part of an E3-ubiquitin ligase complex, as a critical cell cycle regulator by targeting substrates such as the CDK inhibitor p21 for proteasomal degradation.

Altogether I conclude that *dre-1* mutants' diverse developmental alterations arise from aberrant accumulation of distinct target proteins. In particular, my work shows that spatiotemporal control of BLMP-1 protein by DRE-1 coordinates developmental timing and other life history traits in *C. elegans*. DRE-1, on the one hand, restrains BLMP-1 abundance in the epidermis to prevent precocious terminal differentiation and, on the other hand, triggers BLMP-1 degradation in distal tip cells to initiate dorso-ventral migratory events. The notion that DRE-1/BLMP-1 work together for multiple processes suggests these proteins comprise a two-protein module that may mediate related metazoan maturation processes. Taken together, my work fundamentally contributes to the understanding of developmental timing coordination by DRE-1/FBXO11 in *C. elegans* and might help to shed light on related processes in higher organisms.

## Zusammenfassung

Die zeitliche und räumliche Koordination zellulärer Ereignisse ist in allen Organismen essentiell für die optimale Entwicklung von Geweben und des gesamten Organismus. Im Besonderen muss dabei die Menge regulatorischer Proteine strikt kontrolliert und reguliert werden. Pionierarbeit im Fadenwurm *Caenorhabditis elegans* (*C. elegans*) führte zur Entdeckung eines genetischen Netzwerkes bestehend aus so genannten ‚heterochronen Genen‘, die die zeitliche Anordnung zellulärer Ereignisse steuern. Dieses ‚heterochrone Netzwerk‘ ist evolutionär weitgehend konserviert und beinhaltet über 30 Gene, die transkriptionelle, translationale und post-translationale Regulatoren codieren.

2007 wurde in unserem Labor ein neues ‚heterochrones Gen‘ entdeckt, *dre-1*. *dre-1* reguliert die Entwicklung der Epidermis und der Gonade in späten *C. elegans* Larvenstadien und codiert ein hoch konserviertes F-box Protein. F-box Proteine agieren generell als Substraterkennungskomponenten von so genannten SCF E3-Ubiquitin Ligase Komplexen und sind somit maßgeblich an der Spezifität des Ubiquitin-Proteasom-Systems beteiligt. Erste Analysen von DRE-1 und seinem Säugetierortholog FBXO11 haben gezeigt, dass beide Proteine Teil eines solchen SCF Komplexes sind. Punktmutationen im *dre-1* Gen führen zu multiplen Entwicklungsveränderungen im Fadenwurm: verfrühte Ausdifferenzierung epidermaler Stammzellen (seam cells), Störung der Häutungsprozesse und ein verändertes Migrationsmuster der Gonade. Analog sind auch Punktmutationen in murinem und humanem FBXO11 mit Entwicklungsstörungen wie der Ausbildung einer Lippen-Kiefer-Gaumenspalte oder einer chronischen Mittelohrentzündung (Otitis Media) assoziiert. Zusätzlich wurde FBXO11 kürzlich als Tumorsuppressorgen eingestuft, da es den Abbau des onkogenen Proteins BCL6 kontrolliert und häufig in malignen Lymphomen mutiert ist. Interessanterweise sind die Substrate von DRE-1 und FBXO11, die möglicherweise zur Ausbildung von Entwicklungsstörungen führen könnten, noch nicht bekannt. Somit stellen sich folgende fundamentale Fragen, die in dieser Doktorarbeit adressiert werden: Was sind die Substrate von DRE-1/FBXO11, die die zeitliche Abfolge entwicklungsbiologischer Prozesse koordinieren? Wie erfolgt diese Regulation auf molekularer Ebene?

Mittels eines RNAi-basierten Ansatzes habe ich versucht Substrate des SCF<sup>DRE-1/FBXO11</sup>-Komplexes zu identifizieren, die die Entwicklungsstörungen in *dre-1* Mutanten auslösen könnten. Dies basierte auf der Hypothese, dass Substrate in *dre-1* Mutanten nicht mehr abgebaut werden und somit in zu hohen Konzentrationen vorliegen, welche die Koordination der Gewebeentwicklung negativ beeinflussen könnten. Folglich sollte eine Reduktion dieser Substrate mittels RNAi, zu einer Linderung der Entwicklungsstörungen führen. Mit diesem

Ansatz identifizierte ich den Zink-Finger-Transkriptionsfaktor BLMP-1 als neues Substrat des SCF<sup>DRE-1/FBXO11</sup>-Komplexes: Erstens führte eine Reduktion der BLMP-1 Menge zu einer Milderung der *dre-1* Phänotypen in Epidermis und Gonade und *blmp-1* Mutanten selbst zeigten entgegengesetzte Phänotypen in beiden Geweben. Weiterhin beeinflussten *dre-1* und *blmp-1* auch den Prozess der dauer Diapause, so wie die Lebensspanne des Fadenwurms in entgegengesetzte Richtungen. Zweitens war die BLMP-1-Proteinkonzentration in *dre-1* Mutanten und nach Inhibition des 26S Proteasoms deutlich erhöht. Interessanterweise unterlag der BLMP-1-Spiegel einer strikten zeitlichen Regulation, die in *dre-1* Mutanten gestört war und eng verknüpft mit den entsprechenden Phänotypen war. Drittens konnte ich eine direkte Interaktion zwischen DRE-1 und BLMP-1 *in vivo* in *C. elegans* und *in vitro* in kultivierten Säugerzellen nachweisen. Schließlich konnte ich zeigen, dass auch die humanen Orthologe FBXO11 und BLIMP-1 direkt interagieren und FBXO11 den Abbau von humanem BLIMP-1 kontrolliert.

Zusätzlich zu BLMP-1 charakterisierte ich ein weiteres FBXO11 Substrat im Fadenwurm, CDT2, welches erst kürzlich entdeckt wurde. Dabei fand ich eine genetische Interaktion zwischen *dre-1* und *cdt-2* für die Bildung spezifischer, extrazellulärer Strukturen der Fadenwurmepidermis. Lücken dieser Struktur, die von epidermalen Stammzellen synthetisiert wird, treten häufig in *dre-1* Mutanten auf. Meine Daten deuten darauf hin, dass diese Lücken durch eine Dysregulation von CDT-2 verursacht sein könnte, die in epidermalen Stammzellen zu Defekten im Zellzyklus führt. Unsere Ergebnisse unterstützen Forschungsergebnisse aus Säugerzellen, in denen FBXO11-abhängigem CDT2 Abbau regulatorische Funktionen im Zellzyklus zugesprochen werden.

Insgesamt zeigt meine Arbeit, dass den diversen Phänotypen in *dre-1* Mutanten nicht die aberrante Akkumulation eines bestimmten Proteins, sondern vielmehr die Anhäufung multipler Substrate zugrunde liegt. Im Besonderen konnte ich zeigen das DRE-1 den BLMP-1-Proteinspiegel kontrolliert, was für die zeitliche Abfolge gewebespezifischer Entwicklungsprozesse von zentraler Bedeutung ist. Weiterhin koordinieren DRE-1 und BLMP-1 Prozesse, die den gesamten Organismus betreffen, wie Häutungsvorgänge, dauer Diapause und die Regulation der Lebensspanne. Analog könnten die orthologen Proteine FBXO11 und BLIMP-1 zusammen verwandte Prozesse in Säugetieren regulieren. Zusammenfassend erweitert meine Arbeit das Verständnis über die Koordination zeitlicher Entwicklungsabläufe durch DRE-1/FBXO11 im Fadenwurm *C. elegans*, Erkenntnisse, die möglicherweise direkt auf verwandte Prozesse in Säugetieren übertragbar sind.

# **Chapter 1 - INTRODUCTION**

*Life itself is adamantly intertwined with the passing of time. During a life cycle metazoans develop through successive stages and mature to reproductive adults. At the organismal level, development is often marked by dramatic transitions such as metamorphosis and puberty. At the cellular level, temporal and positional fates are precisely regulated to coordinate proliferative, morphogenetic and differentiation events. Molecularly, transcriptional, translational and post-translational mechanisms must act in concert to control rates of protein synthesis, activity and degradation, thereby ensuring sequential action of differentiation and maturation factors.*

*How do organisms keep track of time and in turn coordinate the proper chronology of distinct developmental events on a molecular level?*

## **1.1 Temporal Control of *C. elegans* Development**

### **1.1.1 The Concept of Heterochrony**

Heterochrony denotes a change in the relative timing of developmental events in evolution and its definition has varied since its introduction in 1860. The term heterochrony (from Greek: *heteros* different, changed; *khronos* timing) was first introduced by Ernst Haeckel to describe cases in which an ontogenetic sequence of events does not recapitulate the evolutionary stages of phylogeny and thus constitutes an exception from the biogenetic law (Russell, 1916). In the 1950<sup>ies</sup> Gavin de Beer (De Beer, 1951) and later Gould redefined the scope of heterochrony for the next decades (Gould, 1977; Alberch et al., 1979): In contrast to Haeckel, Gould described heterochrony as the mechanism that produces parallels between ontogeny and phylogeny. Thereby he distinguished between acceleration and retardation of maturation versus body development, also shifting the focus of heterochrony from the relative timing of developmental events to changes in the relation between size and shape (growth heterochrony or allometry). More recently, Smith untangled the different histological meanings of heterochrony by differentiating growth- and sequence heterochrony (Smith, 2001; 2002; 2003). The latter refers to changes in the order of developmental events, extended to the cellular level, and often induced by experimental intervention (e.g. genetically). Such developmental events include cell proliferation, cell differentiation, the appearance of structures, or even the induction of specific genes.

The paradigm for heterochrony is the Mexican axolotl *Ambystoma mexicanum*: this salamander reaches sexual maturity without undergoing metamorphosis, such that its somatic tissue retains larval features of its ancestors and other salamanders. Interestingly, metamorphosis in salamanders is triggered by thyroid hormones, which highly vary in abundance and activity between different axolotl species, indicating that rather few genetic changes in endocrine signaling can alter organismal developmental timing (Frieden, 1981).

Notably, in the last decades the nematode *C. elegans* became the major tool to dissect heterochronic phenomena, amongst others due its genetic tractability, the ability to follow cell fates in living animals and its essentially invariant and entirely determined cell lineage (Brenner, 1974; Sulston and Horvitz, 1977).

### 1.1.2 *C. elegans* Life Plan

Under favorable environmental conditions (abundant food, low population density and moderate temperature) *Caenorhabditis elegans* (from Greek: *caeno* new, recent; *rhabditis* rod-like and Latin: *elegans* elegant) develops from egg through four larval stages to reach reproductive maturity within 3-5 days.

After hatching young larvae consist of 558 cells and rapidly develop through the larval stages, each marked by ecdysis and characterized by stage-specific patterns of cellular events. These basically invariant patterns include cell divisions, mostly in neuronal, epidermal, and gonadal cell lineages as well as morphogenetic events such as gonad and vulval formation that lead to the final 959 somatic cells in hermaphrodite adults. Hermaphrodite animals are reproductive for a 5-day period and live for another two to three weeks post-reproductively.

In unfavorable conditions such as food scarcity, elevated temperature, and high population density indicated by ascaroside pheromones (Golden and Riddle, 1984; Butcher et al., 2007), *C. elegans* can arrest development at certain checkpoints and run alternative life plan programs. First, in the absence of food L1 larvae arrest and survive for several days, and can return to continuous development upon re-feeding, demonstrating that food availability is key to the initiation of postembryonic development (Johnson et al., 1984). Second, *C. elegans* can enter an alternative third larval stage called dauer diapause, characterized by stress resistance, longevity and multiple metabolic and morphological changes including the synthesis of a thick stress and desiccation resistant cuticle, which contains characteristic cuticular threads called dauer alae (Cassada and Russell, 1975). When returned to favorable conditions dauer

larvae resume reproductive development even after periods of over 4 months without food (Wood, 1988). Finally, starvation of larvae at the mid L4 stage, induces the adult reproductive diapause (ARD) (Angelo and Van Gilst, 2009), which is a quiescent state of extended survival thought to be analogous to overwintering in the fruitfly *Drosophila melanogaster* (Tatar and Yin, 2001; Saunders et al., 1989). In *C. elegans* arrested adults can survive for weeks without food while they harbor one or two arrested embryos inside the uterus and halt reproductive development and growth. When returned to food, they regenerate their germline, give rise to normal broods and live a normal adult lifespan (Gerisch, unpublished).

### 1.1.3 Dauer Diapause Signaling

The dauer diapause is the best-characterized developmental arrest in *C. elegans*, and allows worms to survive extended periods of food scarcity in the wild. The dauer decision is governed by a molecular switch (Figure 1): environmental cues are transduced through an endocrine signaling network and converge on the nuclear hormone receptor DAF-12, a key regulator of reproductive vs. arrested development (Fielenbach and Antebi, 2008; Antebi et al., 1998; 2000). DAF-12 contains an N-terminal DNA-binding- and a C-terminal ligand-binding domain (DBD and LBD). Similar to its mammalian homologs, the Vitamin-D (VDR), Liver-X (LXR) and Farnesoid-X (FXR) receptors DAF-12 drives transcription upon binding of its ligands, the cholesterol-derived bile-acid-like dafachronic acids (DAs) (Antebi et al., 2000; Motola et al., 2006). The presence of DAs in young larvae reflects a healthy metabolic state and, then liganded DAF-12 leads to reproductive development (Figure 1). Conversely, the absence of DAs reflects an unfavorable metabolic state. In this case unliganded DAF-12 binds its corepressor DIN-1 and triggers developmental arrest, dauer diapause, and longevity (Ludewig et al., 2004). Besides *daf-12*, genetic screens have revealed more than 30 *Daf* (abnormal dauer formation) loci that modulate dauer diapause formation and comprise the endocrine network upstream of DAF-12 (Riddle et al., 1981; Albert and Riddle, 1988; Gerisch et al., 2001; Fielenbach and Antebi, 2008). Dauer defective (*Daf-d*) mutants fail to form dauer largely independent of the environmental triggers, while dauer constitutive (*Daf-c*) mutants enter the dauer stage even under normal or low stress conditions. These *Daf* loci include components of the sensory neuronal circuits, cGMP signaling (Birnby et al., 2000), and serotonergic neurotransmission (Sze et al., 2000) that under favorable conditions stimulate TGF- $\beta$  (Ren et al., 1996) and Insulin/IGF signaling (Figure 1) (Kimura et al., 1997). In turn, both signaling cascades impinge on rate limiting enzymes within the DA biosynthetic pathway leading to increased DA levels that enforce the reproductive fate (Figure 1) (Gerisch

and Antebi, 2004). Therein, *daf-9/CYP27A1* catalyzes the last step in the biosynthesis of the most potent DAF-12 ligand,  $\Delta^7$ -DA and thus acts directly upstream of DAF-12 within the dauer signaling circuits (Figure 1) (Gerisch et al., 2001; Jia et al., 2002; Motola et al., 2006). Interestingly, both feedforward and feedback loops modulate the activity of DA biosynthetic enzymes to assure this binary organismal fate choice.

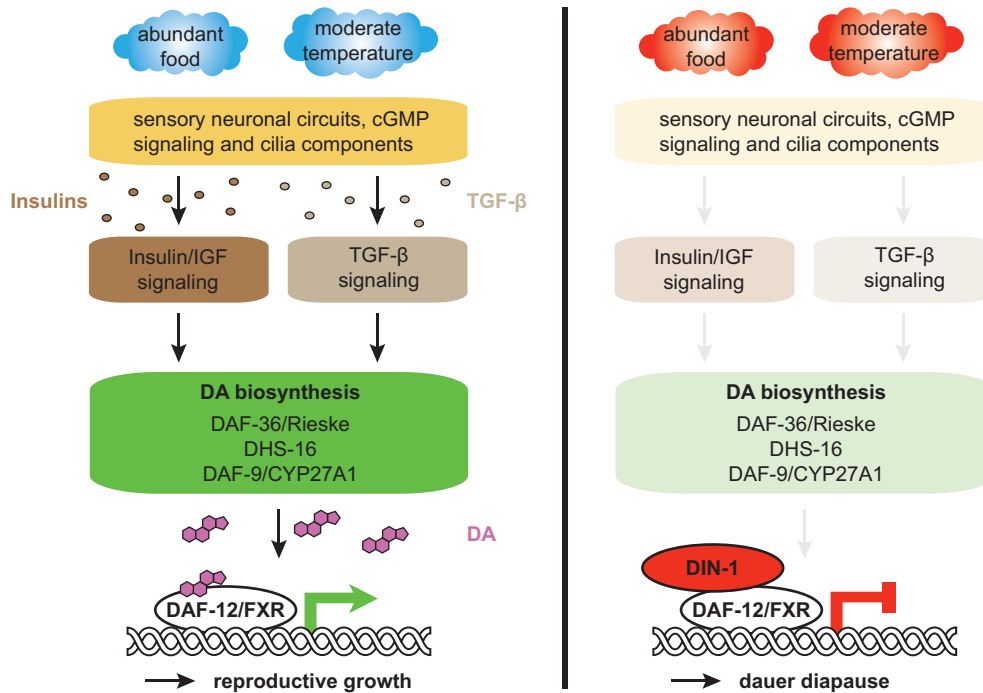


**Figure 1: Dauer Diapause Signaling**

Simplified schematic representation of the signaling cascade governing the dauer decision. Under favorable environmental conditions upstream signaling cascades such as TGF- $\beta$ - and Insulin/IGF signaling trigger DA biosynthesis leading to reproductive growth via ligand-bound DAF-12. Conversely unliganded DAF-12 forms a repressor complex together with DIN-1 and induces dauer diapause upon unfavorable environmental conditions.

## 1.1.4 *C. elegans* Landmarks of Developmental Time

### 1.1.4.1 Molt Cycle

Invertebrate species with exoskeletons often undergo the process of molting as part of growth and maturation. Across molting species, hatching and ecdysis (the shedding of the cuticle) function as major landmarks to define the chronological age of individual animals.

In the fruitfly *Drosophila melanogaster* molting events are triggered by hormonally driven transcriptional cascades. In a cyclic behavior ecdysteroid hormones such as 20-hydroxiecdysone trigger downstream target gene expression including DHR-3, FTZ-F1, and others, through the ecdysone receptor and its coreceptor ultraspiracle/RXR (Riddiford, 1993;

Riddiford et al., 2000; 2003; King-Jones and Thummel, 2005; Thummel, 1996; Koelle et al., 1992; 1991).

In *C. elegans* regulation of the molt cycle is less understood, but initial studies suggest that it is also controlled by an endocrine mechanism. The orphan nuclear hormone receptors *nhr-23* and *nhr-25*, homologs of *Drosophila* DHR3 and FTZ-F1, respectively, have been implicated in regulating the molts. Their expression oscillates with the molt cycle and their mutation leads to severe molting defects (Asahina et al., 2000; Gissendanner and Sluder, 2000; Kostrouchova et al., 1998; 2001; Kouns et al., 2011). However, neither ecdysone nor its receptor have been identified in *C. elegans*.

Although chronological age is a very convenient measure for *C. elegans* temporal boundaries, close inspection indicates that the molt itself is only the termination of a process that was initiated during the intermolts by synthesizing collagens (Johnstone and Barry, 1996). Similarly seam cells, which are lateral epidermal blast cells, divide around the molts, but the cell cycle entry was triggered during intermolts, suggesting developmental programs to run from intermolt to intermolt (Ambros and Horvitz, 1984; Antebi et al., 1998). Based on the description of the entire *C. elegans* cell lineage I will refer to developmental age as hours post-hatching as staged by specific landmarks of developmental progression described in Sulston and Horvitz's landmark work (Sulston and Horvitz, 1977).

#### 1.1.4.2 Tissue- and Stage-Specific Developmental Programs

Each larval stage is characterized by a highly invariant pattern of traceable cellular events including cell proliferation, differentiation and migration in various tissues. *C. elegans* epidermis consists of the hypodermal syncytium and the seam cells, which collectively synthesize and secrete new collagenous cuticles before shedding the old (Singh and Sulston, 1978; Edwards and Wood, 1983; Chisholm and Hsiao, 2012). Seam cells, named H0–H2, V1–V6, and T, are situated along the lateral midline on each side of the worm and display the most conspicuous and best studied temporal patterning events (Figure 2A and 2B). During post-embryonic development they undergo stem cell divisions once during each larval stage roughly coinciding with the molts. These divisions give rise to an anterior hypodermal daughter, which fuses to the hypodermal syncytium, whereas the posterior seam cell retains its stem cell character. Uniquely during the L2 stage subsets of seam cells undergo an additional proliferative division, thus increasing the number of seam cells from 10 to 16 on each side of adult worms. Finally, early in the L4 stage seam cells exit the cell cycle, fuse into

a syncytium and synthesize a continuous ridged cuticular structure called adult alae, a hallmark of the adult cuticle (Figure 2B) (Singh and Sulston, 1978; White, 1988).

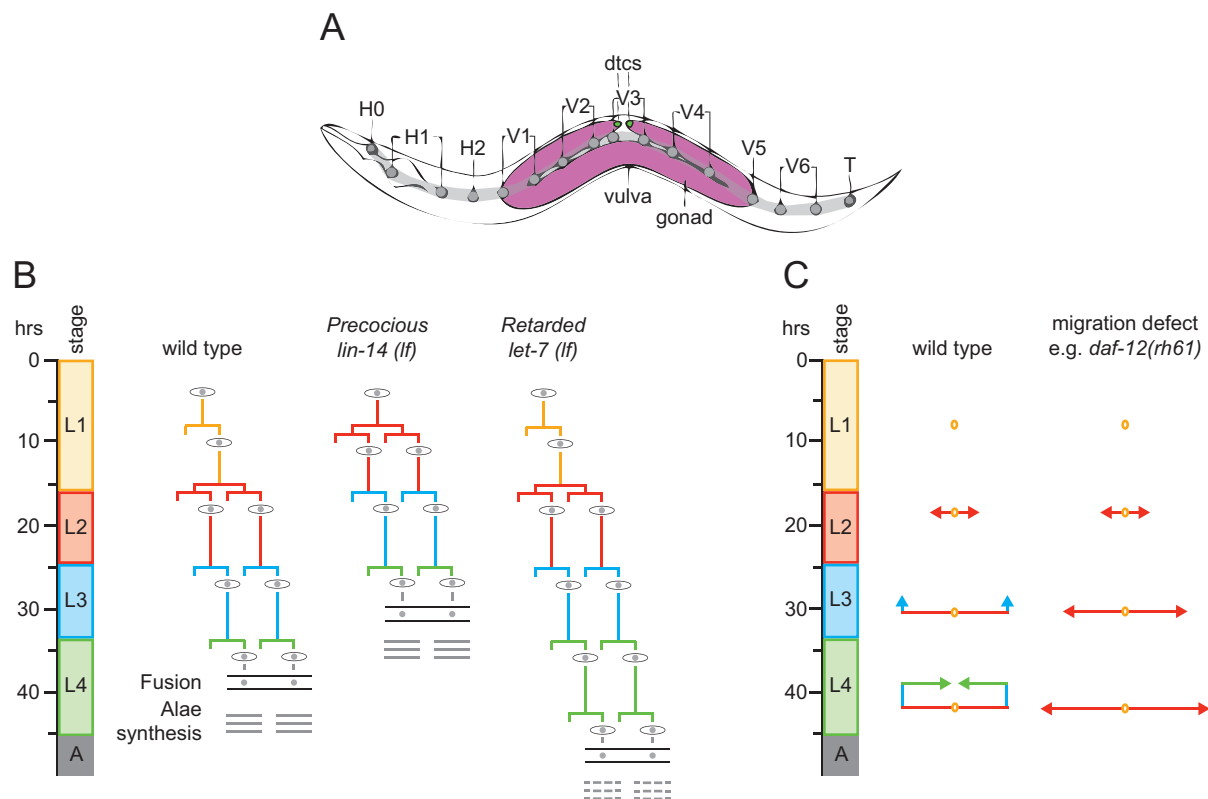


**Figure 2: Stage-Specific Developmental Programs in Epidermis and Gonad**

(A) Schematic representation of an adult worm, showing seam cell nuclei (grey), which comprise the left seam-cell syncytium (grey line). The nuclei are indicated by the name of the blast cell from which they were derived, with the exception of H0, which does not divide post-embryonically. Distal tip cells (dtcs), which lead gonad migration, are shown in green, the whole gonad in purple. (B) Seam cell lineages (V1-V4, V6) from WT worms and two representative heterochronic mutants. Terminal differentiation is indicated by fusion of the seams (eye-shaped cells) and adult alae formation (three horizontal bars). (C) Gonad migration program of WT worms and retarded mutants such as *daf-12(rh61)*, where gonadal arms fail to reflex. Arrowheads indicate positions of the dtcs. Figure modified from (Rougvie, 2001).

Temporal development not only manifests in epidermal blast cells, but also emerges in other tissues: Similar to seam cell programs, intestinal nuclei undergo repetitive endoreplications during each larval stage, with a modification during L2 that gives rise to binucleate cells. Moreover, linear non-repetitive patterns exist that also exhibit strict temporal control such as neuronal remodeling, vulval formation, and gonadal outgrowth. The hermaphrodite gonad undergoes a stereotyped morphogenesis during the larval stages that is readily visible by microscopy (Figure 2C): In L1 larvae the gonad primordium consists of just four cells Z1-Z4, whereby Z2 and Z3 are the germ cell precursors and Z1 and Z4 the somatic gonadal precursor cells. The latter give rise to the distal tip cells (dtcs), which remain located at the distal ends of the two gonadal arms throughout development (Hedgecock et al., 1987). Led by these two dtcs, the gonad migrates from midbody in opposite directions toward head and tail during L2.

In the L3 stage, dtcs reflex dorsally and centripetally back toward the midbody to form two U-shaped gonadal arms in adult animals (Figure 2C).

### 1.1.5 Heterochronic Genes

A rich signaling network of temporal selector genes, the heterochronic genes, orchestrate *C. elegans* stage- and tissue-specific cellular patterns. Forward genetic screens identified a class of mutants called lin (cell lineage abnormal) mutants. A handful of these, including *lin-4*, *lin-14*, *lin-28*, and *lin-29*, were further classified into a subgroup termed heterochronic mutants due to their alteration of cellular developmental timing events (Ambros and Horvitz, 1984; Chalfie et al., 1981). Heterochronic genes work in a highly tissue- and stage-specific manner to coordinate developmental progression throughout the whole organism. Mutations in these genes cause stage-specific cellular events to be expressed earlier (precocious) or later (retarded) than normal, which often manifests as a deletion or repetition of such temporal patterns. Currently, there are over 30 identified heterochronic loci which encode various highly conserved transcriptional, translational and post-translational regulators including the first discovered microRNAs *lin-4* and *let-7* (Table 1) (Reinhart et al., 2000; Lee et al., 1993; Resnick et al., 2010). The hierarchy of the heterochronic circuitry has been built on genetic epistasis and synergy experiments as well as the study of molecular interactions and expression profiles. Although affecting multiple tissues, developmental timing mechanisms have been most extensively studied in *C. elegans* epidermis.

### 1.1.6 Seam Cell Heterochronic Circuitry

Despite the extensive complexity of the *C. elegans* developmental timing regulatory network, its basic framework relies on three microRNA-mediated switches shutting down previous developmental programs to allow for subsequent ones (Figure 3 and Table 1) (Ambros, 2011; Rougvie and Moss, 2013). microRNAs, which encode 21-25 nucleotide RNA stretches, bind to partially complementary sequences in the 3'UTR of a target mRNA to specifically inhibit translation or induce mRNA degradation (Olsen and Ambros, 1999; Pillai et al., 2007; Ambros, 2004). Ultimately they control levels of key regulatory components, which connect the developmental phases by initiating transcriptional programs in a time-specific fashion.

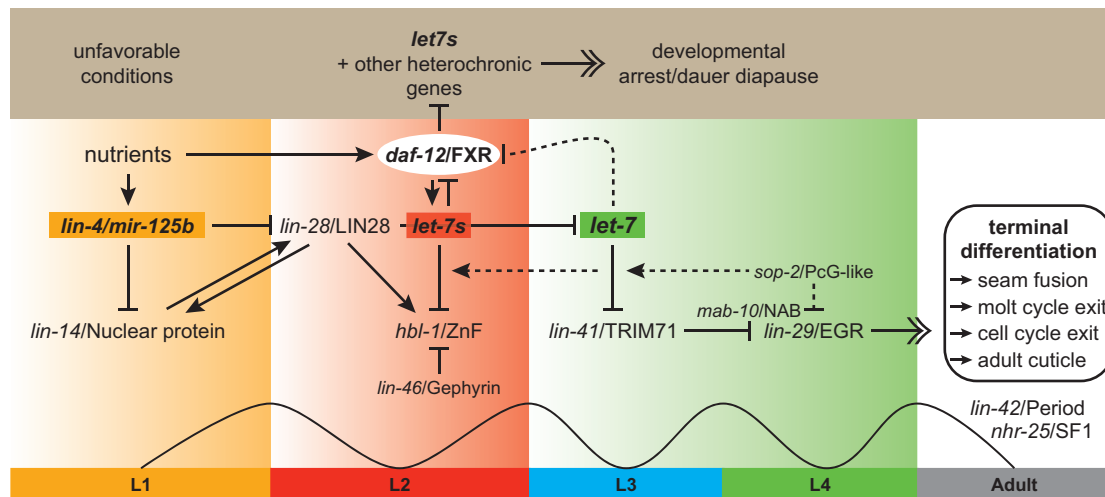


**Figure 3: Seam Cell Heterochronic Circuitry**

Schematic representation of the seam cell heterochronic circuitry that is organized around three microRNA-mediated switches indicated in orange, red and green color. Under favorable conditions heterochronic genes catalyze developmental progression toward terminal differentiation, while adverse environment induces dauer diapause via the nuclear hormone receptor DAF-12.

The canonical heterochronic network can be divided into three phases (Figure 3). First, *lin-4/mir-125b* microRNA accumulates toward the end of the L1 stage to downregulate the novel nuclear protein *lin-14/nuclear protein*, which specifies the L1 fate (Chalfie et al., 1981; Ambros and Horvitz, 1984; Ruvkun and Giusto, 1989; Arasu et al., 1991; Lee et al., 1993; Wightman et al., 1993). *lin-4* transcriptional activation requires the abundance of food, as well as multiple components of Insulin/IGF signaling and various microRNAs (Arasu et al., 1991; Feinbaum and Ambros, 1999; Baugh and Sternberg, 2006; Fukuyama et al., 2006; Karp et al., 2011; Kasuga et al., 2013). Recent studies suggest timely *lin-4* accumulation also relies on auto-regulatory action of the *lin-4* microRNA itself to lock the fate decision (Turner et al., 2014). *lin-4* loss of function results in a strong retarded phenotype where L1 stage patterns are incessantly reiterated and seam cell terminal differentiation never occurs. Likewise, *lin-14* recessive mutation causes L1 patterns to be skipped and all subsequent patterns to advance precociously, such that seam cells undergo the proliferative division already in the L1 stage and seam terminal differentiation occurs late in L3. Intriguingly, *lin-14* gain-of-function alleles were identified, which lack *lin-4* binding sites in the 3'UTR and thus aberrantly stabilize *lin-14* through withdrawal from *lin-4* mediated degradation (Ambros and Horvitz, 1987; Wightman et al., 1991). This observation was key to the discovery of microRNAs.

The RNA-binding protein *lin-28/LIN28* and the homolog of the *Drosophila* hunchback transcription factor, *hbl-1/ZnF* specify second larval stage fates (Fay et al., 1999; Moss et al., 1997). *lin-28(lf)* results in precocious phenotypes whereby L2 programs are skipped and L3 stage and subsequent programs are expressed one stage ahead of schedule (Ambros and

Horvitz, 1984). Like *lin-14*, *lin-28* is also targeted by *lin-4* microRNA, but slightly later in development to initiate the L2-to-L3 transition (Moss et al., 1997). In addition to the sequential downregulation of *lin-14* and *lin-28* by *lin-4*, a positive feedback loop between *lin-14* and *lin-28* reinforces early larval fate specifications (Arasu et al., 1991; Moss et al., 1997; Seggerson et al., 2002). The second switch is mediated by the redundant *let-7*-family microRNA members *mir-48*, *-84*, and *-241*, termed *let-7s*. During L2, *hbl-1* is stabilized by *lin-28*, but just as *lin-28* is downregulated by *lin-4*, *hbl-1* too, becomes targeted by *let-7s* microRNAs. (Vadla et al., 2012; Abrahante et al., 2003; Abbott et al., 2005). *hbl-1* mutants skip L2-specific patterns whereas *let-7s* triple mutants show misexpression of *hbl-1* within the L3 stage, causing reiteration of the L2-specific proliferative seam cell division (Abrahante et al., 2003; Abbott et al., 2005).

Finally, the third phase is initiated by derepression of *let-7* microRNA, which ultimately results in seam cell terminal differentiation. During early larval stages, *lin-28* recruits a poly(U) polymerase *pup-2* to stimulate *let-7* precursor degradation (Lehrbach et al., 2009; Moss et al., 1997; Vadla et al., 2012; Van Wynsberghe et al., 2011). At later stages, during which *lin-28* is repressed, *let-7* accumulates to downregulate its major target *lin-41/TRIM71*, which results in expression of the terminal transcription factor *lin-29/EGR* (Reinhart et al., 2000; Slack et al., 2000; Vella et al., 2004; Rougvie and Ambros, 1995). Thus LIN-28 on the one hand drives L2 programs by stabilizing *hbl-1* and on the other hand inhibits microRNA biogenesis to prevent execution of subsequent programs (Vadla et al., 2012).

*let-7* mutants are lethal. However temperature sensitive (ts) *let-7* alleles such as *let-7(n2853ts)* display retarded heterochronic phenotypes, as seam cells fail to exit the cell cycle and adult alae are not formed until an additional fifth molt. Evidence suggests that rather than repeating L4 programs, *let-7* mutants might reiterate L3-specific programs (Vadla et al., 2012).

*lin-41/TRIM71* encodes a highly-conserved TRIM-NHL-family RNA binding protein that affects mRNA function across species (Ecsedi and Grosshans, 2013). *lin-41(gf)* mutants display retarded phenotypes, largely resembling *let-7* ts alleles (Slack et al., 2000). Likewise, in *lin-41(lf)* mutants seam cells terminally differentiate precociously in L3 larvae due to early elevated LIN-29 levels (Slack et al., 2000). However the concrete mechanism of *lin-29* inhibition by *lin-41* remains poorly understood. Although LIN-41 harbors a RING domain and few studies reported mammalian LIN-41/TRIM-71 to act as ubiquitin ligase on the microRNA machinery component AGO2 (Duchaine et al., 2006; Rybak et al., 2009; Loedige

et al., 2013), its ubiquitin ligase activity seems to be highly context-specific and was reported to be dispensable for repression of mRNA function (Chen et al., 2012; Chang et al., 2012; Loedige et al., 2013).

Finally, increasing LIN-29 levels drive an adult-specific transcriptional pattern including the expression of several collagens, such as *col-7* and *col-19*, which serve as markers of the adult fate (Rougvie and Ambros, 1995; Liu et al., 1995). The Krüppel family zinc-finger transcription factor *lin-29* functions as the most downstream gene in *C. elegans* heterochronic pathways and consequentially is epistatic to all known heterochronic genes affecting seam cell development (Rougvie and Ambros, 1995; Resnick et al., 2010). In other words, all known heterochronic genes directly or indirectly affect the temporal control of *lin-29* expression to specify the timing of seam cell terminal differentiation.

### 1.1.7 Additional Layers of Seam Cell Fate Coordination - a Link Between Developmental Timing, the Molt Cycle and Environmental Cues

The components of the canonical heterochronic pathway described above constitute key players, which when mutated result in strong and penetrant heterochronic phenotypes. In addition to these genes a large number of heterochronic genes has been identified that fine-tune temporal progression in the epidermis and link it to environmental cues and the molting timer. Most of them affect the second and the last of the three microRNA-mediated switches (Figure 3 and Table 1).

#### 1.1.7.1 Additional Modulators of the Second microRNA Switch (L2-to-L3 Transition):

The scaffold protein *lin-46*/Gephyrin, as well as the nematode-specific transcription factor *sel-7* have been reported to act in parallel to the *let-7s* microRNAs to downregulate *hbl-1* and allow developmental progression to L3 (Pepper et al., 2004; Xia et al., 2009). Consistent with LIN-46 levels peaking once in each larval stage, *lin-46* mutation also affects developmental timing at later stages (Pepper et al., 2004; Moss, 2007). Not surprisingly, also mutations in components of the microRNA biogenesis machinery including the Argonaute homologs *alg-1/2*, the GW182 homologs *ain-1/2*, and the Dicer homolog, *dcr-1*, affect *C. elegans* developmental timing as corresponding mutants reiterate L2-specific patterns, most likely through impaired regulation of *hbl-1* by *let-7s* (Morita and Han, 2006; Grishok et al., 2001).

DAF-12 functions as a molecular switch between reproductive vs. dauer development and thereby links environmental cues to developmental timing and progression. One of DAF-12's

major and direct transcriptional outputs includes the *let-7s* microRNAs (Antebi et al., 1998; 2000; Fielenbach and Antebi, 2008; Bethke et al., 2009). In favorable environmental conditions ligand-bound DAF-12 moderately activates *let-7s* expression, which in turn downregulate *hbl-1* to allow reproductive growth and developmental progression. In contrast, ligand-free DAF-12 is a potent repressor of these microRNAs. In the *daf-12* null mutant allele *daf-12(rh61rh411)*, which harbors point mutations in both the DBD and the LBD, *let-7s* microRNAs are slightly reduced and accordingly, these mutants exhibit only weak developmental timing alterations (Bethke et al., 2009; Hammell et al., 2009a; Antebi et al., 1998; 2000). In contrast, *daf-12* LBD mutants such as *daf-12(rh61)* show a striking decrease in *let-7s* microRNAs resulting in aberrantly high HBL-1 levels in L3 larvae. Consequentially, LBD mutants repeat L2-specific seam cell programs leading to delayed or impaired terminal differentiation (e.g. adult alae formation) later in life (Antebi et al., 2000; 1998; Motola et al., 2006). Multiple studies suggest that these allele-specific *daf-12* phenotypes are based on the loss-of-activation and repression function in the *daf-12*(null) mutants, whereas the LBD mutant only impairs *daf-12*-dependent activation, still allowing potent suppression of microRNA expression (Antebi et al., 2000; Bethke et al., 2009). In particular, DAF-12 is a potent repressor of the *let-7s* microRNAs during dauer formation. Of note, the *daf-12*-dependent regulation of *let-7s* is not a linear relation, but fine-tuned by negative feedback loops to lock fate decisions based on environmental stimuli in a cell-autonomous fashion (Hammell et al., 2009a; Grosshans et al., 2005; Bethke et al., 2009). Recently, Chip on Chip analysis suggests a global role for *daf-12* in regulating heterochronic genes at various stages, as *daf-12* resides at the promoters of the heterochronic loci *alg-2*, *lin-46*, *lin-14*, *lin-66*, *lin-28*, *lin-41*, *dre-1*, and *lin-42* (Hochbaum et al., 2011). In sum, DAF-12 functions as key modulator of the second microRNA-mediated switch, which is directly linked to the perception of environmental conditions.

#### 1.1.7.2 Additional Modulators of the Third microRNA Switch (Larval-to-Adult Transition):

In addition to its function at the L2-to-L3 transition the transcription factor *hbl-1* works in parallel to *lin-41* to redundantly specify L4-specific cellular fates by preventing *lin-29* expression (Abrahante et al., 2003). *hbl-1* is not only targeted by *let-7s* microRNAs, but also by *let-7* itself, whose accumulation initiates late larval and finally adult-specific programs (Abrahante et al., 2003; Lin et al., 2003). Both *lin-41* and *hbl-1* are epistatic to *let-7*, as the double mutants display precocious seam phenotypes, consistent with their role downstream of the microRNA (Slack et al., 2000; Abrahante et al., 2003).

Moreover, the *C. elegans* polycomb-group-like (PcG-like) gene *sop-2* specifies spatial and temporal identities of the seams (Cai et al., 2008; Zhang et al., 2003). Null mutants arrest early in L1, whereas ts alleles of *sop-2* show various developmental alterations at permissive temperatures: e.g. seam cells undergo precocious terminal differentiation at the L3- or even the L2 molt. Furthermore, *sop-2* genetically interacts with heterochronic loci controlling early and late developmental programs, acting presumably largely in parallel to the ‘canonical’ pathways. Initial evidence suggests that *sop-2(+)* might generally hamper microRNA-mediated gene repression, consistent with a role at multiple steps in *C. elegans* developmental timing (Cai et al., 2008).

*mab-10/NAB* encodes a NAB (NGFI-A-binding protein) transcriptional cofactor and was recently shown to regulate the larval-to-adult transition in concert with *lin-29*. In *mab-10* loss-of-function mutants seam cells fail to exit the cell cycle and worms undergo supernumerary molts. MAB-10 protein directly binds to LIN-29 via a conserved motif to promote its activity, including downregulation of *nhr-25* and *nhr-23* to prevent extra molts and induction of the CDK inhibitor *cki-1* to trigger exit from the cell cycle (Harris and Horvitz, 2011; Hong et al., 1998).

*nhr-25/SF1*, the homolog of *Drosophila*  $\beta$ -FTZ-F1 and mammalian SF1, encodes a nuclear hormone receptor not only regulating *C. elegans* molting, embryogenesis and reproduction, but also epidermal developmental timing (Gissendanner and Sluder, 2000; Gissendanner et al., 2004; Silhánková et al., 2005; Hada et al., 2010; Chen et al., 2004). In contrast to many other heterochronic genes that are expressed for continuous temporal blocks working in a sequential manner, NHR-25 levels oscillate with the molt cycle, with peaks around the molts (Gissendanner et al., 2004). Intriguingly, *nhr-25* mutants show inconclusive phenotypes regarding their role in epidermal timing regulation: Although these mutants exhibit precocious expression of the adult-specific collagen *col-19*, seam cells do not fuse, undergo an extra division and fail to synthesize adult alae (Hada et al., 2010).

Similar to NHR-25, LIN-42/Period levels oscillate in a 8-10 hour period synchronized with the molt cycle (25°C) (Jeon et al., 1999; Tennessen et al., 2006). *lin-42* encodes the *C. elegans* homolog of the *Drosophila* circadian rhythm gene *Period*, a PAS domain containing protein that cycles in a daily pattern (Jeon et al., 1999). In *C. elegans*, *lin-42* acts as a global regulator of life history, affecting dauer formation, molting, and epidermal developmental timing (Tennessen et al., 2006; 2010). Loss-of-function mutants are hypersensitive to dauer

formation (Tennessen et al., 2010) and exhibit precocious seam cell fusion and adult alae formation, suggesting *lin-42(+)* to specify late larval development in the epidermis (Tennessen et al., 2006; Abrahante et al., 1998). Genetic epistasis experiments place *lin-42* in close proximity to *hbl-1* and *lin-41*, as it mutually suppresses retarded *let-7* phenotypes (Tennessen et al., 2006). Further, *lin-42* acts in opposition to *daf-12* for multiple phenotypes in seam and gonadal heterochrony, as well as dauer formation (Tennessen et al., 2010). *lin-42* also genetically interacts with *lin-14*, *lin-46*, and others, suggesting *lin-42* works at multiple steps of *C. elegans* development consistent with its cycling expression (Abrahante et al., 1998; Pepper et al., 2004; Ren and Zhang, 2010).

Also other key circadian rhythm regulators affect *C. elegans* developmental timing. *tim-1* and *kin-20* are *C. elegans* homologs of the *Drosophila* circadian clock genes *timeless* and *doubletime*, respectively and prevent premature terminal differentiation in the seams (Jeon et al., 1999; Banerjee and Slack, 2002).

Strikingly, multiple heterochronic genes not only have homologs regulating circadian rhythms in vertebrates, but they also directly affect *C. elegans* molting. Besides *nhr-23* and *-25*, the heterochronic gene *lin-42* is a key player within the molt cycle. Its misregulation elicits molting defects at all four molts (Monsalve et al., 2011). Interestingly, heterochrony in *C. elegans* is directly linked to the molt cycle as precocious heterochronic mutants cease the molt cycle at earlier stages than wild type and conversely, retarded mutant animals frequently undergo supernumerary molts, e.g. in *let-7* or *mab-10* mutants. In particular, *let-7/let-7s* microRNAs, as well as *lin-29* together with *mab-10* were shown to directly downregulate NHR-25 levels to trigger exit from the molt cycle at the larval-to-adult transition (Hayes et al., 2006; Harris and Horvitz, 2011). Taken together, molecular pathways governing circadian rhythms in vertebrates and *C. elegans* developmental timing and molting show striking parallels and interactions, suggesting a conserved molecular mechanism to be applied for various types of biological timing control. Intriguingly, then iterant cycling modules are coordinated with molecular switches to ensure proper succession of cellular temporal fates.

**Table 1: Heterochronic Genes Affecting Developmental Timing in *C. elegans* Epidermis**

Summary of known heterochronic genes, including the phenotype in seam cells upon loss of function, as well as the closest mammalian homolog.

Gene	Seam phenotype	Mammalian homolog	References
<b>Switch 1</b>			
<i>lin-4</i>	Retarded, Repeat L1	<i>mir-125b</i>	(Wightman et al., 1993; Lee et al., 1993)

<i>lin-14</i>	Precocious, Skip L1	Novel nuclear protein	(Ambros and Horvitz, 1987; 1984; Ruvkun and Giusto, 1989)
<b>Switch 2</b>			
<i>hbl-1</i>	Precocious, Skip L2	ZnF	(Lin et al., 2003; Abrahante et al., 2003)
<i>lin-28</i>	Precocious, Skip L2	LIN28	(Moss et al., 1997)
<i>mir-48,84,241</i>	Retarded, Repeat L2	<i>let-7s</i>	(Abbott et al., 2005)
<i>lin-46</i>	Retarded, Repeat L2	Gephyrin	(Pepper et al., 2004)
<i>nhl-2</i>	Retarded, Repeat L2	Trim2/nhl Ring finger	(Hammell et al., 2009b)
<i>sel-7</i>	Retarded, Repeat L2	not conserved	(Xia et al., 2009)
<i>daf-12</i>	Retarded, Repeat L2	FXR/LXR/VDR	(Antebi et al., 1998; 2000)
<i>lin-66</i>	Retarded, Repeat L2	not conserved	(Morita and Han, 2006)
<b>Switch 3</b>			
<i>lin-29</i>	Retarded seam fusion	ZnF362/EGR	(Rougvie and Ambros, 1995)
<i>let-7</i>	Retarded seam fusion	<i>let-7</i>	(Reinhart et al., 2000)
<i>dre-1</i>	Precocious seam fusion	FBXO11	(Fielenbach et al., 2007)
<i>lin-41</i>	Precocious seam fusion	Trim71/nhl Ring finger	(Slack et al., 2000)
<i>lin-42</i>	Precocious seam fusion	Period	(Jeon et al., 1999; Tennessen et al., 2006)
<i>tim-1</i>	Precocious seam fusion	Timeless	(Banerjee et al., 2005)
<i>kin-20</i>	Precocious seam fusion	Doubletime kinase	(Banerjee et al., 2005)
<i>sop-2</i>	Precocious seam fusion	Polycomb-group-like	(Cai et al., 2008)
<i>nhr-25</i>	Retarded seam fusion	SF1	(Gissendanner and Sluder, 2000; Hada et al., 2010)
<i>apl-1</i>	Let-7 suppressor	APP homolog	(Niwa et al., 2008)
<b>Wingless Signaling</b>			
<i>pop-1</i>	Synthetic Precocious	TCF/LEF Tcf factor	(Ren and Zhang, 2010)
<i>wrm-1</i>	Synthetic Precocious	$\beta$ -catenin	(Ren and Zhang, 2010)
<b>MicroRNA Biogenesis</b>			
<i>dcr-1</i>	Retarded Repeat L2	Dicer	(Grishok et al., 2001)
<i>alg1/2</i>	Retarded, Repeat L2	Argonaute	(Grishok et al., 2001)
<i>ain1/2</i>	Retarded, Repeat L2	GW182 protein	(Ding et al., 2005)

### 1.1.8 Gonadal Heterochronic Circuitry

Heterochronic genes have been demonstrated to coordinate developmental timing across tissues, but their timing, circuitry, and outcome can be highly tissue-specific (Hallam and Jin, 1998; Antebi et al., 1998; Ambros and Horvitz, 1984). The molecular network underlying temporal control of gonadal migration is poorly understood, except for some key regulators. Similar to the situation in the seams, *daf-12* null mutants show a near WT-like gonadal migration pattern, whereas *daf-12* LBD mutants, which render *daf-12* a constitutive repressor, exhibit a penetrant gonadal migration defect (mig): dtcs fail to turn, repeat L2-stage specific linear ventral movement and migrate straight into head and tail (Figure 2) (Antebi et al., 1998). As in the epidermis, these developmental alterations are partly suppressed by mutation

of the DAF-12 corepressor DIN-1 (Ludewig et al., 2004). Interestingly, mutations in the DA biosynthetic pathway, e.g. *daf-36*/Rieske or *daf-9*/CYP27A1 (previously termed *mig-8*) also cause gonadal migration defects, supporting the idea that ligand-free DAF-12 prevents the dorsal gonadal turn (Antebi et al., 1998; Rottiers et al., 2006; Gerisch et al., 2001). Furthermore, *daf-12* null mutants exhibit synthetic gonadal migration defects in sensitized backgrounds, such as *lin-29(lf)*, indicating *daf-12*-parallel functions to redundantly activate gonadal L3 programs, which could be thwarted by a constitutive DAF-12 repressor (Antebi et al., 1998; Fielenbach et al., 2007). In contrast to retarded migration defects, *lin-42* depletion precedes the dorsal gonadal turn (Tennessen et al., 2006). Thereby genetic epistasis experiments place *lin-42* upstream or parallel to *lin-29* and *daf-12* (Fielenbach et al., 2007; Tennessen et al., 2006). Finally, evidence suggests that temporal signals in the dtcs collectively trigger expression of the netrin receptor *unc-5*/UNC5 to ultimately initiate the dorsal migratory fate (Su et al., 2000).

### 1.1.9 Dauer Diapause - a Reset of Developmental Timing

An unexpected phenomenon was discovered about 25 years ago, which suggests that temporal fates can be reprogrammed. Heterochronic mutants that affect early larval stages show wild type epidermal fates when they developed through dauer diapause (Liu and Ambros, 1991; Abrahante et al., 2003; Euling and Ambros, 1996). Most strikingly, precocious formation of the adult vulva is prevented by reprogramming a subset of vulval precursor cells to reset them to their ancestral fates. The molecular mechanisms underlying the reset of developmental timing are currently investigated, but still very poorly understood (Hochbaum et al., 2011; Karp and Ambros, 2012).

### 1.1.10 Heterochronic Genes – Parallels in Higher Organisms

Importantly, most heterochronic genes are remarkably conserved throughout evolution and fulfill essential functions in plants, flies, and mammals directing proliferation, differentiation, and stem cell dynamics (Geuten and Coenen, 2013; Ambros, 2003; Sokol, 2012). Some extraordinary examples of structural and functional conservation are depicted in the following, highlighting the importance of *C. elegans* heterochronic genes in vertebrate biology.

DAF-12 is homologous to the mammalian nuclear hormone receptors FXR, LXR, and VDR and works at the interface of dauer diapause and heterochronic pathways in *C. elegans* epidermis and gonad. Similar to DAF-12, its mammalian homologs bind steroid ligands to

read out the metabolic state and in turn regulate metabolism homeostasis and developmental progression. For example ligand-bound LXR promotes keratinocyte differentiation in the epidermis (Kömüves et al., 2002). Likewise, lack of VDR prevents skin stem cell differentiation (Xie et al., 2002; Cianferotti et al., 2007; Zhang et al., 2011), indicating that cellular fate decisions are coordinated by a hormone-dependent switch, similar to *C. elegans*.

Even more striking, microRNAs, as well as genes involved in their biogenesis, are highly conserved up to humans. Both *lin-4/mir-125b* and *let-7/let-7* have been demonstrated to direct proliferation and differentiation in various tissues across species (Zhang et al., 2011; Caygill and Johnston, 2008; Yu et al., 2007a). *let-7* is fully conserved throughout all major taxa and has been shown to function as a maturation factor in *C. elegans*, *Drosophila*, and mice (Sokol et al., 2008; Caygill and Johnston, 2008; Büssing et al., 2008; Reinhart et al., 2000). Across species, *let-7* levels are low early in undifferentiated tissues and rise during development to direct differentiation (Pasquinelli et al., 2000). In the fruitfly, *let-7* accumulation triggers terminal maturation of neuronal and abdominal muscles (Sokol et al., 2008; Caygill and Johnston, 2008). Interestingly, the steroid hormone 20-hydroxiecdysone, which pulses before each molt, has been shown to activate *let-7* expression (Chawla and Sokol, 2012). This hormone-driven switch in *Drosophila* shows remarkable similarities to the regulation of developmental progression by DAF-12 and *let-7s* microRNAs in *C. elegans*.

In mammals, *let-7* levels increase during embryogenesis, brain development, and upon differentiation of mouse embryonic stem cells and levels are maintained in various adult tissues (Wulczyn et al., 2007; Thomson et al., 2006; Sempere et al., 2004). Not surprisingly, decreased *let-7* levels have been found to be a hallmark of a variety of different cancers, including lung cancer, breast cancer, hematopoietic cancers, and others (Takamizawa et al., 2004; Thornton and Gregory, 2012). These tumor cells are characterized by a low differentiation state, harboring a high proliferative and self-renewal potential. Likewise, *let-7* deregulation has been demonstrated to significantly contribute to the determination of breast cancer stem cell populations, which have a high proliferative capacity allowing cancers to repopulate after cancer therapy (Yu et al., 2007a). These findings largely reflect the situation in the nematode, where lack of *let-7* results in impaired terminal differentiation and aberrantly ongoing cell divisions, reflecting a cancer-cell-like state (Reinhart et al., 2000). Interestingly, also *let-7* target genes show a substantial overlap between worms and mammals. Amongst them, the oncogene *Ras* (homolog of *let-60*) provides a link between reduced *let-7* levels and tumor formation, establishing *let-7* as a tumor suppressor (Grosshans et al., 2005; Johnson et

al., 2005; Jérôme et al., 2007). Furthermore, TRIM71 (homolog of *lin-41*) is targeted by *let-7* and involved in a feedback-loop regulating *let-7* activity in stem cells (Rybak et al., 2009). Although the hypothesis that LIN-41/TRIM-71 acts as ubiquitin ligase to AGO2 to regulate microRNA and mRNA function has recently been challenged (Loedige et al., 2013; Chen et al., 2012; Chang et al., 2012), still LIN-41/TRIM-71 action has been demonstrated to prevent terminal differentiation in mammals – analogous to the situation in *C. elegans* epidermis (Slack et al., 2000; Ecsedi and Grosshans, 2013).

In addition to *let-7*, *lin-28* is highly conserved and is of extraordinary importance to human stem cell biology. First in mammals LIN28 was shown to inhibit *let-7* maturation by distinct mechanisms, thereby preventing (precocious) stem cell terminal differentiation (Viswanathan et al., 2008; Rybak et al., 2008; Nam et al., 2011; Piskounova et al., 2011). In worms and mammals *lin-28* is highly expressed early in undifferentiated cells and then decreases to allow *let-7* accumulation and cell differentiation. Importantly, mammalian LIN28 works as pluripotency factor, which when overexpressed together with OCT4, SOX2 and NANOG can even dedifferentiate terminally differentiated cells to give rise to induced pluripotent stem cells (Yu et al., 2007b). This activity might in part depend on the decrease of *let-7* levels to re-induce pluripotency (Shyh-Chang et al., 2013). Not surprisingly, mammalian LIN28 overexpression has been demonstrated to drive cancer progression and metastasis in a variety of tumors (Zhou et al., 2013; Thornton and Gregory, 2012). Thereby strong repression of *let-7* shifts transformed cells toward self-renewal and a high proliferative capacity, hallmarks of these tumors (Thornton and Gregory, 2012; Murray et al., 2013). However, the regulation of *let-7* by *lin-28* is not unidirectional, but comprises an autoregulatory feedback as *lin-28*/LIN28 belongs to the conserved *let-7* targets (Rybak et al., 2008; Grosshans et al., 2005). Notably also the *lin-4* homolog *mir-125b* has a conserved role in regulating *lin-28*/LIN28 levels and consequentially affects differentiation across tissues (Rybak et al., 2008; Zhang et al., 2011; Wu and Belasco, 2005).

Finally, in addition to the pivotal role of LIN-28 in stemness and tumorigenesis, LIN-28 polymorphisms have recently been associated with the precocious onset of puberty in humans, revealing a remarkable degree of functional conservation not only on the molecular, but also on the organismal level (Park et al., 2012; Zhu et al., 2010; Ong et al., 2009).

In sum, *C. elegans* and mammalian developmental timing mechanisms show many analogies on a cellular and a molecular level, although their life histories are apparently different. Thus

studying developmental timing mechanisms in lower organisms might further inform temporal control of developmental progression and differentiation in mammals, and might lead to the discovery of novel molecular timing devices. Across species, the specific and precise regulation of protein abundance is key to coordinated developmental progression, but the particular specificity of such processes is yet poorly understood.

## 1.2 Ubiquitin-Mediated Proteolysis

### 1.2.1 Ubiquitin Proteasome System (UPS)

Already more than 70 years ago, Schoenheimer and coworkers discovered the dynamic state of cellular proteins (Schoenheimer, 1942). They found that isotope-labeled amino acids fed to rats were not entirely excreted, but isotopes were present in extracted proteins, indicating their partial or full renewal. However, the biochemical mechanisms underlying protein homeostasis and in particular protein turnover have begun to be uncovered only decades later.

Notably, the discovery of the canonical ubiquitin-dependent proteolysis pathway early in the 1980s was honored with a Nobel prize in chemistry in 2004 (Ciechanover et al., 1980; Hershko et al., 1980; Wilkinson, 2005). The 76 amino acid polypeptide ubiquitin was initially purified from bovine thymus, but later shown to be ubiquitously expressed and extremely conserved among all eukaryotes (Goldstein et al., 1975; Hershko and Ciechanover, 1998). It constitutes the most prominent member of a class of ubiquitin-like modifiers, which change the properties of a target protein upon post-translational covalent linkage (Komander and Rape, 2012; Vertegaal, 2007). Today we know that thousands of proteins get modified by ubiquitination, which most predominantly triggers their subsequent proteasomal degradation, but also can induce a variety of alternative fates, including lysosomal degradation, as well as non-proteolytic fates such as regulation of protein interactions, activity, and localization (Figure 4) (Komander and Rape, 2012; Pickart and Fushman, 2004).

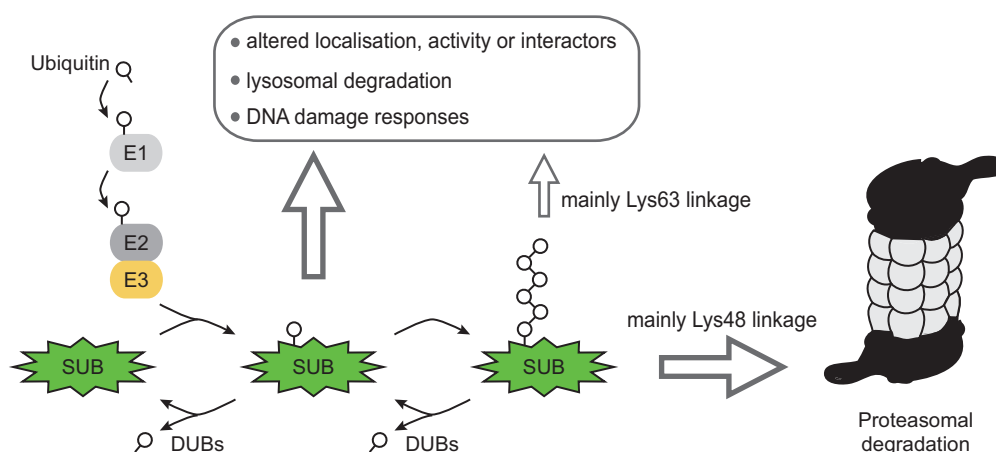


**Figure 4: Mechanism and Cellular Fates of Protein Ubiquitination**

Target proteins are ubiquitinated by an enzymatic cascade of E1, E2 and E3 enzymes. Number and linkage of ubiquitin moieties can direct the target protein to distinct cellular fates. Poly-ubiquitination (mainly Lys48 linked) predominantly triggers degradation of the target protein via the 26S proteasome. Deubiquitinating enzymes (DUBs) antagonize the ubiquitination machinery and recycle ubiquitin molecules.

Covalent ligation of ubiquitin to a target protein is catalyzed by a 3-step enzymatic cascade (Figure 4): ubiquitin-activating enzymes (E1) form a thioester bond between the C-terminal Gly of ubiquitin and a Cys residue of the E1 enzyme in an ATP-dependent reaction. Activated ubiquitin is then transferred to a Cys residue in the active site of an ubiquitin-conjugating enzyme (E2). In the final step an ubiquitin ligase (E3) links the ubiquitin C-terminus via an isopeptide bond to the  $\epsilon$ -amino group of a target proteins Lys residue. The attachment of a single ubiquitin to a target protein (monoubiquitination) is commonly thought to regulate protein interaction or localization (Hicke, 2001). Repetitive action of an E3 ligase results in polyubiquitin chains through conjugation of ubiquitin to one of the seven Lys residues of a preceding ubiquitin (Lys6, -11, -27, -29, -33, -48, or -63) (Hershko and Ciechanover, 1998). Notably, ubiquitin chain elongation can be supported by a 4<sup>th</sup> class of enzymes (E4 ligases), which specifically promote polyubiquitination of short ubiquitin chains (Koegl et al., 1999; Hoppe et al., 2004; Hoppe, 2005). Depending on the linkage between the ubiquitin molecules, the chain on a target protein can be recognized by linkage-specific adapters, which couple the chain topology to a particular outcome (Dikic et al., 2009; Dikic and Dötsch, 2009; Komander and Rape, 2012; Pickart and Fushman, 2004; Thrower et al., 2000). While Lys63 linkages predominantly affect DNA damage responses and protein trafficking (Spence et al., 1995; Galan and Haguenauer-Tsapis, 1997; Hicke and Dunn, 2003), polyubiquitin chains linked via Lys11, Lys29, and Lys48 mainly label target proteins for subsequent degradation via the 26S proteasome (Chau et al., 1989; Finley et al., 1994; Komander and Rape, 2012).

The 26S proteasome is a multi-subunit complex present in cytosol and nucleus, consisting of a multi-catalytic core subunit (20S) and two regulatory caps (19S) on each site of the barrel-shaped core (Bedford et al., 2010; Wójcik and DeMartino, 2003). Proteins labeled for proteasomal degradation are recognized by ubiquitin binding domain-containing receptors exposed on the proteasome surface, then get unfolded, deubiquitinated, and proteolyzed to small polypeptides. Deubiquitination is carried out by C-terminal hydrolases (deubiquitinases, DUBs), which function as natural counterparts to the ubiquitination machinery and constantly recycle ubiquitin molecules (Figure 4) (Komander et al., 2009). Recent studies unraveled a major role, in particular for linkage-specific DUBs, in the sophisticated process of ubiquitin chain editing (Komander and Rape, 2012). Although extensive research on the ubiquitin code and its encoding has been performed, still many ubiquitin-mediated functions remain poorly understood.

In sum, posttranslational modification by ubiquitin, and in particular ubiquitin-dependent proteolysis of regulatory proteins, such as cyclins, transcription factors, oncoproteins, and tumor suppressors directs distinct cellular fates in health and disease. Therefore the UPS is a key contributor to the control of intracellular protein homeostasis and acts in an active and highly time- and substrate-specific manner. The diversity of ubiquitin's biological targets and functional outcomes of ubiquitination raises the question of how specificity is ensured within the ubiquitination pathway.

### 1.2.2 Specificity of the Canonical UPS Pathway – E3-Ubiquitin Ligases

The large protein superfamily of E3-ubiquitin ligases selects target proteins and directly or indirectly determines the topology of conjugated ubiquitin moieties by recruiting specific E2 enzymes and mediating the terminal ubiquitin transfer.

Across species, the number of E3 ligases largely exceeds the number of E1 and E2 enzymes. For example in humans, there are only two E1 enzymes (1 in *C. elegans*), about 38 E2 enzymes (20 in *C. elegans*), but more than 600 E3 ligases (about 170 in *C. elegans*) (Kipreos, 2005; Skaar et al., 2009b; Deshaies and Joazeiro, 2009). One distinguishes two major classes of E3 ligases in eukaryotes depending on the presence of either a HECT (Homologous to the E6-AP Carboxyl Terminus) or a RING (Really Interesting New Gene) domain, which both are involved in the recruitment of the E2-conjugating enzyme. Interestingly, these two classes also catalyze ubiquitin-transfer by distinct mechanisms: While HECT domain E3-ligases contain a conserved Cys-residue that forms an intermediate thioester bond with the ubiquitin C-terminus, RING domain E3 ligases facilitate the direct transfer of ubiquitin from the conjugating E2 enzyme to the target's Lys by bringing them in close spatial proximity (Passmore and Barford, 2004; Scheffner et al., 1995). In addition to these two major classes there is a third, small family of E3-ubiquitin ligases, containing a U-box domain, a specified RING finger (Fang et al., 2003).

Given the substrate diversity, additional mechanisms must exist to ensure target specificity. While HECT E3s and many RING E3 ligases act as monomers, some RING E3 ligases form multimeric complexes (Feldman et al., 1997; Deshaies and Joazeiro, 2009). Pioneering work in *C. elegans* and yeast uncovered this large class of E3 ligases termed Cullin-RING ubiquitin ligases (CRL) which are built on different Cullin scaffolds (8 in humans, 6 in *C. elegans*) and can incorporate an enormous variety of substrate-recognition subunits (SRS) (Petroski and Deshaies, 2005; Deshaies and Joazeiro, 2009; Sarikas et al., 2011). The archetypal CRLs,

which are built on CUL1, are named S phase kinase-associated protein 1 (SKP1)- Cullin1 (CUL1)- F-box protein complexes (SCF complexes) and are the by far best characterized (Table 2 and Figure 5) (Feldman et al., 1997; Petroski and Deshaies, 2005). The modular composition of related CRLs is summarized in Table 2.

**Table 2 : Overview of Cullin-RING Ligase Complex Components**

*BTB* broad complex, tramtrack, bric-a-brac; *SOCS* suppressor of cytokine signaling; *DDB1* DNA damage binding protein-1; *DCAF* DDB1 and CUL4 associated factor; *RBX* ring-box protein; *SKP1* S phase kinase-associated protein-1; *APC* adenomatous polyposis coli-2. The SCF complex is indicated in blue.

Cullin	Adapter	Substrate recognition subunit	RING
CUL1	SKP1	F-Box protein	RBX1
CUL2	Elongin C/B	SOCS-box protein	RBX1
CUL3	BTB-domain protein		RBX1
CUL4A	DDB1	DCAF	RBX1
CUL4B	DDB1	DCAF	RBX1
CUL5	Elongin C/B	SOCS-box protein	RBX2
Atypical and Cullin-related ligases			
CUL7*	SKP1	FBXW8	RBX1
CUL9*/PARC	?	?	RBX1
APC2	?	CDC20 or CDH1	APC11

\*not conserved in nematodes

### 1.2.3 SCF E3-Ubiquitin Ligase Complexes

SCF complexes are assembled on a CUL1 scaffold that bridges the two essential biochemical functions (Figure 5): the CUL1 C-terminus binds the small RING domain protein RBX1 that recruits the E2 enzyme, while the N-terminus is linked to the F-box protein through a SKP1 adapter. In humans there is only one adapter protein, SKP-1, whereas the *C. elegans* genome encodes 21 *skp-1* related genes (*skr*) (Yamanaka et al., 2002). Eight of the *skr* genes were found to interact with *C. elegans cul-1*, of which *skr-1* and -2 show the closest homology to human SKP-1 (Yamanaka et al., 2002; Nayak et al., 2002). Importantly, target specificity of SCF complexes is ensured by the F-box protein, which functions as SRS that directly binds the substrate (Skowyra et al., 1997).

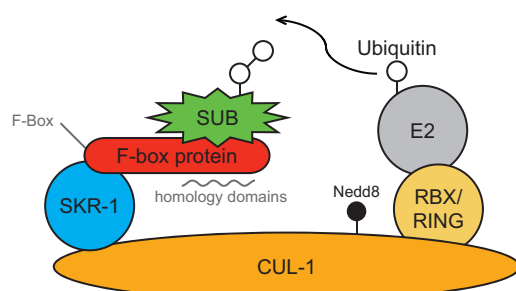


**Figure 5 Schematic Structure of SCF E3-Ubiquitin Ligase Complexes**

Schematic representation of a CUL1-based SCF E3-ubiquitin ligase complex: E2 enzyme and substrate (SUB) get closely linked to facilitate ubiquitin transfer. A ring finger containing protein (e.g. RBX1) recruits the E2 enzymes, while the F-box protein binds the substrate. SKR1 functions as adapter to attach the F-box protein to the CUL1 core scaffold. Neddylolation of the Cullin base increases SCF complex activity.

In addition to their substrate specificity, CLRs are themselves regulated in abundance and activity: First, multiple SCF complexes have been shown to have autocatalytic ubiquitination activity targeting the F-box protein for degradation, in particular in the absence of substrates, which can have shielding function (Yen and Elledge, 2008; Galan and Peter, 1999; Li et al., 2004). Second, SCF complexes and most other CRLs (except for CUL7-based) can be activated by neddylation, whereby the small ubiquitin-like protein Nedd8 gets covalently linked to a specific Lys residue of the Cullin scaffold itself (Hori et al., 1999; Pan et al., 2004). This modification induces a conformational change that brings the E2 enzyme in closer proximity to the F-box protein-bound substrate and thus facilitates the ubiquitin transfer (Duda et al., 2008). Like ubiquitination, neddylation is catalyzed by an enzymatic triad, whereby Cullin functions as its own E3 ligase (Kamura et al., 1999). Nedd8 can be removed from Cullins via the COP9 signalosome, a large multisubunit complex (Cope and Deshaies, 2003). Third, the conserved Cullin-associated and neddylation-dissociated protein-1 (CAND1) can bind unneddylated Cullins by competing with the adapter/SRS to sequester the complex in an inactive and disassembled state (Liu et al., 2002; Zheng et al., 2002). Cycles of SCF complex assembly and disassembly can prevent autoubiquitination of the F-box protein and enable binding of alternative SRS to the core scaffold (Pierce et al., 2013). Thus, neddylation and deneddylation act in concert with CAND1 to modulate SCF complex specificity and activity. Finally, additional levels of SCF complex regulation have more recently been uncovered, including allosteric regulation by small molecules, inhibition by pseudosubstrates, and substrate competition (Deshaies and Joazeiro, 2009).

#### **1.2.4 F-box Proteins – the Key to Substrate Recognition**

F-box proteins function as the substrate-recognition components of SCF complexes, thus conferring substrate-specificity to the UPS. Across species, a variety of F-box proteins can bind to the core SCF scaffold, each targeting multiple substrates, thus enabling SCF complexes to specifically label hundreds of proteins for subsequent degradation (Jin et al., 2004; Skaar et al., 2009a; 2009b). The human genome encodes ‘only’ 69 F-box proteins, whereas the number of predicted F-box proteins in the nematode exceeds 500 (Skaar et al., 2009b; Thomas, 2006). However only a handful of *C. elegans* F-box proteins are conserved across all major taxa (Table 3). The F-box domain describes a conserved 40 amino acid stretch that was termed after its presence in cyclin F/FBXO1 and that mediates binding to the SKP1 adapter and therefore the core scaffold (Bai et al., 1996). F-box proteins can be categorized into three classes depending on the presence of homology domains besides the F-

box (Jin et al., 2004): FBXW proteins contain WD40 repeats (12 members in humans), FBXL proteins contain Leu-rich repeats (21 members in humans), and all other F-box proteins are referred to as F-box only (FBXO). However, FBXO proteins also contain conserved recognizable domains that they do not share with multiple other F-box proteins, but which have been shown to be involved in direct substrate binding (D'Angiolella et al., 2012; Duan et al., 2012). Therefore the term FBXO more recently refers to F-box and other domains.

In response to certain triggers, for example during cell cycle coordination, F-box proteins must rapidly and specifically bind their target to promote its ubiquitination. Thereby substrate recognition generally requires prior post-translational modification of the target, which makes substrate recruitment the ultimate regulatory level of SCF complex-mediated ubiquitination. In the canonical model F-box proteins have a high affinity for short, defined degradation motifs termed degrons, predominantly when they are phosphorylated (phosphodegrons) (Ravid and Hochstrasser, 2008). Prime examples include  $\beta$ -TRCP/FBXW1 and FBXW7, which recognize specific phosphodegrons of their targets through the WD40 repeats (Wu et al., 2003; Hao et al., 2007). Besides phosphodegrons multiple regulatory mechanisms of substrate-recognition have emerged: F-box proteins can bind unmodified degrons, glycosylated degrons, require cofactors or small molecules for degron binding, or even detect larger domain structures (Skaar et al., 2013). Together with the regulation of the SCF core scaffold described above, substrate recruitment confers temporal and context-dependent specificity to SCF-complex mediated protein degradation.

Physiologically, F-box protein-substrate modules affect a wide range of cellular processes in health and disease states, including cell death and survival, cell differentiation as well as developmental timing (Skaar et al., 2013). However F-box proteins are predominantly studied in the context of cell proliferation, as they target multiple cell cycle regulators. Not surprisingly dysregulation of F-box proteins such as truncation or hyperactivation has been closely linked to the onset of tumorigenesis by aberrantly modulating levels of substrates with oncogenic or tumor suppressive activity. Examples include  $\beta$ -TRCP, FBXL7, and SKP2. The latter is an oncogene that when overexpressed degrades the CDK inhibitor and tumor suppressor p27/Kip1. In contrast FBXL7 is found to be inactivated in numerous tumor tissues (Welcker and Clurman, 2008; Frescas and Pagano, 2008). In addition to their key role in tumorigenesis, F-box proteins such as  $\beta$ -TRCP, FBXL3, and FBXL21 govern circadian rhythms by degrading PER1 and 2 as well as CRY1 and 2, which constitute major regulators

of the core circadian clock system (Busino et al., 2007; Yoo et al., 2013; Shirogane et al., 2005).

In *C. elegans* only a few F-box proteins have been carefully investigated, which led to the discovery of several conserved F-box protein-substrate modules (Table 3). Most conserved F-box proteins, including *mec-15*/FBXW9, *sel-10*/FBXW7, *lin-23*/β-TRCP, and *fsn-1*/FBXO45 contribute to the regulation of axon guidance and synapsis dynamics in the nematode (Ding et al., 2007; Sun et al., 2013; Liao et al., 2004; Mehta et al., 2004; Segref and Hoppe, 2009). Furthermore, *lin-23* was shown to affect cell cycle progression, while *fsn-1* regulates germ cell apoptosis through CEP-1/p53 (Kipreos et al., 2000; Gao et al., 2008). Taken together, these findings highlight the diversity of F-box protein regulated processes across species and exemplifies their context and time-specific mode of action. However, although multiple orphan F-box proteins have been associated with biological processes particularly in disease states, their cognate proteolytic substrate remain elusive.

**Table 3: Conserved *C. elegans* F-box Proteins and Substrates Identified**

Conserved *C. elegans* F-box proteins and identified substrates are shown. Substrates depicted in grey yet require additional experimental evidence. If conserved, also confirmed mammalian substrates are listed. For additional mammalian substrates see (Skaar et al., 2009b). References: **1** Jin et al., 2004; **2** Thomas et al., 2006; **3** Shaye et al., 2011

<b><i>C. elegans</i> gene</b>	<b>Substrates (<i>C. elegans</i>)</b>	<b>Closest human homolog</b>	<b>Selected substrates (mammals)</b>
C10E2.2		(FBXO30, FBXO40) <sup>3</sup>	
T28B11.1		ZCCHC10 <sup>2</sup>	
<i>mec-15</i>		FBXW9 <sup>1,2,3</sup>	
<i>dre-1</i>	CED-9/BCL2 (Chiorazzi et al., 2013)	FBXO11 <sup>1,2,3</sup>	BCL2 (Chiorazzi et al., 2013)
<i>sel-10</i>	LIN-12/Notch (Hubbard et al., 1997); LIN-45/BRAF (la Cova and Greenwald, 2012)	FBXW7 <sup>1,2,3</sup>	Notch1 (Tsunematsu et al., 2004)
<i>lin-23</i>	BAR-1/β-Catenin (Dreier et al., 2005)	(β-TRCP, FBXW11) <sup>1,2</sup>	β-Catenin (Latres et al., 1999)
<i>skpt-1</i>		SKP2 <sup>2,3</sup>	
T28B4.1 ( <i>skpt-1</i> paralog)		SKP2 <sup>2</sup>	
C02F5.7		FBXL2 <sup>1,2,3</sup>	
C14B1.3		(NCCRP1, FBXO10, FBXO27, FBXO2, FBXO44, FBXO6) <sup>1,2</sup>	
<i>fsn-1</i>	SCD-1/ALK (Liao et al., 2004) CEP-1/p53 (Gao et al., 2008)	FBXO45 <sup>2,3</sup>	p73 (Peschiaroli et al., 2009)
<i>mfb-1</i> <sup>1,2,3</sup>		(FBXO25, FBXO32) <sup>1,2,3</sup>	

### 1.2.5 F-box Protein-Substrate Pair Identification

In the 15 years of research on SCF complexes more than 100 substrates have been identified by distinct experimental approaches. However, many studies demonstrated that the F-box protein-substrate interaction is very transient and target identification still remains one of the most important challenges in the SCF complex field.

The combination of a wealth of genetic and biochemical approaches in yeast led to the discovery of the first SCF<sup>CDC4/FBXW7</sup> complex including the associated E2 ligase and the first substrate Sic1/p27Kip1 (Willems et al., 1996; Bai et al., 1996; Skowyra et al., 1997; Feldman et al., 1997; Mathias et al., 1996). Typically, involvement of an SCF complex in the turnover of an unstable protein was examined genetically, by either using temperature-sensitive SCF-complex mutants, RNAi/shRNA depletion, or by overexpressing a dominant negative form of CUL1 (DN-CUL1) (Koepp et al., 2001; Donzelli et al., 2002; Jin et al., 2005). DN-CUL1 lacks the C-terminus and thus the ability to recruit the E2 ligase, but retains its interaction with the SKP1 adapter, ultimately stabilizing the target protein (Jin et al., 2005). Biochemical approaches using libraries of F-box expression constructs in yeast two-hybrid systems were generally applied to identify the cognate F-box protein (Drury et al., 1997; Thomas et al., 1995). In these assays, F-box deletion mutants have been successfully used to identify binding partners as they sequester the target protein from the degradation machinery (Margottin et al., 1998). Also in *C. elegans* a genetic approach based on an EMS mutagenesis screen for reversion of *sel-10*//*FBXW7* egg-laying defects resulted in the discovery of a highly conserved F-box substrate *lin-12*/Notch (Hubbard et al., 1997; Sundaram and Greenwald, 1993). More recently, GFP fusion libraries allowed an unbiased approach to identify mammalian F-box substrates by expressing a library of ORFs fused to GFP in a wild type and F-box mutant background screening for GFP accumulation (Benanti et al., 2007; Yen and Elledge, 2008). Pagano's group modified a conventional pull-down assay by adding ubiquitin conjugating components and tagged-ubiquitin to immunopurified SCF complexes to then recover proteins that incorporated the tagged ubiquitin and identify them by mass spectrometry (Peschiaroli et al., 2006). Still today F-box protein purification followed by mass spectrometry combined with the use of DN-CUL-1, proteasome inhibition, or F-box deletion mutants is the standard technique to identify F-box substrates, but it remains a challenging task.

## 1.3 DRE-1/FBXO11 – Connecting Selective Degradation to Developmental Timing Control

### 1.3.1 DRE-1

*dre-1* encodes one of a handful of *C. elegans* F-box proteins that are conserved across all major taxa (Table 3) and it was shown to function in a SCF E3-ubiquitin ligase complex (Fielenbach et al., 2007; Shaye and Greenwald, 2011). Besides the N-terminal F-box domain DRE-1 contains no WD40 or Leu-rich domains, but three CASH (carbohydrate binding and sugar hydrolysis) domains situated in a region of 18 predicted  $\beta$ -sheets (Figure 6). Furthermore, this region is predicted to harbor protein arginine methyl transferase activity, although this could not be confirmed experimentally (Cook et al., 2006; Fielenbach et al., 2007). Finally, at the C-terminus DRE-1 contains a zinc-finger motif homologous to ZnF-UBR, which is associated with the N-end rule of substrate recognition (Figure 6) (Kwon et al., 1998; Tasaki et al., 2005). Thereby a proteins half-life was found to be dependent on the N-terminal amino acid, which can induce UPS-dependent protein degradation after its detection by N-recognins (Bartel et al., 1990; Bachmair et al., 1986; Dougan et al., 2012).

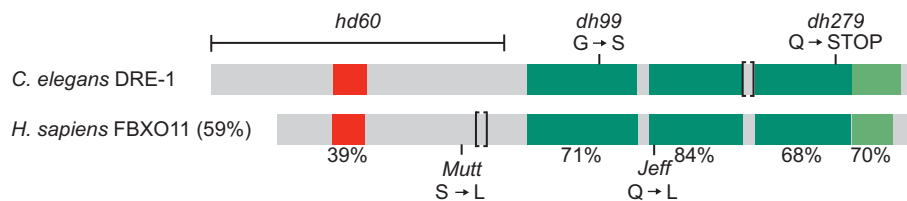


**Figure 6: DRE-1 Protein is Evolutionary Conserved**

Domain structure, mutations and multiple sequence alignment of *C. elegans* DRE-1 and human FBXO11 showing sequence similarity of homologous domains. F-box domain, red; carbohydrate binding and sugar hydrolysis (CASH) domains, dark green; zinc finger, light green. *C. elegans* DRE-1 (NP\_504661); *Homo sapiens* FBXO11 (NP\_079409). Figure modified from (Fielenbach et al., 2007).

*dre-1* was identified in a *daf-12(rh61rh411)* null mutant enhancer screen for *daf-12* redundant functions in gonadal heterochrony (Fielenbach et al., 2007). As mentioned above, *daf-12(rh61rh411)* null mutants show a near WT-like gonad migration pattern, while *daf-12(rh61)* LBD mutants display strong gonadal migration defects, pointing toward potential *daf-12* coactivators to act redundantly with *daf-12* in gonadal heterochrony (Antebi et al., 1998; 2000). *dre-1(dh99);daf-12(rh61rh411)* double mutants, but neither single mutant, give rise to a penetrant synthetic gonadal migration defect (Fielenbach et al., 2007). Similarly *dre-1;lin-29* and *daf-12;lin-29* mutants unveil a strong synthetic migration defect, in which both gonadal arms fail to reflex (Fielenbach et al., 2007). The unreflexed phenotype is interpreted

as a repetition of L2-specific gonadal programs with concomitant prevention of L3-programs and indicates a global redundant function of *dre-1* in gonadal heterochrony.

On their own, *dre-1* hypomorphic mutants also display heterochronic phenotypes in epidermal tissue: seam cells fuse and form adult alae precociously in L3 larvae, a full stage ahead of schedule, suggesting that *dre-1(+)* specifies late larval programs (Fielenbach et al., 2007). Conversely a subset of seam cells display adult alae gaps, which have been reported in various retarded heterochronic mutants (Slack et al., 2000). As both precocious and retarded phenotypes of *dre-1* hypomorphic mutants are not fully penetrant, *dre-1* is assigned a modulatory function at the larval-to-adult transition in the epidermis. This was supported by genetic epistasis experiments, which place *dre-1* upstream of *lin-29* and downstream or parallel to the *let-7* microRNA (Fielenbach et al., 2007). Interestingly, *dre-1* null mutants fail to hatch or arrest in the L1 stage, often displaying molting defects, which places *dre-1* in line with *lin-42/Period* and *nhr-25/SF1* as regulators of both developmental timing and the molt cycle (Fielenbach et al., 2007). Consistent with its diverse phenotypes, *dre-1* is expressed throughout development in a variety of tissues including hypodermis and epidermal seams, dtcs, the anchor cell, and multiple neurons in head, tail, ventral cord and periphery (Fielenbach et al., 2007). More recently, *dre-1* was shown to be expressed in the tail-spike cell and required for its programmed death several hours after birth (Chiorazzi et al., 2013; Sulston et al., 1983). Here, *dre-1* functions through *ced-9/BCL2*, presumably by directly regulating its protein turnover (Chiorazzi et al., 2013). However, the *dre-1* substrate(s) regulating *C. elegans* developmental timing and molting still remain to be elucidated.

### 1.3.2 FBXO11

*C. elegans dre-1* shares 59% sequence homology with its human homolog FBXO11 (Figure 6). In mice, FBXO11 protein is detected from embryonic day 9.5 and expressed in a wide range of tissues during development such as heart, muscle, liver, lung, palatal epithelia, adrenal gland, kidney, osteoblasts, spleen, bone marrow, hematopoietic cells, skin, and the middle ear (Hardisty-Hughes et al., 2006). Homozygous mutation of *Fbxo11* results in facial clefting, cleft palate defects, and perinatal lethality as observed in *Mutt* and *Jeff* mutant mice, which were identified in ENU mutagenesis screens for deafness (Hardisty et al., 2003; Hardisty-Hughes et al., 2006). Furthermore, FBXO11 haploinsufficient mice develop chronic otitis media, an inflammation of the middle ear that affects about 15% of young children (Bluestone and Klein, 2001; Hardisty-Hughes et al., 2006). Interestingly, also in humans FBXO11 SNPs have been correlated with the onset of this hearing impairment (Segade et al.,

2006; Rye et al., 2011). Finally, FBXO11 loss of function contributes to the pathogenesis of diffuse large B cell lymphomas and FBXO11 mutations are frequently found in other cancers, such as colon, neck, ovary, lung, and head tumors (Richter et al., 2012; Yoshida et al., 2011; Stransky et al., 2011; Kan et al., 2010). In particular, FBXO11 functions as tumor suppressor in B cells by controlling the stability of the oncoprotein BCL6, which was the first FBXO11 substrate to be identified (Duan et al., 2012). However, the substrate(s) causative for developmental alterations in *Fbxo11* mutants have yet remained entirely elusive.

## 1.4 Aim of Thesis

Developmental progression is orchestrated by the collective action of microRNAs, transcriptional, translational, and post-translational regulators that integrate environmental cues and translate them into molecular traits. In *C. elegans*, these temporal selectors are termed heterochronic genes and they time cellular fates in a highly tissue-specific manner. In particular in epidermal seam cells three microRNA-mediated switches regulate developmental progression, which are largely regulated by food availability and general environmental conditions in part transduced through the nuclear hormone receptor DAF-12. Originally identified as *daf-12* enhancer in gonadal heterochrony, the highly conserved F-box protein DRE-1 was shown to regulate the larval-to-adult transition in the epidermis (Fielenbach et al., 2007). F-box proteins function as substrate-recognition components of SCF E3-ubiquitin ligase complexes, thus conferring substrate specificity to the UPS. Interestingly, also the mammalian homolog of DRE-1, FBXO11 has been linked to developmental alterations in mice and men, including facial clefting and otitis media. Moreover, it was recently shown to be a tumor suppressor by controlling BCL6 turnover in lymphocytes. Despite extensive research on the about 70 SCF complexes in humans, many F-box proteins remain orphan receptors or the discovered targets cannot fully explain their cellular and organism-wide functions. The temporal control of protein abundance and activity is largely mediated by the UPS and naturally essential for the control of developmental progression. In particular oscillating or transiently peaking proteins underlie a quick and precise degradation process. Two of the over 30 heterochronic genes, LIN-41 and DRE-1 encode proteins that harbor ubiquitin ligase activity. However, besides controversial work on mammalian LIN-41, which might target mammalian Argonaute proteins, the cognate substrates regulating developmental timing and cellular differentiation remain largely elusive.

During my doctorate I aimed to identify novel substrate(s) of the SCF<sup>DRE-1/FBXO11</sup> complex that coordinate developmental progression to shed light on the mechanisms of post-translational control of biological timing. I expected to find heterochronic genes that, if unknown, would be characterized with regard to their function in *C. elegans* maturation to further deepen our understanding of regulatory developmental timing circuits

## **Chapter 2 - RESULTS**

In parallel and simultaneous approaches, the group of Michele Pagano and our group identified two conserved substrates of the SCF<sup>DRE-1/FBXO11</sup> E3-ubiquitin ligase complex, CDT2 and BLMP-1.

## 2.1 CDT2 – a Cell Cycle Regulator Targeted by DRE-1/FBXO11

### 2.1.1 Identification of CDT2 as FBXO11 Substrate by the Pagano

#### Laboratory

After identification of the first FBXO11 substrate BCL6 (Duan et al., 2012), Pagano and coworkers aimed to identify novel substrates of FBXO11 in an unbiased fashion to further elucidate its physiological functions. Therefore, they expressed FLAG-HA-tagged FBXO11 or a tagged version of the paralog FBXO10 as control in HEK293T cells and stabilized potential substrates by either coexpressing a DN-CUL1(1-385) or by inhibiting the proteasome (Rossi et al., 2013). Immunopurified SCF complexes were analyzed by multidimensional protein identification technology (MudPIT) (Florens and Washburn, 2006). CDT2 peptides were present specifically in the FBXO11 purifications that were treated with DN-CUL1 or proteasome inhibitor (Rossi et al., 2013). Likewise, in a parallel approach using siRNA-based screening, the Dutta group found FBXO11 to be a major regulator of CDT2 stability (Abbas et al., 2013a).

CDT2 (Cdc10-dependent transcript 2) encodes a highly conserved DBB1 (DNA damage-binding protein 1) and CUL4 associated protein that functions as substrate recognition component of a CUL4A-based CRL. CRL4<sup>CDT2</sup> has been shown to be a major regulator of cell cycle progression and the DNA-repair machinery by targeting the replication initiation factor CDT1 (Cdc10-dependent transcript 1), the CDK inhibitor p21, and the histone 4 methyltransferase (H4K20) Set8 for proteasomal degradation (Abbas et al., 2010; Abbas and Dutta, 2011; Terai et al., 2010; Abbas et al., 2008; Centore et al., 2010; Kim et al., 2008; Jørgensen et al., 2011). In particular, CRL4<sup>CDT2</sup> ubiquitinates its targets during S phase and in response to DNA damage in a PCNA-dependent manner to promote cell cycle progression, prevent aberrant re-replication, and induce DNA repair mechanisms (Abbas and Dutta, 2011). As described above, SRS stability of E3 ligases is frequently controlled by autoubiquitination (Galan and Peter, 1999; Yen and Elledge, 2008), which was recently also demonstrated for CDT2 (Abbas et al., 2013a). However, through extensive biochemical analysis, both Rossi et

al. and Abbas et al. independently showed CDT2 stability to be additionally controlled by the SCF<sup>FBXO11</sup> complex (Figure 7) (Rossi et al., 2013; Abbas et al., 2013a). Interestingly, Pagano and colleagues found CDK-mediated Thr464 phosphorylation of CDT2 in proliferating cells to prevent FBXO11-dependent CDT2 ubiquitination and degradation (Rossi et al., 2013). This finding is in contrast to the paradigm of phosphorylation-dependent substrate recognition by F-box proteins and describes a novel mechanism of substrate recruitment to SCF-complexes (Skaar et al., 2013). Physiologically, serum starvation or TGF- $\beta$  treatment inhibits CDKs and promotes exit from the cell cycle via FBXO11-dependent degradation of then unphosphorylated CDT2. Consistently, FBXO11 depletion delays cell cycle exit through stabilized CDT2 (Figure 7) (Rossi et al., 2013). Furthermore, FBXO11 restrains TGF- $\beta$  responses within a cell via CDT2 degradation and stabilization of its target Set8, which in turn prevents accumulation of the TGF- $\beta$  downstream effector PhosphoSMAD2 by an unknown mechanism (Figure 7) (Abbas et al., 2013a; 2013b). Consistently, PhosphoSMAD2 levels have been found to be aberrantly elevated in epithelia of homozygous *Fbxo11* *Jeff* mutant mice (Tateossian et al., 2009).

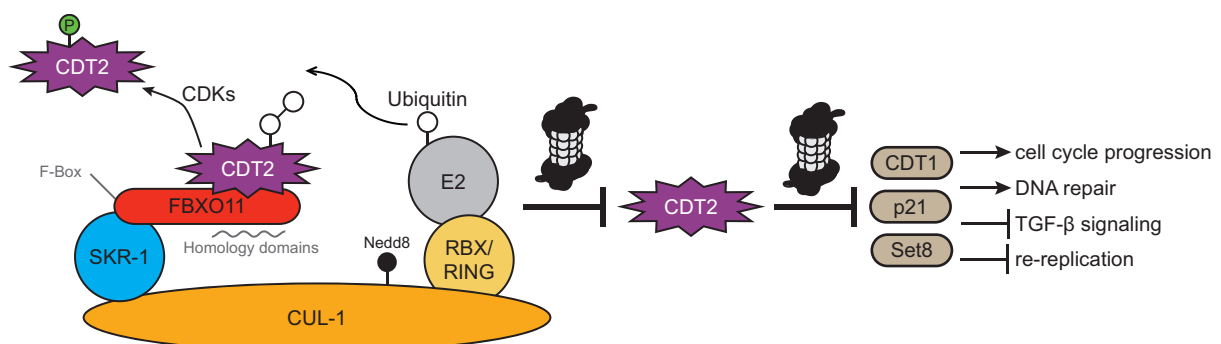


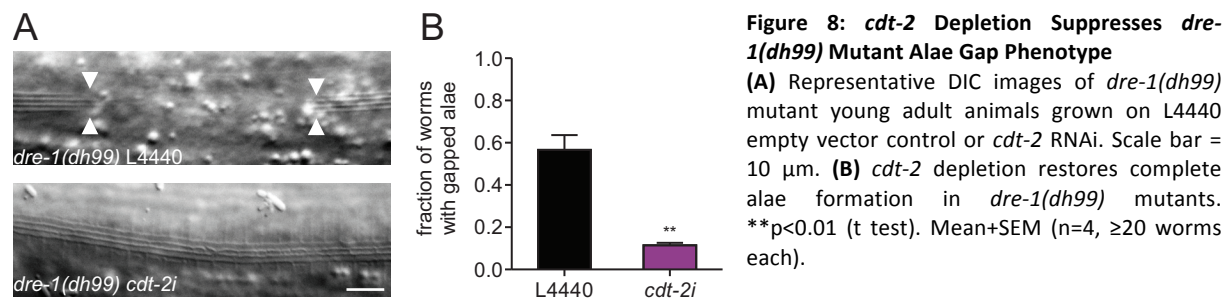
**Figure 7: FBXO11 Regulates CDT2-Dependent Processes by Controlling its Turnover**

Model of FBXO11/CDT2 function in mammals: FBXO11 triggers CDT2 degradation via the proteasome and thus interferes with CDT2-dependent processes such as cell cycle progression, TGF- $\beta$  signaling, and DNA repair mechanisms. Notably CDT2 itself is part of a CRL complex and controls the proteasomal turnover of multiple substrates including Set8, CDT1 and p21, which are key mediators of CDT2-dependent processes. CDT2 phosphorylation by cyclin-dependent kinases (CDKs) prevents the CDT2-FBXO11 interaction and stabilizes CDT2.

### 2.1.2 *dre-1* and *cdt-2* Genetically Interact in *C. elegans*

Since both FBXO11 and CDT2 are highly conserved in *C. elegans*, and also their physical association was shown to be conserved (Rossi et al., 2013), I used *C. elegans* as a model to validate some of the major findings *in vivo*. During terminal differentiation *C. elegans* seam cells fuse, exit the cell cycle, and synthesize a continuous cuticular structure called adult alae. *dre-1* mutants show various alterations in seam cell fates including precocious seam cell fusion and gaps in the adult alae. The latter have been reported in a variety of retarded

heterochronic mutants, such as *let-7*, where individual cells fail to exit the cell cycle (Slack et al., 2000). Furthermore, *dre-1;daf-12* mutants exhibit a synthetic gonadal migration defect in which both dtcs fail to reflex and continue migrating straight into head and tail (Fielenbach et al., 2007). Given that DRE-1 functions as substrate recognition component of a SCF complex, we hypothesized elevated substrate levels to cause *dre-1* mutant developmental alterations. If CDT-2 were a cognate substrate, its depletion should ameliorate such phenotypes.



Knockdown of *cdt-2* by RNAi was confirmed by qRT-PCR and by a significant increase in nuclei size of blast cells, such as the seams (Kim et al., 2008). Importantly, *cdt-2* depletion strikingly reduced the appearance of gaps in the adult alae of *dre-1(dh99)* mutants from 56% to 13% (Figure 8). Surprisingly, the precocious seam cell fusion, as well as the synthetic gonadal migration defects of *dre-1* mutants were fully *cdt-2* independent (Figure 9), indicating that *dre-1* and *cdt-2* only interact for the process of adult alae formation. On its own, *cdt-2* depletion did not show overt heterochronic phenotypes in the seam or gonad.

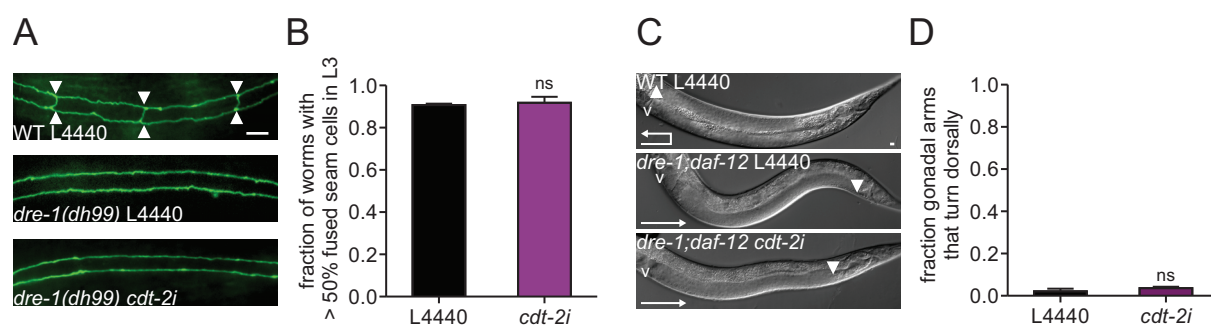


**Figure 9: *cdt-2* Depletion does not Affect Related *dre-1* Mutant Phenotypes**

**(A)** Representative fluorescence images of seam cell adherence junctions as visualized by *ajm-1::gfp* in WT and *dre-1(dh99)* L3 larvae grown on L4440 empty vector control or *cdt-2* RNAi. Arrowheads indicate seam-seam boundaries. **(B)** *cdt-2* depletion does not affect *dre-1(dh99)* mutant precocious seam cell fusion in L3 larvae. Mean+SEM (n=3,  $\geq 20$  worms each). **(C)** Representative DIC images of WT and *dre-1(dh99);daf-12(rh61rh411)* young adult worms grown on L4440 empty vector control or *cdt-2* RNAi, showing one gonadal arm. Arrowheads indicate position of the dtc. v = vulva. **(D)** *cdt-2* depletion does not suppress *dre-1(dh99);daf-12(rh61rh411)* gonadal migration defects. Mean+SEM (n=3,  $\geq 40$  gonadal arms each).

To further investigate the cellular fate underlying *cdt-2* dependent alae gap formation, I analyzed CKI-1::GFP expression in seam cells of *dre-1* mutant animals. *cki-1* encodes a

homolog of the mammalian cyclin-dependent kinase inhibitor p27/Kip1 that promotes cessation from the cell-cycle in *C. elegans* and that is highly expressed in arresting cells (Fukuyama et al., 2003; Hong et al., 1998). I followed CKI-1::GFP expression throughout larval development and found it to be strongly expressed in all seam cells of WT young adult worms right after cell cycle exit and adult alae synthesis. Conversely, CKI-1::GFP expression was not visible in the region of the alae gaps in *dre-1(dh99)* mutants ( $n>15$ ), although neighboring seam cells were strongly CKI-1::GFP positive (Figure 10). Next, I also analyzed CDT2 levels upon *dre-1* depletion using a full-length *cdt-2::gfp* fusion construct (Poulin and Ahringer, 2010). CDT-2::GFP was very dynamic in the seam and hypodermal cells peaking prior to cell divisions (data not shown). However, I could not observe increased accumulation or altered expression of CDT-2::GFP upon *dre-1* depletion by RNAi (data not shown). It is possible that changes in CDT-2 levels might only be observable during a narrow time window or there may be functional redundancy for CDT-2 turnover in *C. elegans*. Nevertheless, the observation of genetic suppression, and the coexpression of *dre-1* and *cdt-2* in the seams, argues for an important functional interaction.

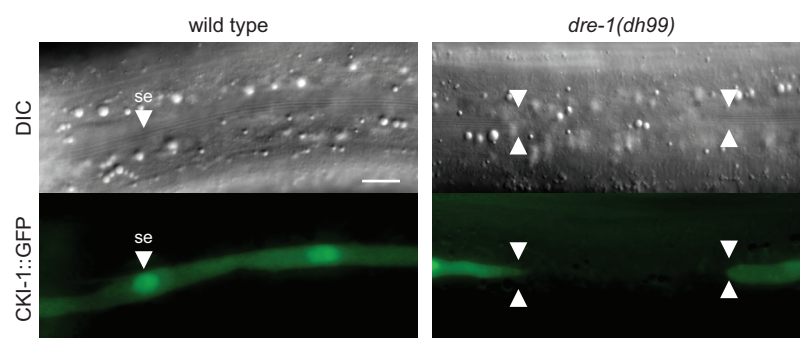


**Figure 10: CKI-1::GFP is Absent from Seam Cells Underneath the Alae Gaps**  
Representative DIC and fluorescence images of WT and *dre-1(dh99)* mutant young adult animals expressing CKI-1::GFP (*mals105*), a marker of arresting cells. Arrowheads indicate seam (se) nuclei (left panel) and the area of an alae gap (right panel). Scale bar = 10  $\mu$ m.

Taken together, my findings suggest that alae gaps in *dre-1* mutants could arise from a failure of cell cycle exit in seam cells, which might be induced by aberrantly regulated CDT-2 levels. The observed genetic interaction in *C. elegans* is consistent with the situation in mammals and supports the notion that FBXO11-mediated degradation of CDT2 controls cell cycle exit across species.

## 2.2 BLMP-1/BLIMP-1 - a Novel DRE-1/FBXO11 Target

### 2.2.1 *blmp-1* and *nhr-25* Suppress *dre-1* Epidermal Heterochrony

Similar to our genetic approach with the candidate interactor *cdt-2*, we reasoned that client substrates aberrantly accumulate in *dre-1* mutants and cause developmental timing alterations in epidermis and gonad. If so, then knockdown of such substrates should suppress *dre-1* mutant defects. Thus, I performed an RNAi-based suppressor screen in *dre-1(dh99)* hypomorphic mutants that was initially focused on transcription factors and a handful of heterochronic gene candidates. I identified the Zn-finger transcription factor BLMP-1 and the nuclear hormone receptor NHR-25 as potent suppressors of *dre-1* heterochronic phenotypes in the epidermis and therefore as potential substrate candidates.

The predicted *C. elegans* BLMP-1 protein contains an N-terminal SET domain, a proline rich domain, and 5 paired-domain Zn fingers at the C-terminus (Andersen and Horvitz, 2007; Tunyaplin et al., 2000). An existing deletion allele *tm548* lacks part of exon 3 leading to a frameshift that disrupts the SET domain and all subsequent Zn fingers, suggesting it is null. In a previously published genome-wide RNAi screen in *C. elegans*, *blmp-1* was found to affect male tail tip morphogenesis as its depletion results in precocious retraction of the male tail tip (Nelson et al., 2011). Moreover, *blmp-1* was shown to modulate adult lifespan and cuticle morphogenesis, but altogether its function in the nematode is poorly understood (Samuelson et al., 2007; Greer et al., 2010; Zhang et al., 2012). In contrast, mammalian BLIMP-1 is extensively studied in different cellular contexts: BLIMP1 is necessary and sufficient to drive terminal differentiation of B cells into antibody-secreting plasma cells and also governs various cell fate decisions, including primordial germ cell specification and skin differentiation, generally working as a transcriptional repressor (Horsley et al., 2006; Ohinata et al., 2005; Turner et al., 1994; Shapiro-Shelef et al., 2003). Importantly, *C. elegans* BLMP-1 and mammalian BLIMP-1 show striking domain conservation, with 43% similarity in the SET domain and 70% similarity in the Zn fingers (Tunyaplin et al., 2000).

I found both *blmp-1* and *nhr-25* loss of function to suppress *dre-1* phenotypes in the epidermis. In *dre-1* partial loss-of-function mutants, such as *dre-1(dh99)*, seam cells undergo precocious terminal differentiation in L3, a full stage ahead of schedule. Using the adherens junction marker *ajm-1:gfp*, I observed that RNAi-mediated knockdown of *blmp-1* reduced *dre-1(dh99)* precocious seam cell fusion from 90% to 15% of the animals (Figure 11).

Similarly, only 7.5% of *dre-1(dh99);blmp-1(tm548)* double mutant animals showed precocious seam cell fusion in L3 larvae (Figure 11).

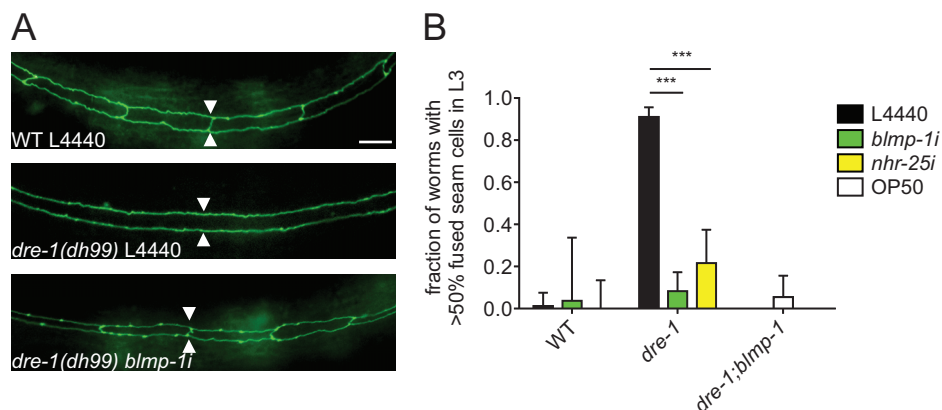


**Figure 11: *blmp-1* and *nhr-25* Suppress *dre-1(dh99)* Precocious Seam Cell Fusion**

**(A)** Representative fluorescence images of seam cell adherence junctions as visualized by *ajm-1::gfp* in WT and *dre-1(dh99)* L3 larvae grown on L4440 empty vector control or *blmp-1* RNAi. Arrowheads indicate seam-seam boundaries. Scale bar = 10  $\mu$ m. **(B)** *blmp-1* and *nhr-25* RNAi suppress *dre-1(dh99)* precocious seam cell fusion in L3 larvae. \*\*\* $p < 0.001$  (Fisher's exact). Mean+95%CI (n>30).

Notably, *blmp-1* mutants themselves displayed heterochronic phenotypes: Surprisingly they showed no alteration in seam cell division and fusion patterns (data not shown), but as reported previously in a different context, *blmp-1* mutants exhibited incomplete adult alae formation, a phenotype reminiscent of retarded mutants such as *let-7* (Figure 12) (Slack et al., 2000; Zhang et al., 2012). Notably, incomplete alae formation was rescued by introducing a fosmid-based *blmp-1::gfp* translational fusion construct (*wgIs109*, (Sarov et al., 2012)), demonstrating that the phenotype arises from lesions in *blmp-1* (Figure 12B). Of note, the poor alae formation phenotype precluded the analysis of *dre-1* mutant alae gap appearance upon *blmp-1* knockdown.

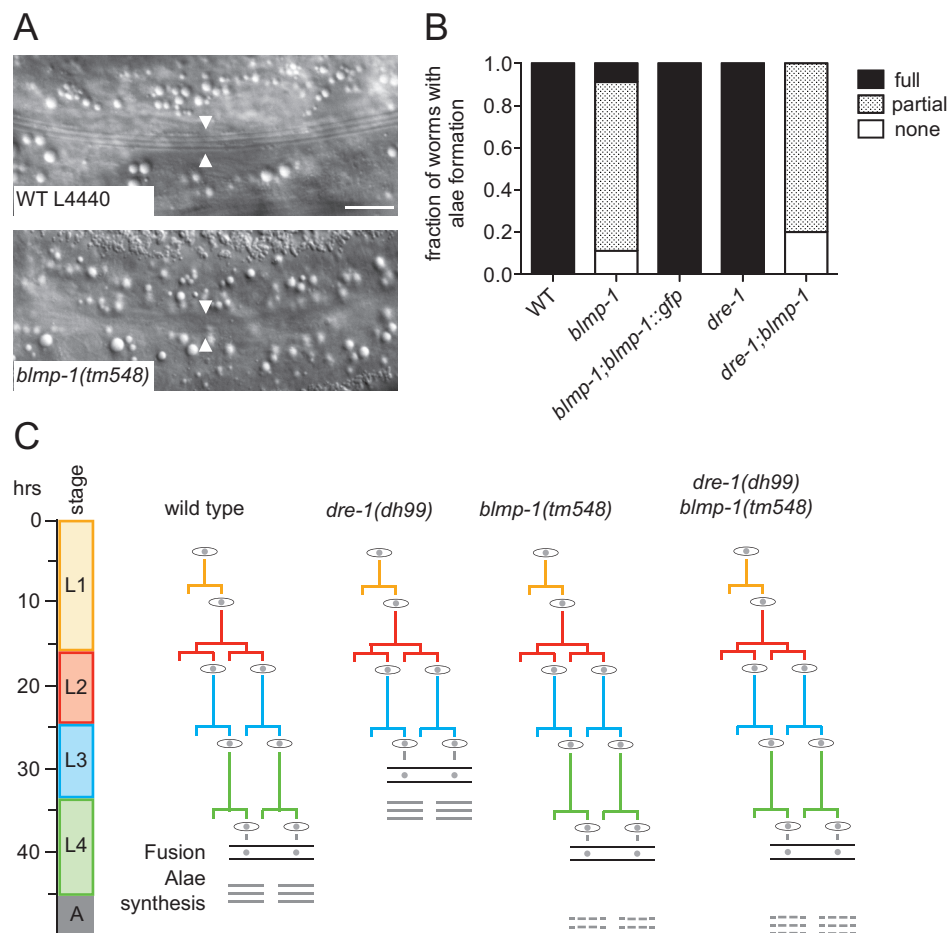


**Figure 12: *blmp-1* Promotes Terminal Differentiation in the Hypodermis**

(A) Representative DIC images of young adult WT and *blmp-1(tm548)* mutant worms. Arrowheads indicate seam cell positions, the origin of adult alae synthesis. (B) *blmp-1(tm548)* and *dre-1(dh99);blmp-1(tm548)* mutants show poor formation of adult alae ( $n > 20$ ). (C) Seam cell lineages (V1-V4, V6) from WT worms and various mutants as inferred from inspection. Terminal differentiation is indicated by fusion of the seams (eye-shaped cells) and adult alae formation (three horizontal bars). *dre-1* mutants exhibit precocious seam cell terminal differentiation, whereas *blmp-1* and the double mutants show incomplete formation of adult alae (three dashed horizontal bars).

Besides *blmp-1*, also knockdown of the nuclear hormone receptor *nhr-25* using RNAi substantially reduced *dre-1* precocious seam cell fusion from 90% to 21.5% of the animals (Figure 11B). Of note, *nhr-25* depletion reportedly induces retarded seam cell fusion in WT worms and prevents precocious adult alae formation in several precocious mutants (Hada et al., 2010). Taken together, complete terminal differentiation of epidermal stem cells depends on both *blmp-1* and *nhr-25* and both transcriptional regulators constitute potential targets of the SCF<sup>DRE-1</sup> ubiquitin ligase.

### 2.2.2 *blmp-1* Suppresses *dre-1* Gonadal Heterochrony

We next asked whether *blmp-1* and *nhr-25* also influenced *dre-1* developmental timing phenotypes in the gonad. In WT hermaphrodites, dtcs guide gonadal migration to form two U-shaped gonadal arms in adult animals. Whereas *dre-1* mutants on their own show only a

weak retarded gonadal migration phenotype, combinations with other heterochronic loci, such as *daf-12*/FXR/LXR/VDR or the *lin-29*/EGR null mutants, unveil a strong synthetic retarded phenotype in which both gonadal arms entirely fail to reflex (mig).

Strikingly, RNAi-mediated depletion of *blmp-1* suppressed the strong retarded phenotype of *dre-1(dh99);daf-12(rh61rh411)* mutants, restoring the dorsal turn in more than 80% of the animals (Figure 13). In contrast, *nhr-25* knockdown failed to ameliorate the gonadal migration defect (Figure 13B). To investigate specificity of *blmp-1*-mediated mig suppression, the effect of *blmp-1* reduction was analyzed in related mig mutants. *blmp-1* depletion also restored gonadal reflection in *dre-1(dh99);lin-29(n546)* mutants, whereas gonadal migration defects in *daf-12(rh61rh411);lin-29(n546)* and the strong heterochronic *daf-12* allele *rh61* remained unaffected (Figure 13B). These observations reveal that *blmp-1* depletion specifically suppresses gonadal heterochronic phenotypes arising from *dre-1*, and not *daf-12* or *lin-29* lesions, again suggesting that *dre-1* and *blmp-1* work in a unified pathway.

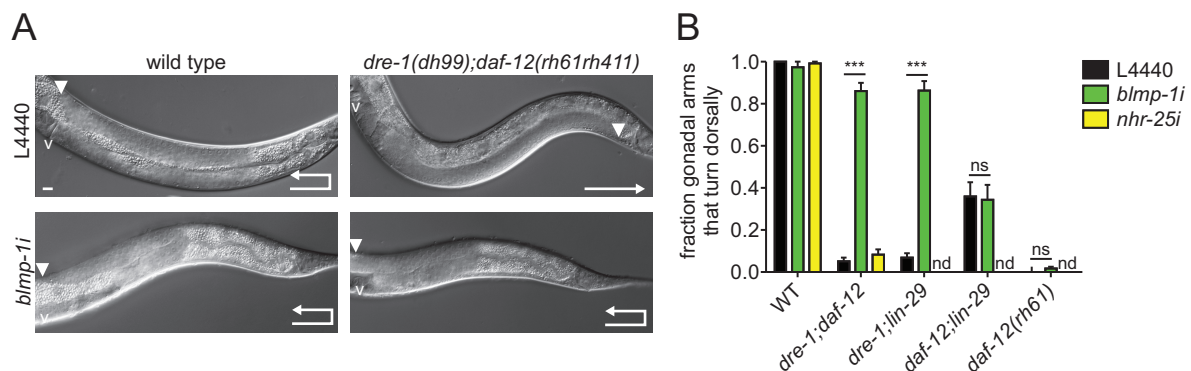


**Figure 13: *blmp-1*, but not *nhr-25* Depletion Specifically Suppresses *dre-1* Synthetic Gonadal Migration Defects**

(A) Representative DIC images of WT and *dre-1(dh99);daf-12(rh61rh411)* young adult worms grown on L4440 empty vector control or *blmp-1* RNAi, respectively, showing one gonadal arm each. Arrowheads indicate position of the dtc. v = vulva. Scale bar = 10  $\mu$ m. (B) *blmp-1* depletion specifically suppresses gonadal migration defects of *dre-1(dh99);daf-12(rh61rh411)* and *dre-1(dh99);lin-29(n546)* mutants, but does not affect *daf-12(rh61rh411);lin-29(n546)* and the strong heterochronic *daf-12* allele *rh61*. \*\*\* $p < 0.001$  (ANOVA). Mean+SEM (n=3, 40 gonadal arms each).

To test whether *blmp-1* regulates WT gonadal morphogenesis I analyzed dtc migration in *blmp-1(tm548)* mutant animals. Consistent with a role in gonadal developmental timing, *blmp-1* mutants showed precocious gonadal migration: dtcs navigated the first turn dorsally 2-3 hours ahead of schedule, but often failed the second turn and continued migration toward head and tail (Figure 14). Again, these phenotypes were rescued by the full-length *blmp-1::gfp* transgene (Figure 14B). Notably, *blmp-1(lf)* early gonadal migration defects prevailed in *dre-1(dh99);daf-12(rh61rh411)* mutants grown on *blmp-1* RNAi, consistent with *blmp-1* acting downstream of *dre-1* (Figure 14B and 14C).

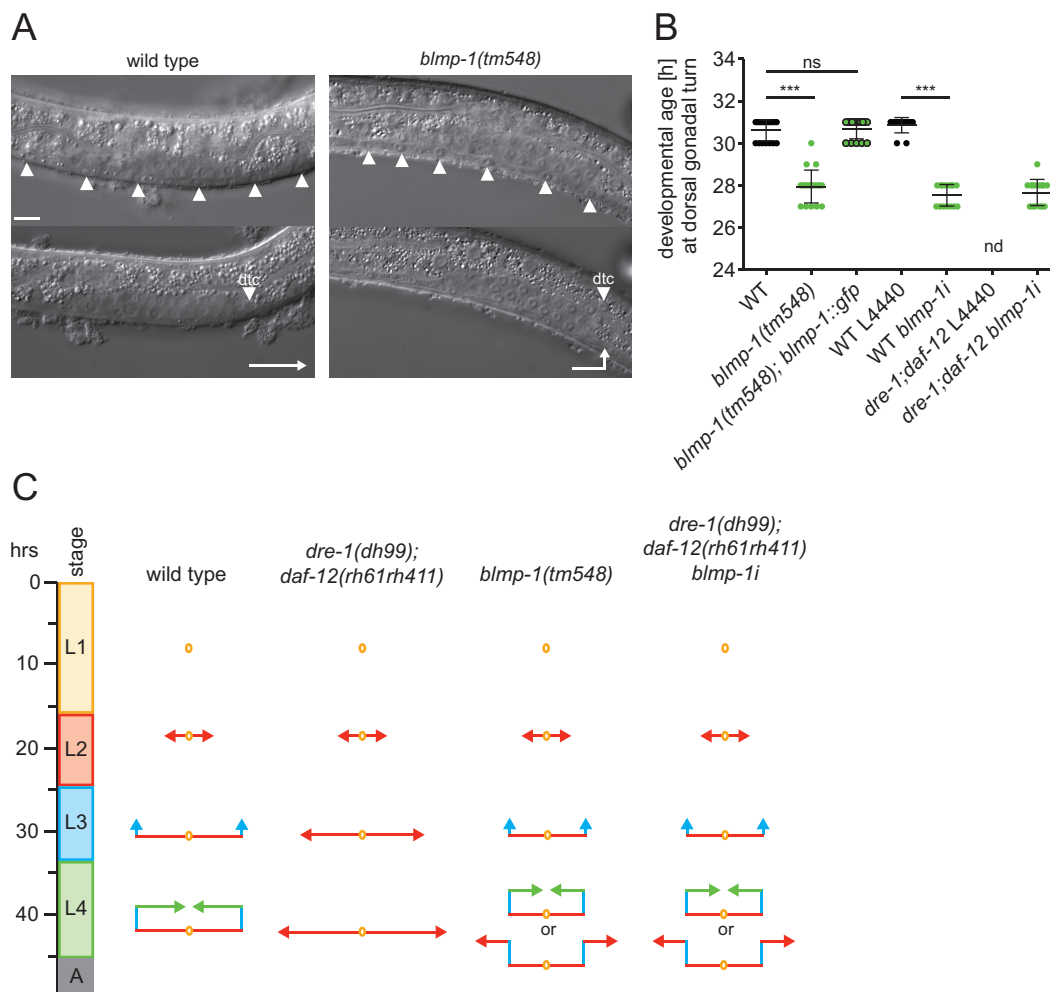


**Figure 14: *blmp-1*(+) Impedes Dorsal Migration of the Gonad**

(A) Representative DIC images of 27 hrs post-hatching WT and *blmp-1* mutant larvae staged by vulval precursor cells (arrowheads, upper panel). Dtc's migrate precociously in the *blmp-1(tm548)* mutant (arrowheads, lower panel). Scale bars = 10  $\mu$ m. (B) In *blmp-1(tm548)* mutants, as well as WT and *dre-1(dh99);daf-12(rh61rh411)* mutants grown on *blmp-1* RNAi dtcs turn dorsally ahead of time. \*\*\* $<0.001$  (ANOVA). Mean $\pm$ SD. ns = not significant. nd = not determined. (C) Gonad migration program of WT worms and various mutants as inferred from inspection. Arrowheads indicate positions of the dtcs.

Taken together, these results show that *dre-1/blmp-1* also function together to coordinate temporal patterning of gonadal outgrowth. Because *blmp-1* and not *nhr-25* suppressed *dre-1* phenotypes in multiple tissues, we focused our further analyses on *blmp-1*.

### 2.2.3 *blmp-1* Works at a Late Step in the Seam Cell Heterochronic Circuit

To further elucidate the role of *blmp-1* in the seam cell heterochronic gene network I performed genetic epistasis and synergy experiments with known heterochronic loci that regulate the larval-to-adult transition. First, I tested *blmp-1* knockdown in a variety of precocious heterochronic mutants (Figure 15). Amongst them, *hbl-1/Hunchback*, *lin-42/Period*, *lin-41/Trim71*, and *sop-2/PcG-like* specify L4 programs by directly or indirectly preventing *lin-29/EGR* expression and thus the adult fate. Accordingly, loss-of-function mutants show impenetrant precocious terminal differentiation phenotypes, in which seam

cells fuse and synthesize adult alae already in L3 larvae, similar to *dre-1* mutants. Notably, knockdown of *blmp-1* variously suppressed precocious seam cell phenotypes of these mutants, suggesting it acts downstream or parallel to these components (Figure 15). Moreover, *blmp-1* retarded or incomplete adult alae formation even strongly prevailed over *hbl-1(ve18)*, *lin-42(n1089)* and *lin-41i* precocious phenotypes, possibly closely linking these genes in a pathway (Figure 15A and 15C). By comparison, suppression of temperature-sensitive hypomorphic *sop-2(bx91)* mutant phenotypes at semi-permissive temperatures was relatively weak, indicating *blmp-1* might work upstream or in parallel to *sop-2* (Figure 15A). However, these results have to be interpreted with caution, since not all alleles used were null.

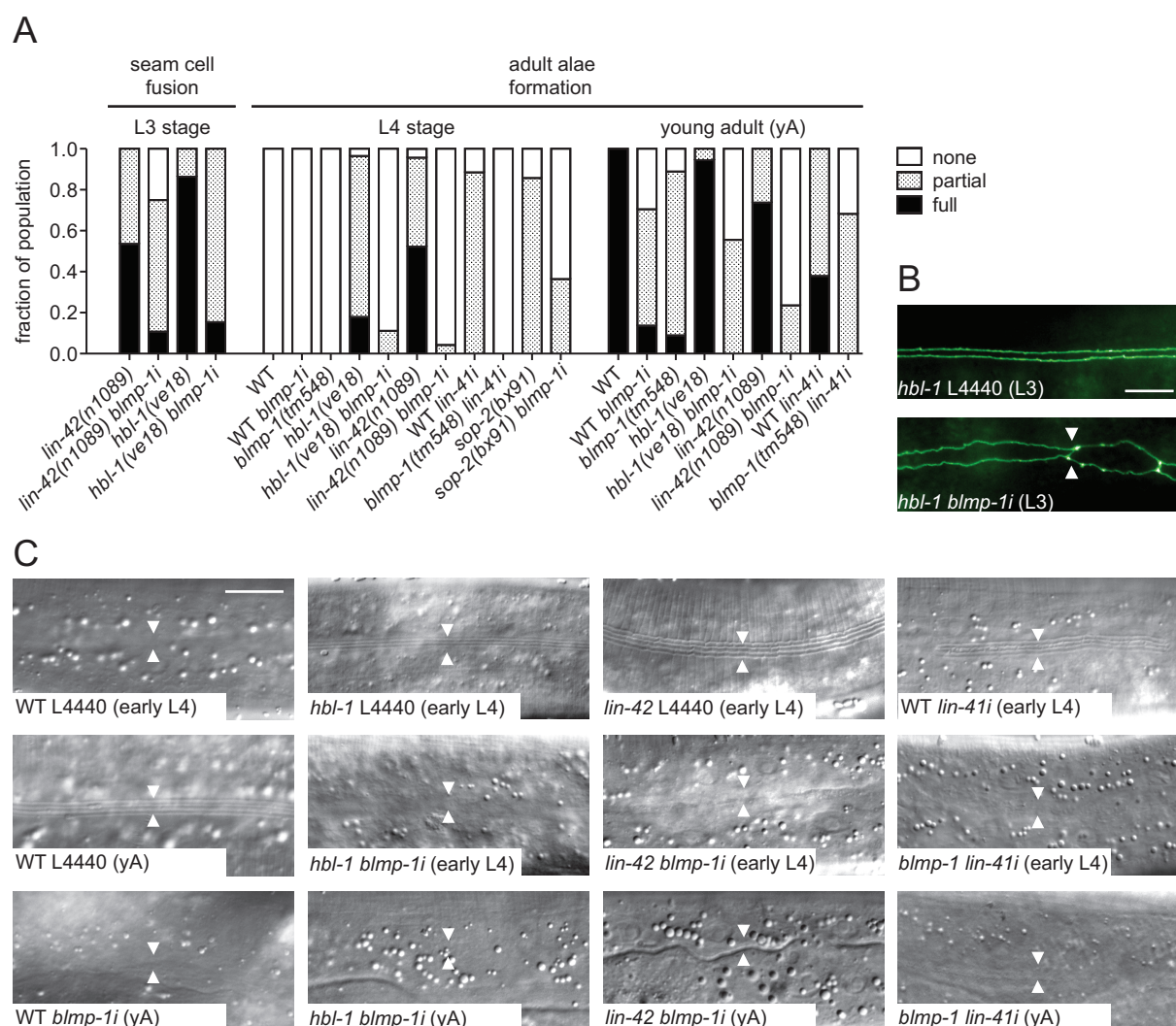


**Figure 15: *blmp-1* Interacts with Precocious Heterochronic Loci in the Epidermis**

**(A)** Epistasis experiments of *blmp-1(tm548)/blmp-1i* with precocious heterochronic loci *hbl-1(ve18)*, *lin-41i*, *lin-42(n1089)*, and *sop-2(bx91)*. ( $n > 20$ ). L4440 empty vector functions as control. Partial seam fusion refers to an incomplete seam syncytium with leftover unfused seam cells. Partial alae formation refers to poorly formed or incomplete adult alae. Temperature-sensitive *sop-2(bx91)* mutants were observed after shifting L1 larvae from 15°C to 23°C. **(B)** Representative pictures of seam cell adherence junctions as visualized by *ajm-1::gfp* in *hbl-1(ve18)* L3 larvae grown on L4440 empty vector control or *blmp-1* RNAi. Arrowheads indicate seam-seam boundaries. **(C)** Representative DIC images of WT worms and selected precocious heterochronic mutants showing adult alae formation under control (L4440) and *blmp-1* depleted conditions at the early L4 or young adult (yA) stage. Arrowheads indicate position of the seam syncytium.

Next I examined *blmp-1* genetic synergy with various retarded heterochronic mutants working at the larval-to-adult transition (Figure 16). *hbl-1* and *lin-41* are downregulated post-transcriptionally by *let-7/let-7s* microRNAs, leading to derepression of *lin-29/EGR*, which then triggers the adult fate. Thus *let-7* and *lin-29* loss of function cause retarded phenotypes: *let-7* mutants display incomplete seam cell fusion and poor or no adult alae formation; in *lin-29* mutants both events fail entirely. RNAi mediated knockdown of *blmp-1* in temperature-sensitive *let-7(n2853ts)* mutants slightly enhanced the *let-7* retarded adult alae formation and the bursting phenotype at a semi-permissive temperature (Figure 16A-C). No enhancement was detected for *lin-29(n546)* as its retarded phenotypes are fully penetrant (Figure 16A and 16B). The transcriptional cofactor *mab-10/NAB* cooperates with *lin-29/EGR* to specify the adult seam fate. Loss-of-function mutations of *mab-10* do not alter seam cell fusion and adult alae formation, but subsets of seam cells undergo an extra nuclear division after they fuse into the seam syncytium (Harris and Horvitz, 2011). *blmp-1* depletion enhanced the penetrance of the extra nuclear division phenotype of *mab-10(e1248)* (Figure 16D and 16E) and corresponding animals rarely formed adult alae (Figure 16A and 16B), indicating that *blmp-1* acts downstream or in parallel to *mab-10*.

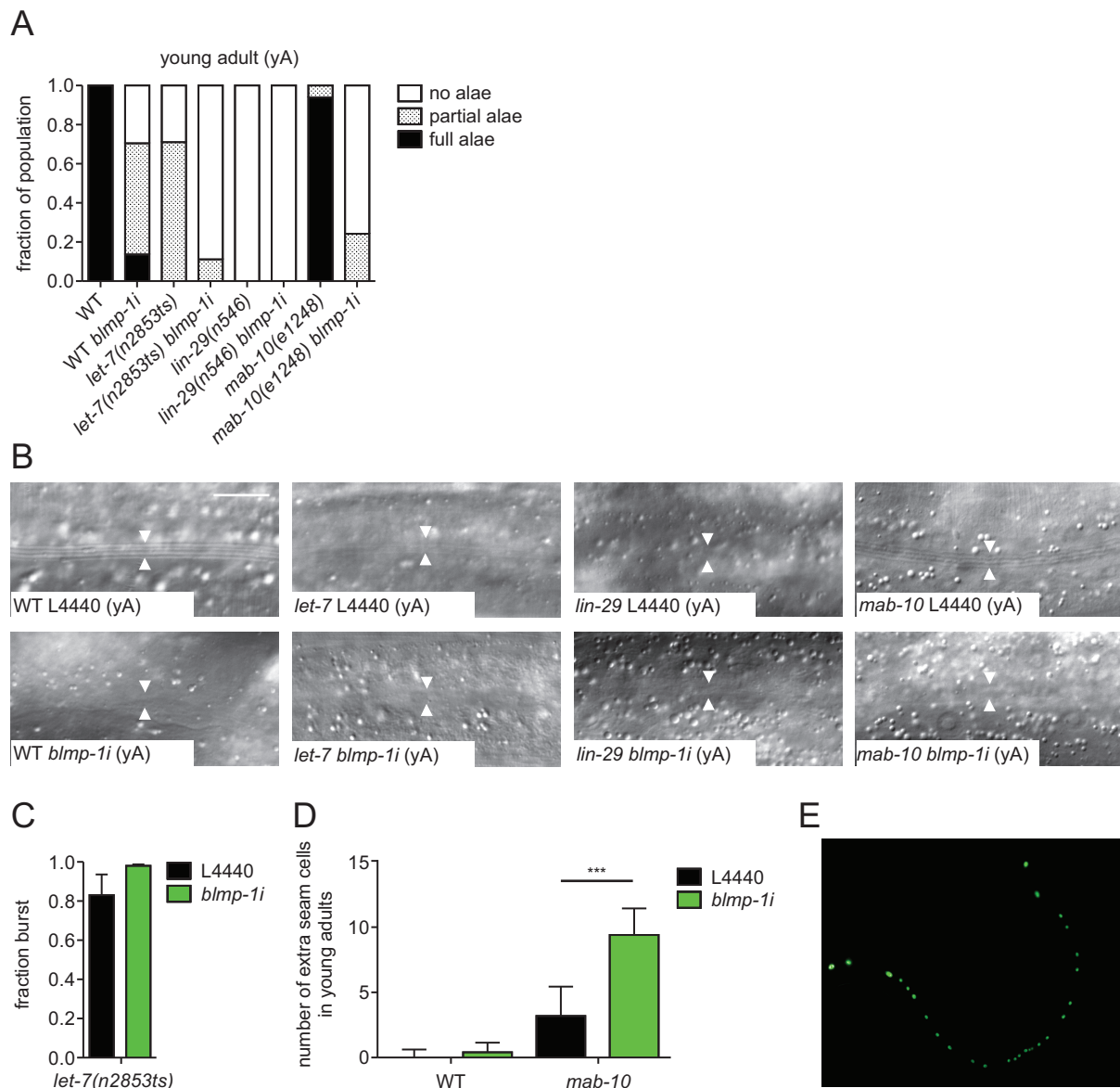


**Figure 16: *blmp-1* Interacts with Retarded Heterochronic Loci in the Epidermis**

**(A)** Synergy experiments of *blmp-1*(RNAi) with retarded heterochronic loci *let-7(n2853ts)*, *lin-29(n546)*, and *mab-10(e1248)*. ( $n > 20$ ). L4440 empty vector functions as control. Partial seam fusion refers to an incomplete seam syncytium with leftover unfused seam cells. Partial alae formation refers to poorly formed or incomplete adult alae. Temperature-sensitive *let-7(n2853ts)* mutants were observed after shifting L1 larvae from 15°C to 20°C. **(B)** Representative DIC images of WT animals and retarded heterochronic mutants showing adult alae formation under control (L4440) and *blmp-1* depleted conditions at the young adult (yA) stage. Arrowheads indicate position of the seam syncytium. **(C)** *blmp-1* depletion slightly enhances *let-7(n2853ts)* bursting phenotype at semi-permissive temperatures (20°C). Mean+SD ( $n=3$ , >50 worms each). **(D)** *blmp-1* knockdown increases the number of seam cells that undergo an extra division after the larval-to-adult transition in *mab-10(e1248)* mutants. The number of seam cells was scored in worms carrying 1-5 eggs using the *scm-1::gfp* marker. The number of theoretically present seam cells per side (16) was subtracted from the results to get the number of cells with extra divisions. \*\*\* $p < 0.001$  (ANOVA). Mean+SD ( $n \geq 17$ ). **(E)** Representative fluorescence image of a *mab-10(e1248)* mutant young adult worm grown on *blmp-1* RNAi expressing *scm-1::gfp* in seam cell nuclei. Scale bar = 10  $\mu\text{m}$ .

Altogether, these analyses reveal a broad role for *blmp-1* as a developmental timing gene promoting many aspects of seam cell terminal differentiation.

### 2.2.4 *dre-1/blmp-1* Regulate *C. elegans* Life History

The genetic interactions described above reveal that *dre-1* and *blmp-1* act in opposition for developmental timing events in epidermis and gonad. Interestingly, I found both *dre-1* and *blmp-1* to also regulate entry into dauer diapause. Under unfavorable environmental conditions, such as food scarcity and heat, *C. elegans* can enter this alternate third larval stage, characterized by stress resistance, longevity, and multiple metabolic and morphological changes including the synthesis of a thick stress and desiccation resistant cuticle. In particular, *blmp-1* mutants were defective in dauer formation (Daf-d), as even under dauer inducing conditions (27°C, low cholesterol) they did not enter the alternate larval stage (Figure 17A). However, they arrested development as L3 or L4 larvae appearing unable to shed their cuticle. Also starvation induced a similar phenotype, but not dauer formation in *blmp-1* mutants (data not shown). Conversely, *dre-1* mutants constitutively formed dauer larvae (Daf-c) under stress conditions, albeit at low levels, suggesting the two genes normally promote and prevent dauer formation, respectively (Figure 17A). Consistent with my previous data, the *blmp-1* mutant phenotype (Daf-d) prevailed in the double mutant (Figure 17A). *blmp-1* depletion was also epistatic to canonical Daf-c loci *daf-2/InsR*, *daf-7/TGF- $\beta$* , and *daf-9/CYP27A1*, placing *blmp-1* downstream of Insulin/IGF, TGF- $\beta$ , and steroidal signaling at a late step in the dauer signaling pathways in close proximity to the key regulator of the dauer decision *daf-12* (Figures 1, 17B, and 17C).

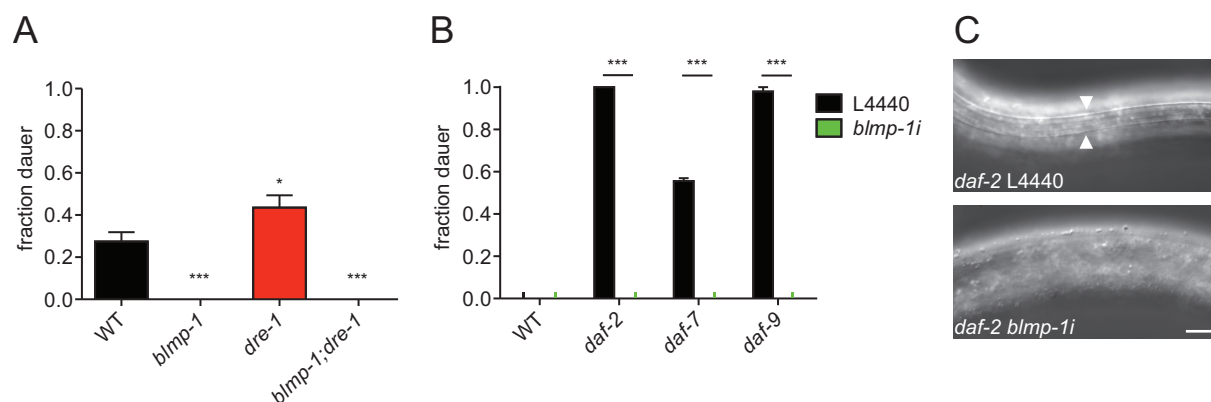


**Figure 17: *dre-1* and *blmp-1* Show Opposite Phenotypes for Dauer Formation**

**(A)** Dauer formation of WT, *dre-1(dh99)*, *blmp-1(tm548)* and *dre-1(dh99);blmp-1(tm548)* animals scored on plates lacking cholesterol at 27°C. \* $p < 0.05$ , \*\*\* $p < 0.001$  (ANOVA). Mean+SEM ( $n \geq 8$ , >100 worms each). **(B)** Dauer formation of WT, *daf-2(e1368)*, *daf-7(e1372)* and *daf-9(dh6)* animals scored on regular NGM plates at 25°C. In the latter three genotypes, *blmp-1* depletion led to L3/L4 arrest without dauer alae and SDS resistance. \*\*\* $p < 0.001$  (ANOVA). Mean+SEM ( $n = 3$ , 15 worms each). **(C)** Representative DIC images of *daf-2(e1368)* mutants on L4440 empty vector control or *blmp-1* RNAi. Arrowheads indicate dauer alae. Scale bar = 10  $\mu$ m.

In addition to dauer formation *blmp-1* and *dre-1* affected organismal life span (Figure 18A). While knockdown of *blmp-1* from L4 onward slightly shortened WT lifespan, similar to

previous reports (Figure 18A) (Samuelson et al., 2007), *dre-1* depletion resulted in a modest, but reproducible lifespan increase (Figure 18A). Interestingly a completely parallel approach in our lab identified *blmp-1* as a modulator of germline longevity. Upon loss of germline precursor cells *C. elegans* lifespan is dramatically increased (Hsin and Kenyon, 1999). Multiple important players in germline longevity have been identified, including a functional somatic gonad, as well as key transcriptional regulators such as *daf-16/FOXO*, *daf-12/FXR/LXR/VDR*, *nhr-80/HNF-4*, and *pha-4/FOXA* (Hsin and Kenyon, 1999; Lapierre et al., 2011; Goudeau et al., 2011; Antebi, 2013). Similar to these key factors, my colleagues found *blmp-1* depletion to abrogate *glp-1/Notch* mutant longevity, mutants, which lack the germline at non-permissive temperatures (Nakamura, Karalay, and Antebi, unpublished; Austin and Kimble, 1987; Arantes-Oliveira et al., 2002). I reproduced this lifespan phenotype together with Dr. Shuhei Nakamura in germ cell precursor-ablated animals, which lived significantly longer than mock-ablated controls, but only in the presence of functional *blmp-1(+)* (Figure 18B). However, *blmp-1* mutation led to general sickness as it also significantly shortened WT lifespan. Moreover, *blmp-1* RNAi treatment from L4 onwards did not completely suppress the lifespan extension upon germline loss induced by germ cell precursor ablation (Figure 18C). Therefore the role of *blmp-1* in germline longevity was not further investigated in this study.

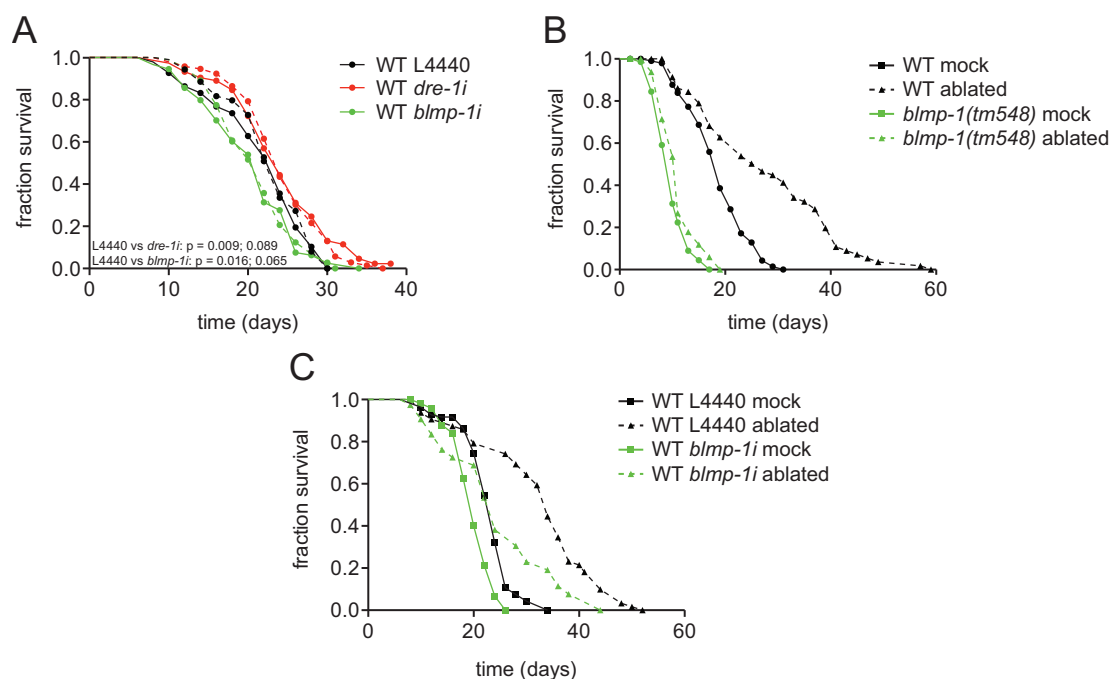


**Figure 18: *dre-1* and *blmp-1* Modulate Longevity**

**(A)** Lifespan analysis: WT animals were grown on RNAi from the L4 stage as indicated. Dashed lines represent an independent repeat of the experiment. First given p value corresponds to the experiment displayed with solid lines (log rank (Mantel-Cox) test). **(B)** Lifespan analysis: Germ cell precursors Z2 and Z3 of WT animals and *blmp-1(tm548)* mutants were ablated by laser microsurgery in young L1 larvae prior to lifespan analysis. Recovered animals that were not ablated

functioned as control (mock). **(C)** Lifespan analysis: After germ cell precursor ablation WT animals were recovered on OP50 bacteria and transferred to RNAi plates at the L4 stage as indicated. Lifespan analysis was performed together with Dr. Shuhei Nakamura.

Taken together, *dre-1* and *blmp-1* not only regulate developmental timing in epidermis and gonad, but also work in opposite ways for the life history traits of dauer formation and longevity in *C. elegans*.

### 2.2.5 BLMP-1 Overexpression Enhances *dre-1* Phenotypes

As *blmp-1* loss of function variously suppressed *dre-1* mutant phenotypes, I examined whether its overexpression can recapitulate or enhance *dre-1* mutant developmental alterations. Surprisingly, BLMP-1::GFP overexpression did not evoke *dre-1* related phenotypes such as precocious seam cell fusion in a WT background (data not shown). However, multiple *dre-1* phenotypes were strongly enhanced: first, the *blmp-1* overexpressor provoked strong retarded gonadal migration defects when grown on *dre-1* RNAi (Figure 19A). Second, it substantially enhanced molting defects of *dre-1* depleted worms (Figure 19B and 19C). Third, it was synthetic lethal in a *dre-1(dh99)* mutant background, similar to *dre-1* null mutants, and could only be recovered in a weaker *dre-1* allele *dre-1(dh279)*. In sum, *blmp-1* overexpression cannot fully recapitulate, but significantly enhance *dre-1* mutant phenotypes.

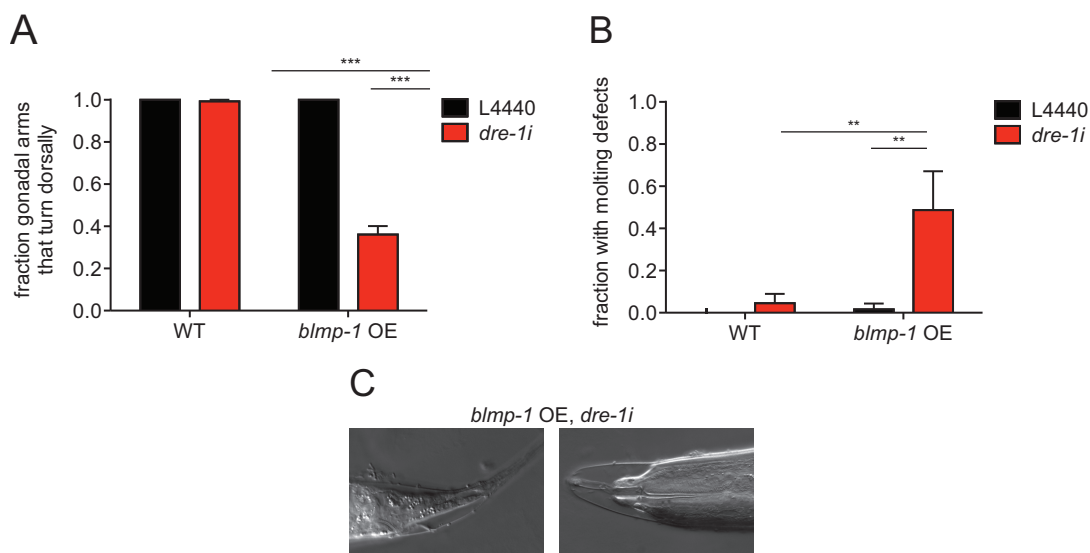


**Figure 19: *blmp-1* Overexpression Enhances *dre-1* Phenotypes**

**(A)** *blmp-1* overexpression (OE) using an integrated *blmp-1::gfp* transgene (*wgls109*, Sarov et al., 2012) induces gonadal migration defects in *dre-1* depleted worms. \*\* $p < 0.01$  (ANOVA). Mean+SEM ( $n=3$ , 40 gonadal arms each). **(B)** Representative DIC images of molting defects observed in *blmp-1* OE worms grown on *dre-1* RNAi. Scale bar = 10  $\mu\text{m}$ . **(C)** Quantification of molting defects induced by *dre-1* depletion in *blmp-1* OE worms. \*\* $p < 0.01$  (ANOVA). Mean+SEM ( $n=3$ , 20 worms each).

## 2.2.6 The SCF<sup>DRE-1</sup> Complex Degrades BLMP-1 via the Proteasome

The genetic epistasis experiments described above place *blmp-1* downstream of *dre-1*, supporting the idea that BLMP-1 could be a substrate of the SCF<sup>DRE-1</sup> E3-ubiquitin ligase. To directly test this hypothesis, I examined the effect of *dre-1* depletion on BLMP-1 protein levels.

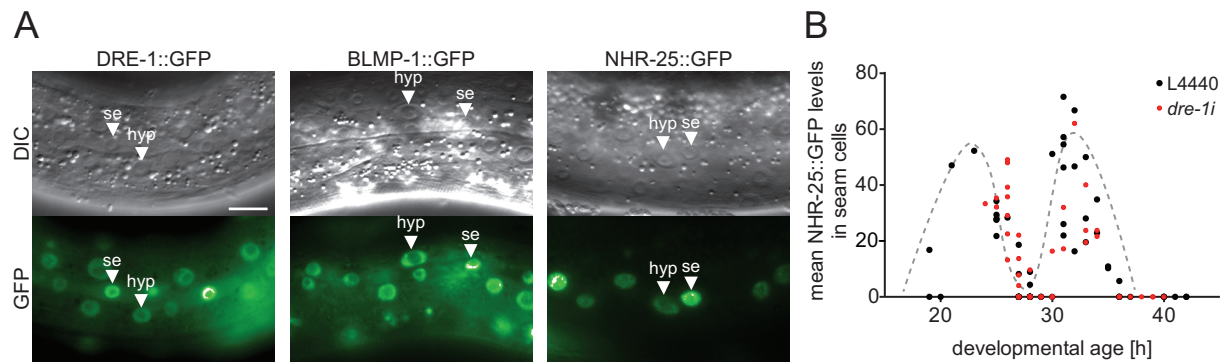


**Figure 20: BLMP-1::GFP and NHR-25::GFP Overlap with DRE-1::GFP Expression, but NHR-25::GFP is *dre-1* Independent** (A) Representative DIC and fluorescence images showing overlapping expression patterns of DRE-1-, BLMP-1- and NHR-25::GFP in seam (se) and hypodermal (hyp) nuclei of L4 larvae. (B) NHR-25::GFP expression in seam cells varies with the molt cycle (indicated by the dashed line), but does not depend on *dre-1*. Each dot represents mean GFP intensity in >5 seam cells of a worm. Developmental age is given in hours (h) post-hatching.

First, BLMP-1::GFP and also NHR-25::GFP showed overlapping expression with DRE-1::GFP in seam and hypodermal cells as well as the dtcs (Figure 20A). NHR-25::GFP expression oscillated with the molt cycle, but showed no obvious *dre-1* dependence during L2-to-L4 larval stages, indicating that NHR-25 indeed is not a primary target of the SCF<sup>DRE-1</sup> complex (Figure 20B). Second, in contrast to NHR-25, I found that knockdown of *dre-1* resulted in a striking 7-8-fold increase in BLMP-1::GFP levels in seam and hypodermal cells (Figure 21A and 21B). Interestingly, BLMP-1::GFP levels were only moderately elevated in a weak *dre-1(dh279)* mutant background and could not be analyzed in *dre-1(dh99)* mutants due to synthetic lethality (Figure 21B and 21E). Third, knockdown of other SCF complex components, such as the scaffold *cul-1* and the *skr-1* adapter also led to a pronounced accumulation of BLMP-1::GFP, whereas knockdown of related molecules, such as *cul-4*, *skr-2* and *skr-3*, had little or no effect (Figure 21B and 21E). Finally, to test whether the UPS mediates BLMP-1 proteolysis, I inhibited the proteasome using the synthetic inhibitor bortezomib or *rpn-8* RNAi, which depletes a subunit of the proteasomal 19S cap (Segref et al., 2011). Both treatments significantly increased BLMP-1::GFP levels in seam and hypodermis (Figure 21C-E).

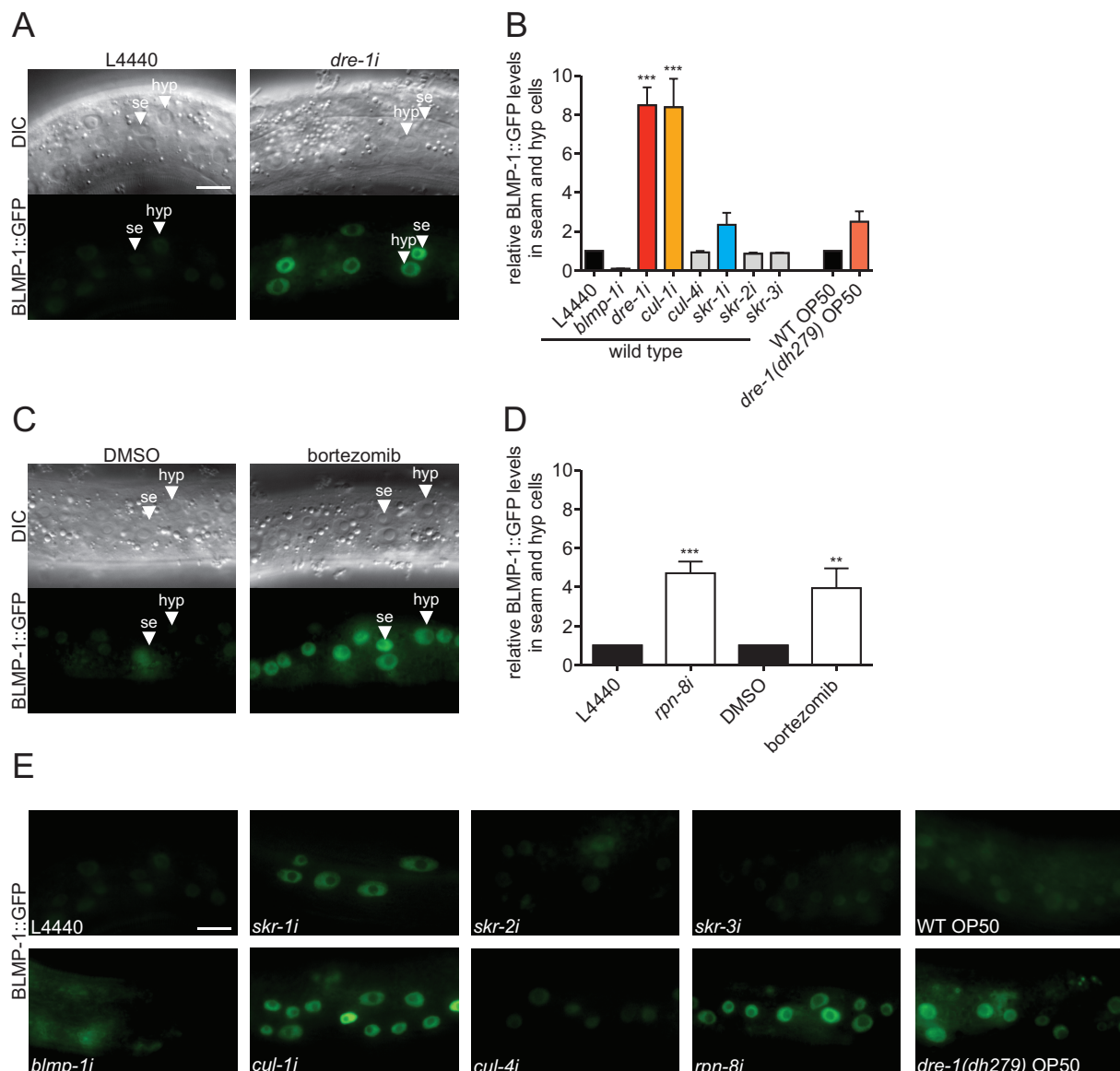


**Figure 21: BLMP-1::GFP Levels are Regulated by the SCF<sup>DRE-1</sup> Complex and the Proteasome**

(A) Representative DIC and fluorescence images of BLMP-1::GFP expressing L4 larvae grown on L4440 empty vector control or *dre-1* RNAi. (B) BLMP-1::GFP levels in seam and hypodermal cells are significantly increased upon *dre-1* and *cul-1* depletion. \*\*\* $p < 0.001$  (ANOVA). Mean+SEM ( $n \geq 3$ ,  $\geq 10$  cells of 5 worms each). (C) Representative DIC and fluorescence images of BLMP-1::GFP expressing L4 larvae treated with 100  $\mu$ M bortezomib or DMSO control. (D) Proteasome inhibition (bortezomib and *rpn-8* RNAi) increases BLMP-1::GFP levels in seam and hypodermal cells. \*\* $p < 0.01$ , \*\*\* $p < 0.001$  (ANOVA). Mean+SEM ( $n \geq 3$ ,  $\geq 10$  cells of 5 worms each). (E) Representative fluorescence images showing BLMP-1::GFP expression in seam and hypodermal nuclei upon various RNAi treatments and in *dre-1(dh279)* mutants. se = seam cell. hyp = hypodermal cell. Scale bars = 10  $\mu$ m.

I next analyzed endogenous BLMP-1 levels by western blotting to visualize the amount of native protein (Figure 22). In accord with my *blmp-1::gfp* transgene results, *dre-1* depletion and proteasome inhibition by *rpn-8* RNAi both resulted in a significant increase in endogenous BLMP-1 protein (Figure 22). Consistent with the genetic data, BLMP-1 levels were also strongly elevated in a *dre-1(dh99)* mutant background (Figure 22).

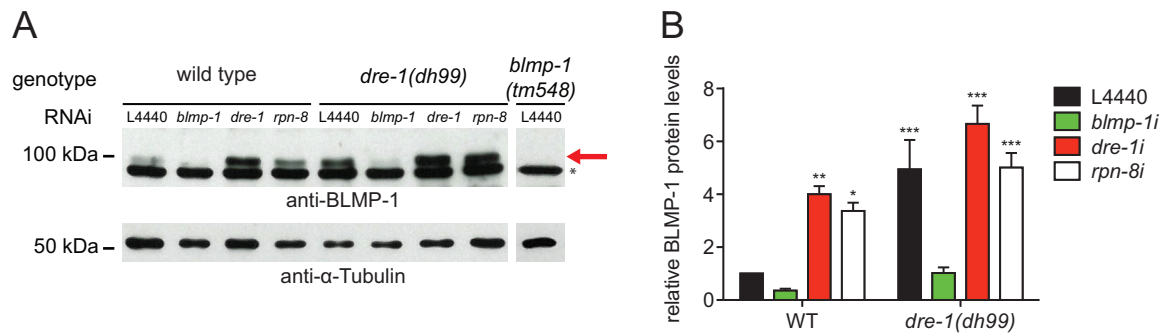


**Figure 22: Endogenous BLMP-1 Levels Depend on *dre-1* and the Proteasome**

**(A)** Western blot analysis of BLMP-1 protein levels in WT, *dre-1(dh99)* and *blmp-1(tm548)* L4 larvae after various RNAi treatments from egg. The asterisk marks a nonspecific band. The arrow points to the BLMP-1 band. **(B)** Quantification of western blot analyses. \* $P < 0.05$ , \*\* $P < 0.01$ , \*\*\* $P < 0.001$  (ANOVA). Mean +SD (n=5).

Conversely, *blmp-1* mRNA levels were unchanged upon *dre-1* depletion or proteasome inhibition as analyzed by qRT-PCR (Figure 23). Altogether, these results strongly support the notion that the SCF<sup>DRE-1</sup> complex post-transcriptionally regulates BLMP-1 through proteasome-mediated degradation. Furthermore, they indicate that DRE-1 C-terminal residues might not be of major importance for mediating BLMP-1 degradation, since the *dre-1(dh279)* allele, which leads to a C-terminal *dre-1* truncation, only marginally elevates BLMP-1 levels (Figure 21B and 21E).

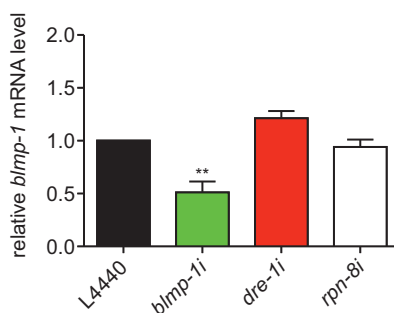


**Figure 23: *blmp-1* mRNA Levels are Largely Independent of *dre-1* and the Proteasome**

qRT-PCR analysis of WT L4 larvae treated with the indicated RNAis starting at the egg stage. \*\* $p < 0.01$  (ANOVA). Mean+SEM (n=3).

If BLMP-1 were a direct substrate of DRE-1, then the two proteins would be predicted to physically interact. To test this, I performed coimmunoprecipitation experiments in worms expressing full-length DRE-1::GFP under its native promoter. Importantly, immunoprecipitation of DRE-1::GFP specifically coprecipitated a small fraction of endogenous BLMP-1 (< 1% of input), whereas a NHR-25::GFP control did not (Figure 24A). NHR-25::GFP was used as control due to its largely overlapping expression pattern and its similar expression intensity compared to DRE-1::GFP. Consistently, when expressed in HEK293T cells FLAG-HA-tagged DRE-1 specifically coprecipitated with 6xHis-tagged *C. elegans* BLMP-1, but not the closely related Zn-finger transcription factor LIN-29

(Figure 24B). Thereby coprecipitation of DRE-1 and BLMP-1 required proteasome inhibition, pointing to a very transient interaction.

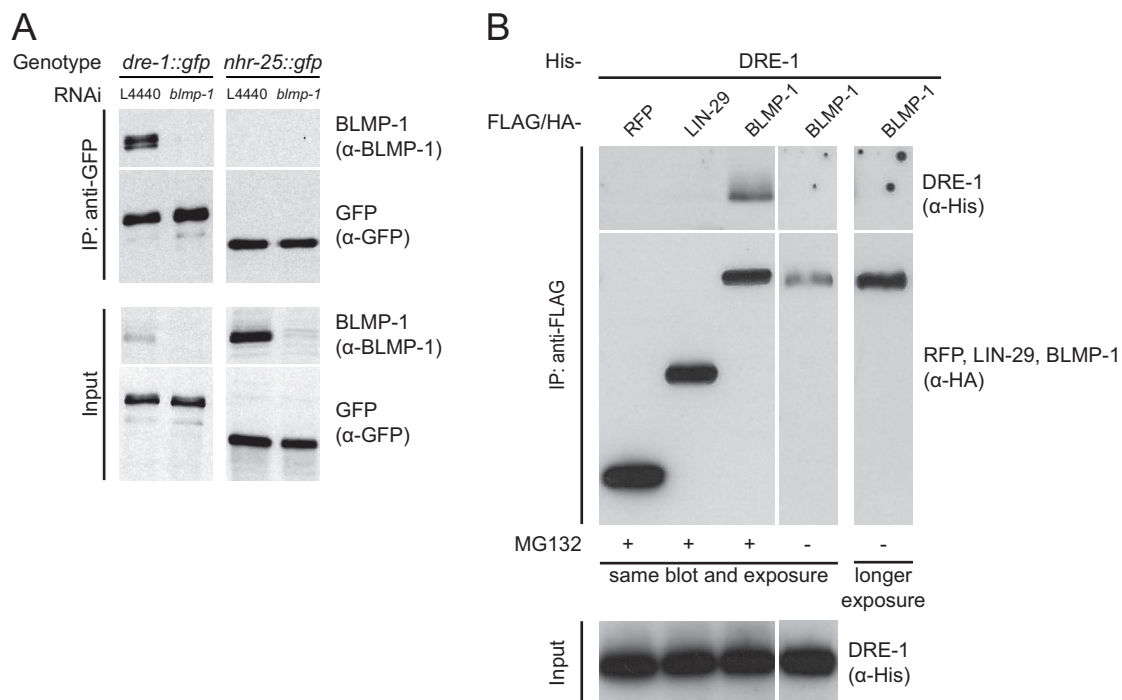


**Figure 24: DRE-1 Physically Interacts with BLMP-1**

(A) L3 larvae expressing integrated DRE-1::GFP or NHR-25::GFP as control were grown from egg stage onwards on L4440 empty vector control or *blmp-1* RNAi expressing bacteria, respectively and utilized for anti-GFP immunoprecipitation (IP). Lysates and IP were analyzed by SDS-PAGE and immunoblotting. (B) His-DRE-1 coprecipitates with FLAG-HA-tagged (F/H) BLMP-1 when cotransfected in HEK293T cells treated with 15  $\mu$ M MG132. F/H-RFP and -LIN-29 serve as negative controls.

Furthermore, I found DRE-1 expression in mammalian cells to destabilize coexpressed BLMP-1 protein after blocking nascent protein synthesis by cycloheximide (CHX) treatment (Figure 25). In these assays BLMP-1 stability was rescued by proteasome inhibition, supporting the *in vivo* findings. However, we failed to detect ubiquitinated BLMP-1 of higher molecular weight in *C. elegans* as well as in cell-based assays (collaboration with the group of Michele Pagano at NYU), but such species might be of low abundance or unstable *in vivo*, and difficult to ubiquitinate in a heterologous system *in vitro*.

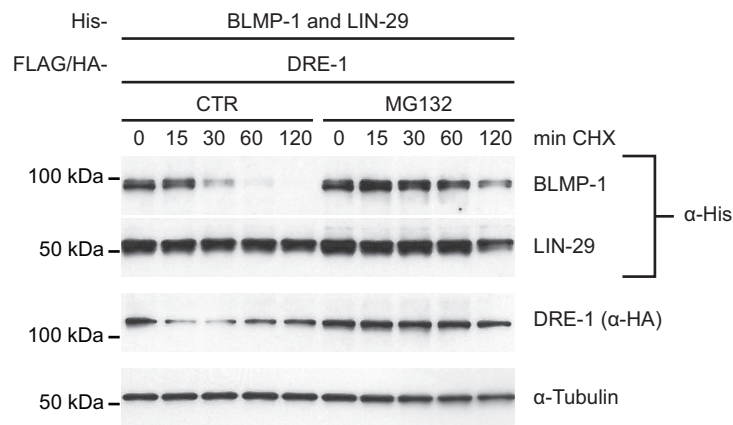


**Figure 25: BLMP-1 is Degraded via the Proteasome**

HEK293T cells were transfected with His-BLMP-1 and -LIN-29 in combination with FLAG-HA-DRE-1. Transfected cells were treated with cycloheximide (CHX) or CHX + 15  $\mu$ M MG132 for the indicated time intervals prior to harvesting and analysis by SDS-PAGE and immunoblotting.

### 2.2.7 BLMP-1 is Dynamically Regulated in a Tissue-Specific Manner

Having established BLMP-1 as a DRE-1 substrate for proteolysis, we sought to better understand the temporal dynamics of BLMP-1 regulation *in vivo*. The genetic studies described above reveal that *blmp-1* acts at an intermediate step in dtc migration, but promotes terminal differentiation in *C. elegans* hypodermis. To clarify the tissue-specific regulation of developmental timing by DRE-1/BLMP-1, I followed BLMP-1::GFP levels in these tissues throughout larval development.

In dtcs BLMP-1::GFP was expressed from mid-L2, when gonadal outgrowth initiates toward head and tail (Figure 26A and 26B). By mid-L3 (28-30 hours of developmental age), just prior to the dorsal gonadal turn, BLMP-1::GFP levels in the dtcs dropped dramatically (Figure 26A and 26B). Correlatively, DRE-1::GFP levels in the dtcs steadily increased from L2-to-L4 larval stages (Figure 26C). In contrast, when worms were fed *dre-1* RNAi, BLMP-1::GFP levels persisted to later ages and the dtcs frequently failed the dorsal turn (Figure 26A and 26B). Altogether, these data strongly suggest that timely DRE-1-mediated BLMP-1 degradation permits the gonadal turn, while high BLMP-1 levels in gonadal dtcs impede this event (Figure 26D).

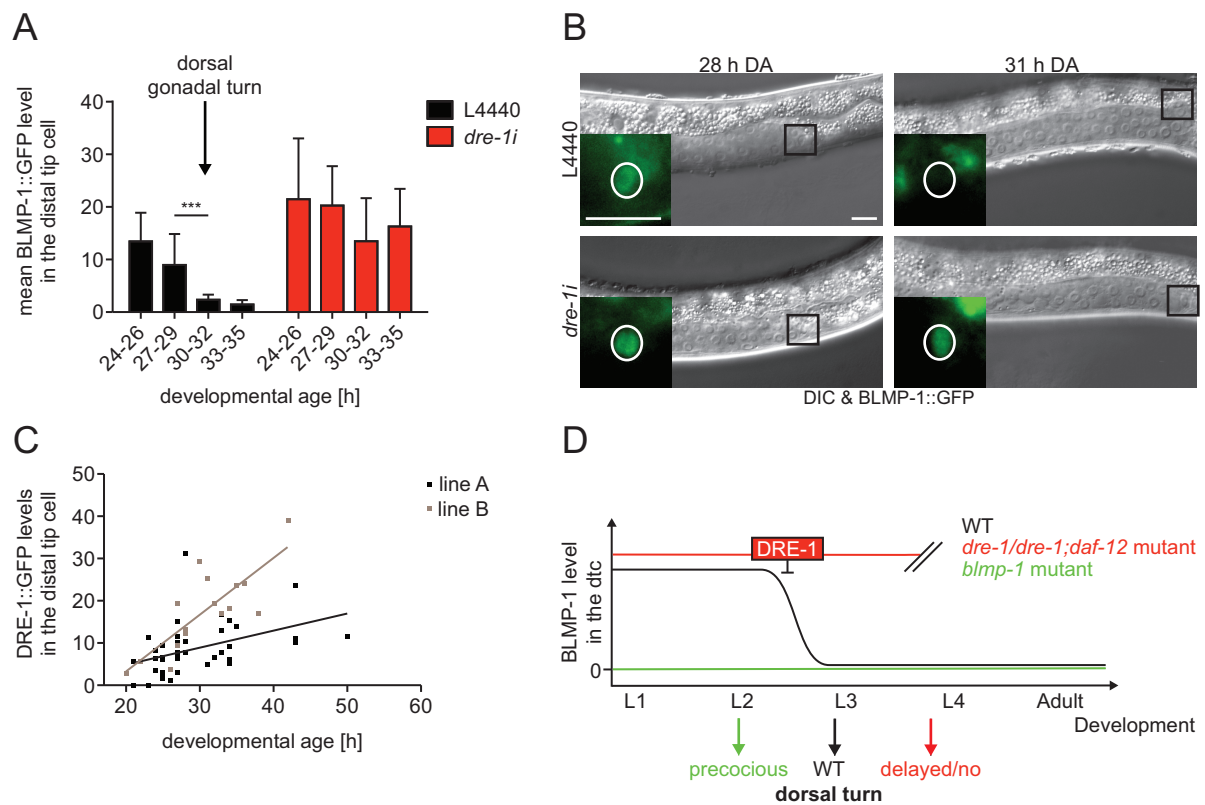


**Figure 26: DRE-1 Degrades BLMP-1 to Initiate the Dorsal Gonadal Turn**

(A) BLMP-1::GFP levels in the dtcs were assessed in  $\geq 5$  worms per grouped developmental age. \*\*\* $p < 0.001$  (ANOVA). Mean+SD. (B) Representative DIC images of age-matched L3 larvae with zoom in on BLMP-1::GFP expression in the dtcs. Black box indicates the area enlarged in the fluorescence image. White circle roughly marks the dtc nucleus. Scale bars = 10  $\mu\text{m}$ . (C) DRE-1::GFP levels were assessed in dtcs of two integrated lines (A and B). Developmental age is given in hours (h) post-hatching. Solid lines represent linear regression fits for illustration. Each dot represents GFP intensity in one dtc. (D) Model for *dre-1/blmp-1* action in gonadal tissue: BLMP-1 is downregulated in a *dre-1*-dependent manner in mid-L3 to allow the dorsal gonadal turn. In *dre-1* or *dre-1/daf-12* mutants BLMP-1 levels persist to later ages, leading to retarded migration defects, whereas the dorsal turn is preceded in the absence of BLMP-1. Double-slashes indicate the end of data assessment.

Surprisingly, in seam and hypodermal cells BLMP-1::GFP levels were largely constant throughout larval development except for a transient peak early in the L4 stage (Figure 27A). Interestingly, this peak coincides with the time of seam cell fusion, indicating this BLMP-1 pulse might trigger the fusion event. Likewise, *dre-1* knockdown provoked a strong increase of seam and hypodermal BLMP-1::GFP expression earlier in development, resulting in seam cell fusion as early as 28 hours of developmental age during the L3 stage (Figure 27A). These observations are consistent with a model in which increased BLMP-1 levels initiate terminal differentiation events in the seams. Unexpectedly, DRE-1::GFP levels in seam and hypodermis did not obviously change during this time, implying that other instructive components or cofactors, such as kinases or phosphatases may contribute toward BLMP-1 regulation (Figure 27B). In sum, my data suggest that DRE-1 maintains a low steady state level of BLMP-1 to prevent precocious terminal differentiation in the epidermis (Figure 27C).

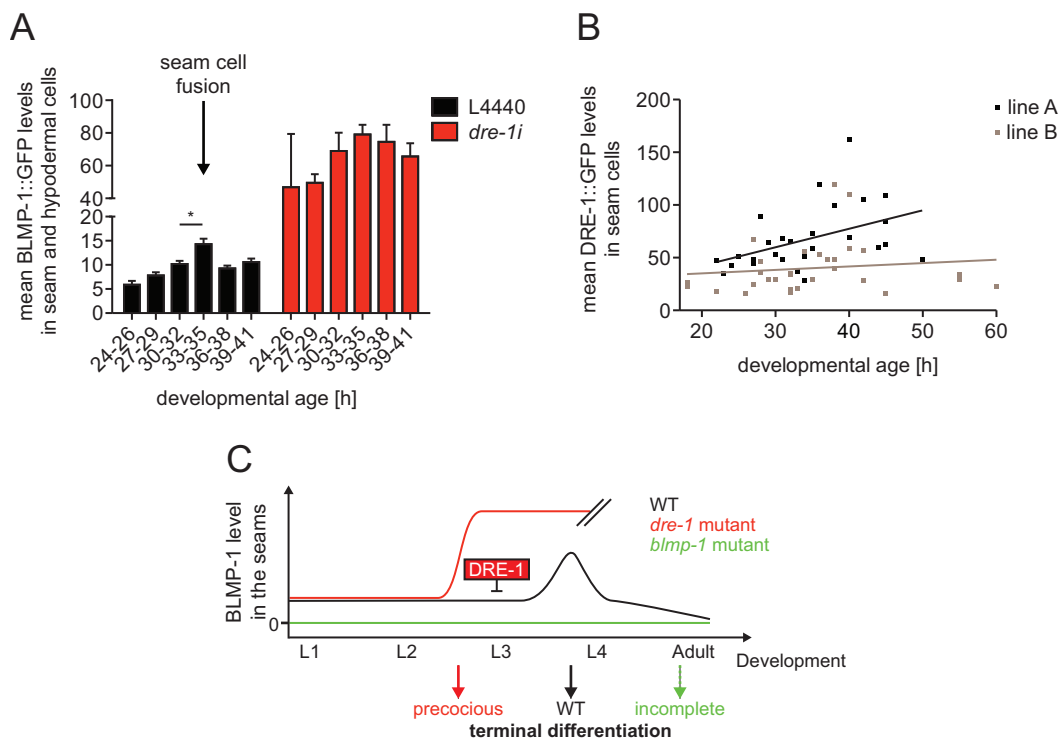


**Figure 27: DRE-1 Restrains BLMP-1 Levels to Prevent Terminal Differentiation in the Seams**

**(A)** BLMP-1::GFP levels in seam and hypodermal cells were assessed in  $\geq 5$  worms per grouped developmental age.  $*p < 0.05$  (ANOVA). Mean+SEM. **(B)** DRE-1::GFP levels in seam and hypodermal cells were analyzed in two integrated lines (A and B). Developmental age is given in hours (h) post-hatching. Solid lines represent linear regression fits for illustration. Each dot represents mean GFP intensity of  $>5$  seam cells of a worm. **(C)** Model for *dre-1/blmp-1* action in somatic tissue: Elevated BLMP-1 levels contribute to seam cell terminal differentiation, leading to precocious terminal differentiation in *dre-1* mutants and consequentially impaired terminal differentiation in the absence of BLMP-1. Double-slashes indicate the end of data assessment.

## 2.2.8 Screen for DRE-1/BLMP-1 Upstream Regulators

As indicated above, additional layers of regulation might contribute to the timing of BLMP-1 turnover particularly in the epidermis. As substrate phosphorylation is oftentimes key to substrate recognition by F-box proteins or, as recently shown, can have the exact opposite effect (Rossi et al., 2013; Skaar et al., 2013), we decided to screen through a RNAi library of kinases and phosphatases with regard to their effect on BLMP-1 protein abundance. Under my supervision a bachelor student, Caroline Hoppe, screened through a library of 393 kinases and 151 phosphatases using BLMP-1::GFP expression as direct readout. Surprisingly we found no striking upregulation of BLMP-1::GFP, but 5 candidates marginally increased BLMP-1::GFP levels in the hypodermis (Table 4). However, multiple RNAi treatments provoked a moderate reduction of BLMP-1::GFP levels, indicating the corresponding proteins to normally prevent BLMP-1 degradation (Table 4). As many of these candidates were tested only once, they are currently confirmed in an RNAi-sensitized *rrf-3(pk1426)* mutant background (Simmer et al., 2002).

Table 4: Kinase and Phosphatase Candidates Found to Modulate BLMP-1::GFP Levels

Kinase library		Phosphatase library		
Gene	Replicates	Gene	Replicates	
<i>vps-34</i>	1	W03F11.4	1	BLMP-1::GFP down
<i>mtk-1</i>	1	ZK973.k	1	BLMP-1::GFP up
<i>cdk-9</i>	1	ZK484.7	1	
Y47G6A_246.a	2	F22D6.9	1	
F46F5.2	2	R03D7.8	1	
<i>vab-1</i>	1	F52H3.6	1	
<i>dkf-2</i>	1	T20H9.6	1	
<i>daf-1</i>	2	C17H12.5	1	
<i>pmk-3</i>	1	<i>cel-1</i>	1	
C49C8.1	1	F53C3.13	1	
W03G9.5	1	T20B6.1	1	
<i>plk-3</i>	1	<i>fem-2</i>	1	
<i>rskn-2</i>	2	C55B7.3	1	
<i>gcy-6</i>	2	T25B9.10	1	
H06H21.8	1			
<i>ttbk-2</i>	1			
<i>gcy-11</i>	1			
<i>elo-3</i>	2			
F49C12.7	1			
<i>pct-1</i>	1			
M04C9.5	1			
ZK507.1	1			

### 2.2.9 *blmp-1* Expression Profiles – Seeking for Downstream Effectors

We not only investigated upstream regulators of DRE-1/BLMP-1, but also aimed to identify cognate downstream effectors regulated by the transcription factor *blmp-1*. Therefore we performed RNA-sequencing analysis of *blmp-1* mutant and WT animals harvested at the mid-L3 stage. We identified 325 significantly up- and 303 downregulated genes ( $\geq 1.5$ -fold difference from WT,  $q$ -value $<0.05$ ), indicating that *blmp-1* might not exclusively fulfill repressor functions in *C. elegans* (see Appendix). Differentially regulated genes included those enriched in the biological processes of molting and cuticle development, sugar and aminosugar metabolism, and protein modification (Figure 28A). The molting and cuticle-related regulated genes were amongst others *ptr-8*, *wrt-2*, *bed-3*, *nas-36*, and collagens (e.g. *col-7*, *col-91* and *col-124*). I further confirmed *blmp-1*-dependent regulation of these genes by qRT-PCR in L3 larvae and also young adult animals. Interestingly, all tested genes were

similarly regulated in both stages (Figure 28B). To initially test whether one target alone causes *blmp-1* retarded seam phenotypes, I depleted multiple downregulated candidates by RNAi in a RNAi-sensitized *rrf-3(pk1426)* mutant background, since I saw no affect on alae formation in WT animals. *wrt-2* and *bed-3* depletion both altered adult alae formation, but only in a small fraction of worms, suggesting that multiple *blmp-1* regulated genes act in concert to control adult alae synthesis (Figure 28C and 28D).

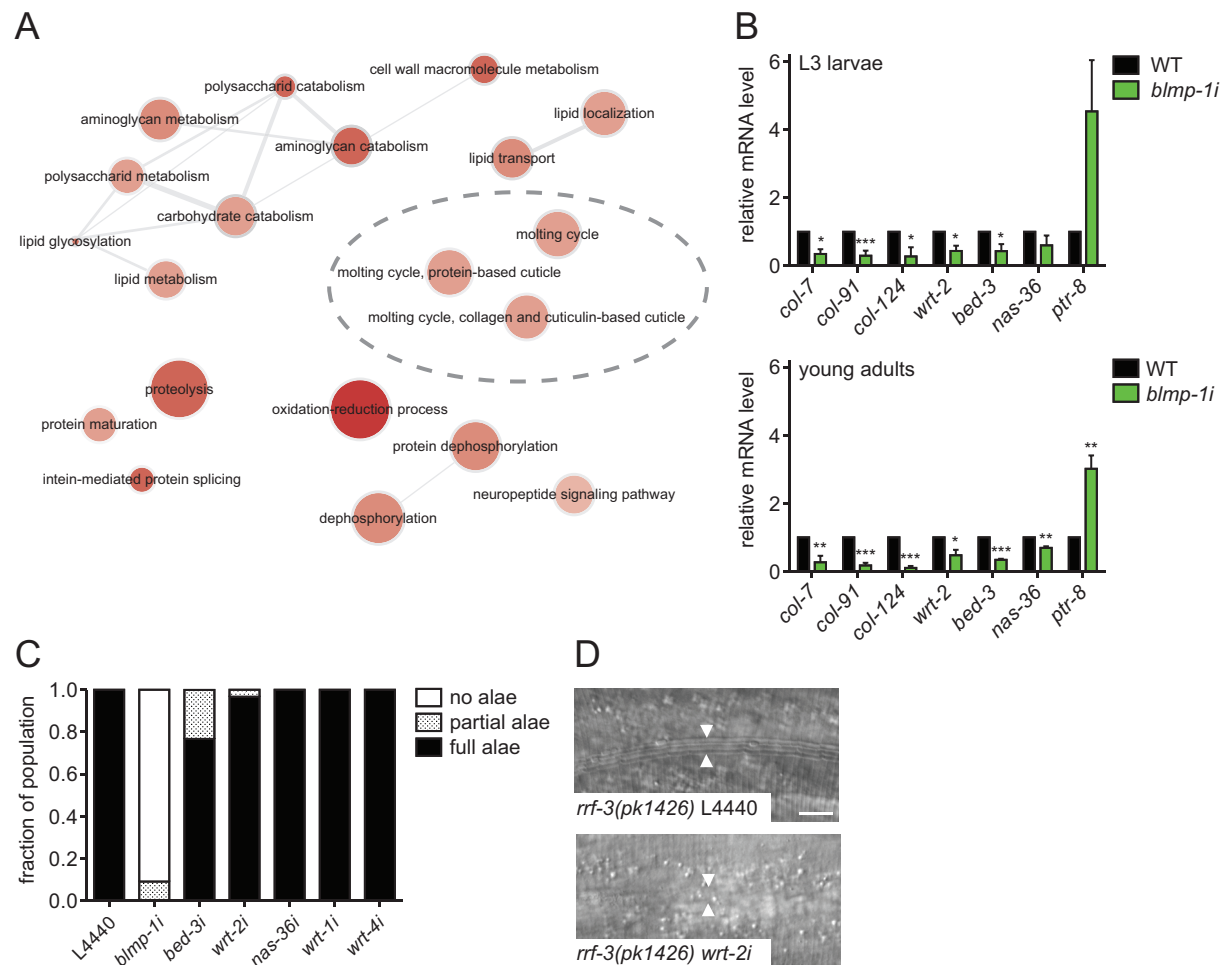


**Figure 28: BLMP-1 Controls Epidermal Maturation via Transcriptional Changes in Molting- and Cuticle Related Genes**

(A) Summary of gene-ontology/biological processes derived from DAVID analysis (Huang et al., 2009) of differentially regulated genes ( $q < 0.05$ , fold change  $\geq \pm 1.5$ ) in WT vs. *blmp-1* mutant animals from RNA-sequencing datasets ( $n = 3$ ). ReviGO was used for visualization of the resulting GO term classes and its semantic similarity (Supek et al., 2011). Bubble color, size, and line widths respectively indicate significance of enrichment, frequency of GO term in underlying data sets, and degree of similarity. More intense colors indicate a higher significance of enrichment. (B) qRT-PCR analysis of *blmp-1*-regulated molting and cuticle-related genes in L3 larvae and young adult worms.  $*P < 0.05$ ,  $**P < 0.01$ ,  $***P < 0.001$  (t-test). Mean  $\pm$  SEM ( $n \geq 3$ ). (C) *bed-3* and *wrt-2* depletion by RNAi hamper adult alae formation in only a small fraction of RNAi-sensitive *rrf-3(pk1426)* mutant animals ( $n > 15$ ). (D) DIC images of young adult *rrf-3(pk1426)* mutant animals grown on L4440 empty vector control or *wrt-2* RNAi. Arrowheads indicate seam cell positions, the origin of adult alae synthesis. Scale bar = 10  $\mu\text{m}$ .

In sum, these data strongly support the idea that *blmp-1* is a key regulator of *C. elegans* epidermal terminal differentiation, by transcriptionally regulating a set of molting and cuticle-related genes.

### 2.2.10 The DRE-1/BLMP-1 Interaction is Conserved to Mammals

Given the remarkable degree of conservation of both BLMP-1 and DRE-1, I next asked whether also human FBXO11 restrains human BLIMP-1 stability. Importantly, I found the regulation of BLMP-1 by DRE-1 to be evolutionary conserved. First, like the worm proteins, human BLIMP-1 specifically coprecipitated with human FBXO11 when coexpressed in cultured HEK293T cells, again only upon proteasome inhibition (Figure 29A and 29B). BLIMP-1 also weakly interacted with the closely related FBXO10, but not other controls (Figure 29A). Interestingly, the ability to bind BLIMP-1 was substantially reduced when the Q491L amino acid substitution identified in the *Jeff* mouse mutant was introduced into human *Fbxo11*, suggesting that the conserved region containing the point mutation may facilitate interaction (Figure 29A).

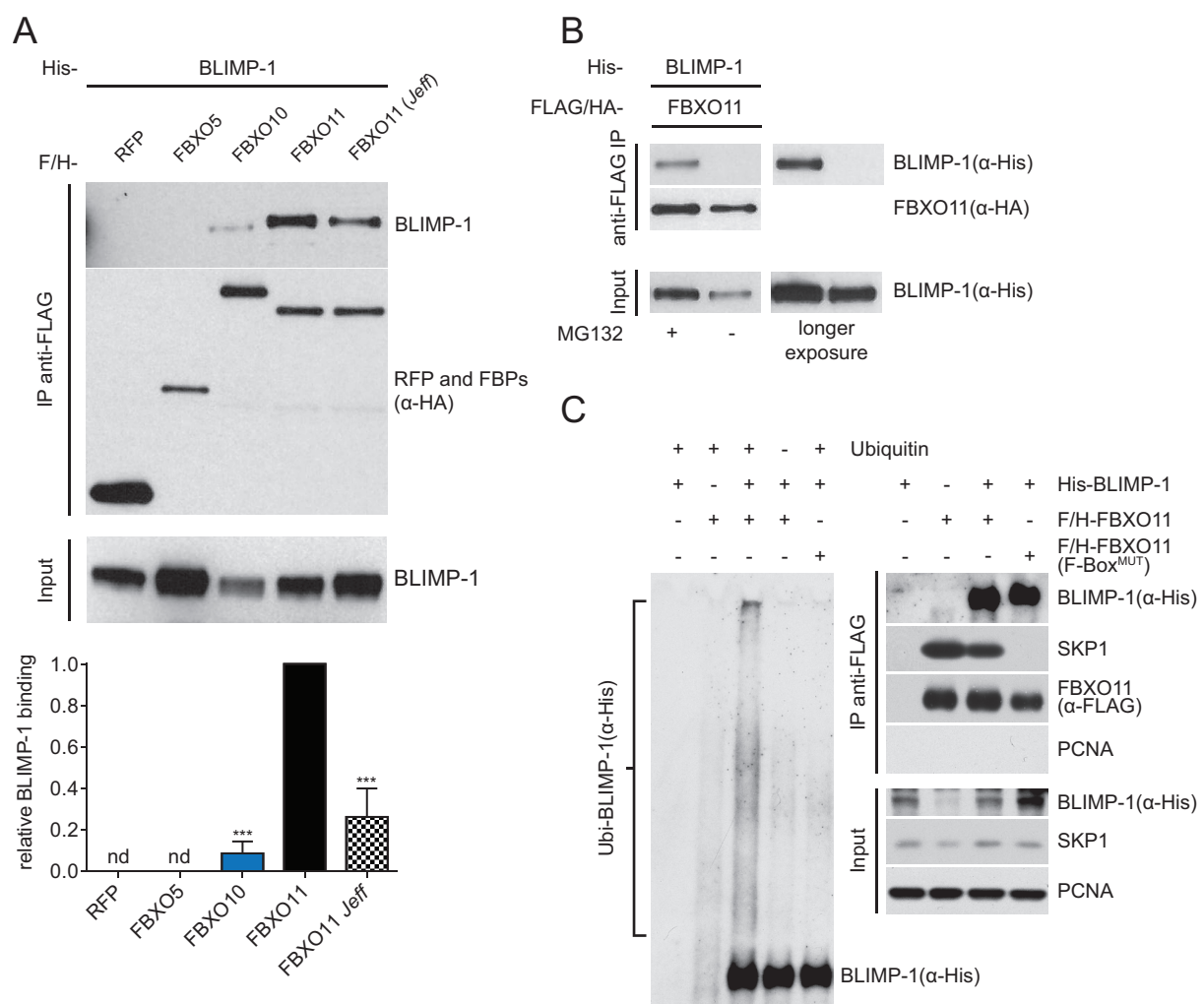


**Figure 29: Human FBXO11 Binds Human BLIMP-1 and Triggers its Ubiquitination**

**(A)** Anti-FLAG IP of human FLAG-HA-tagged (F/H) RFP, -FBXO5, -FBXO10, -FBXO11 and -FBXO11(Q491L/*Jeff*) from HEK293T cells treated with 15  $\mu$ M MG132. Human His-BLIMP-1 was coexpressed. Quantification of RFP/F-box-protein binding intensity to BLIMP-1 was normalized to BLIMP-1 input and FBXO11-BLIMP-1 association. \*\*\* $p$ <0.001 (ANOVA). Mean+SD (n=5). nd = not detectable. **(B)** Human His-BLIMP-1 coprecipitates with coexpressed F/H-FBXO11 from HEK293T cells only when treated with 15  $\mu$ M MG132. **(C, performed by L. Cermak)** HEK-293T cells were transfected with His-tagged BLIMP-1,

FLAG-tagged FBXO11 or -FBXO11(F-box<sup>MUT</sup>), and an empty vector as indicated. After immunopurification with anti-FLAG resin, *in vitro* ubiquitination of BLIMP-1 was performed in the presence of E1 and E2 enzymes. Where indicated, ubiquitin was added. Samples were analyzed by SDS-PAGE and immunoblotting (left panel). Immunoblots of whole-cell extracts and immunoprecipitations are shown in the right panel.

Second, in collaboration with Dr. Lukas Cermak from the Pagano laboratory at NYU, we could show that immunopurified FBXO11 promoted BLIMP-1 ubiquitination *in vitro* (Figure 29C). To this end, Dr. Cermak performed *in vitro* ubiquitination assays after coexpression of tagged FBXO11 and BLIMP-1 and immunopurification of SCF<sup>DRE-1</sup> complexes from HEK293T cells. Notably, the appearance of BLIMP-1 higher molecular weight species in these assays necessitated a functional F-box domain, which tethers FBXO11 to the SCF complex: F-box domain mutation (F-box<sup>MUT</sup>/V98A, C99A, F102A) abolished binding to the SKP1 adapter protein and consistently prevented BLIMP-1 ubiquitination (Figure 29C).

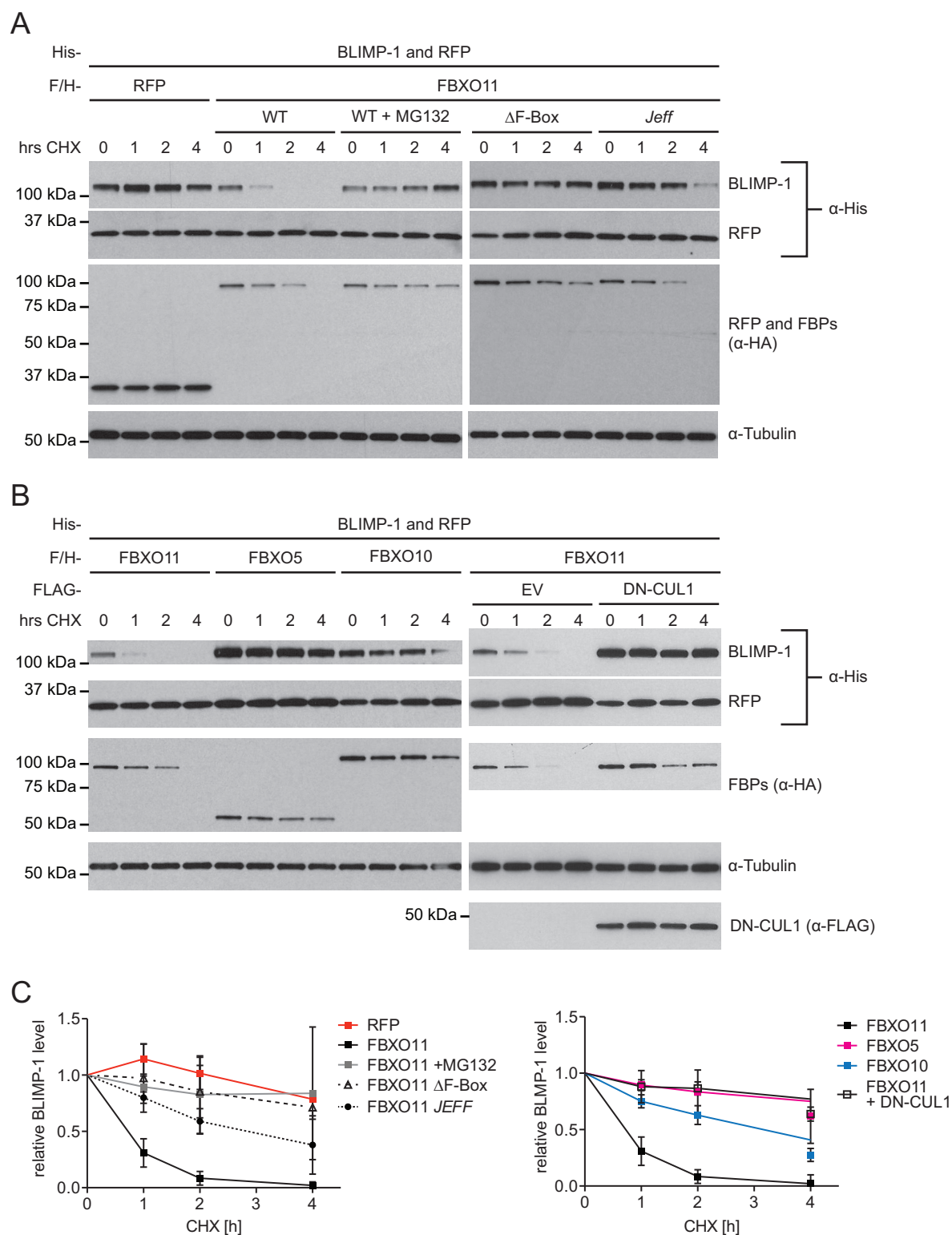


**Figure 30: The SCF<sup>FBXO11</sup> Complex Triggers Human BLIMP-1 Degradation via the Proteasome**

**(A+B)** FBXO11 promotes BLIMP-1 degradation. Human BLIMP-1 stability was assessed in HEK293T cells transfected with His-BLIMP-1 and -RFP in combination with either Flag-HA(F/H)-tagged RFP, -FBXO11  $\pm$  DN-CUL1(1-452), -FBXO11( $\Delta$ F-box), -FBXO11(Q491L/*Jeff*), FBXO5, or FBXO10. Cells were treated with cycloheximide (CHX) or CHX  $\pm$  15 $\mu$ M MG132 for 0, 1, 2 or 4 hrs as indicated prior to harvesting and analysis by SDS-PAGE and immunoblotting. **(C)** Human BLIMP-1 stability was quantified from  $\geq 3$  independent experiments (see A+B) and normalized to BLIMP-1 levels at 0 hrs CHX treatment and coexpressed His-RFP. Mean $\pm$ SD ( $n \geq 3$ ).

Third, like for the *C. elegans* counterparts, CHX treated cells showed progressive proteolysis of transfected human BLIMP-1 upon cotransfection of FBXO11, which strongly depended on a functional proteasome (Figure 30A and 30C). Rates of human BLIMP-1 proteolysis were significantly reduced by deletion of the FBXO11 F-box domain ( $\Delta$ F-box) or by introducing the amino acid substitution FBXO11/Q491L (Figure 30A and 30C). Furthermore, inclusion of a deletion mutant, dominant negative form of the SCF scaffold CUL1, but not other dominant negative Cullins, prevented FBXO11-dependent BLIMP-1 degradation (Figures 30B, 30C and 31). In accord with a low BLIMP-1 binding affinity, also FBXO10 overexpression slightly destabilized BLIMP-1 after CHX treatment, indicating that FBXO10 might also harbor a minor capability to target BLIMP-1 (Figure 30B and 30C).

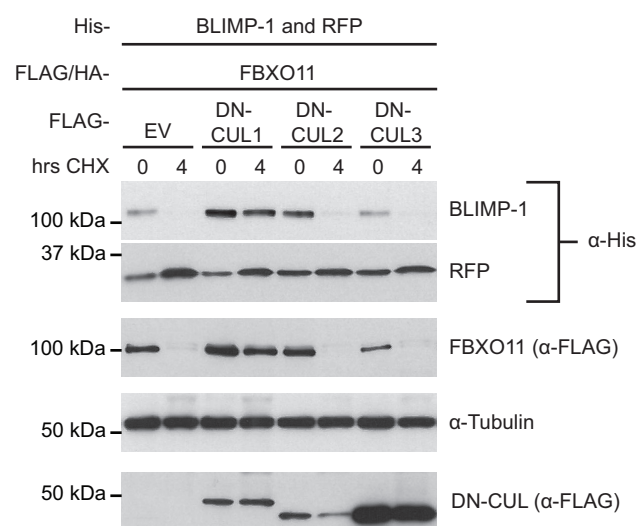


**Figure 31: Specifically DN-CUL1, but not other DN-CULs, Prevents FBXO11-Dependent BLIMP-1 Turnover**  
HEK293T cells were transfected with His-BLIMP-1 and -RFP in combination with F/H-tagged FBXO11  $\pm$  FLAG-DN-CUL1(1-452), -CUL2(1-427), or -CUL3(1-418). Transfected cells were treated with CHX for 0 or 4 hrs as indicated prior to harvesting and analysis by SDS-PAGE and immunoblotting.

Finally, in agreement with accelerated BLIMP-1 degradation Dr. Lukas Cermak found that short hairpin RNA (shRNA)-mediated depletion of FBXO11 in ARP1 multiple myeloma cells using two different shRNAs, led to stabilization of endogenous BLIMP-1 in the presence of CHX (Figure 32). ARP1 cells were used as BLIMP-1 plays a critical role in B cell maturation and also because it was one of few cell lines that showed detectable BLIMP-1 protein levels without additional stimulative treatments (Hardin et al., 1994).

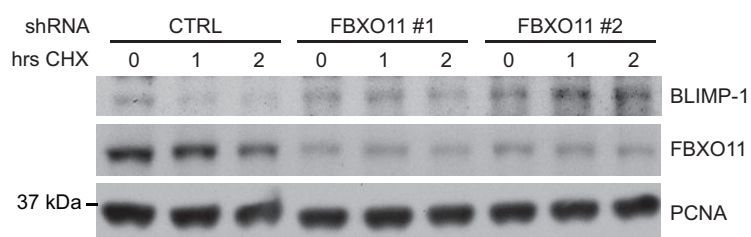


**Figure 32: FBXO11 Restrains Endogenous BLIMP-1 Levels in ARP1 Multiple Myeloma Cells**

**(Performed by L. Cermak)** Stability of endogenous BLIMP-1 was analyzed in ARP1 multiple myeloma cells infected with either viruses expressing two different FBXO11 shRNAs or an empty virus (CTRL), and selected for 72 hrs. Cells were then treated with CHX for 0, 1 or 2 hrs as indicated and protein extracts were analyzed by SDS-PAGE and immunoblotting.

Altogether, these experiments demonstrate that  $SCF^{FBXO11}$  mediates ubiquitin-mediated degradation of BLIMP-1, providing strong evidence for conserved proteolytic regulation across taxa.

## **Chapter 3 - DISCUSSION**

### 3.1 DRE-1 Substrates in *C. elegans*

CED-9/BCL2 was so far the only predicted substrate of DRE-1 in *C. elegans*, a hypothesis solely based on genetic interactions (Chiorazzi et al., 2013). In this work, I validated CDT-2 as a genetic interactor of *dre-1 in vivo* in *C. elegans* and discovered the zinc-finger transcriptional repressor BLMP-1 as a novel target of the highly conserved SCF<sup>DRE-1</sup> E3-ubiquitin ligase. My findings indicate that *dre-1* and *cdt-2* interact genetically to regulate the timing of cell cycle exit, while I found that *dre-1/blmp-1* work together to not only regulate developmental timing in the epidermis and gonad, but also affect molting, dauer diapause formation and adult lifespan in *C. elegans*. Remarkably, our data demonstrate that the *dre-1/blmp-1* interaction is conserved in human cells, suggesting that these two proteins might act together to control related processes across species.

Prof. Michele Pagano and colleagues identified a novel substrate of the SCF<sup>FBXO11</sup> complex, CDT2, which was known to control cell cycle progression and DNA damage responses (Abbas et al., 2013b; Abbas et al., 2013a; Rossi et al., 2013). As the two *C. elegans* counterparts, CDT-2 and DRE-1, specifically interacted in cultured cells, I used the nematode to validate the relation *in vivo*. My data show that *cdt-2* genetically interacts with *dre-1* for the process of adult alae formation, but not seam cell fusion or gonadal migration. Further my findings indicate that *dre-1* mutant alae gaps could arise from a *cdt-2*-dependent failure in cell cycle exit, as a marker of arresting cells, CKI-1::GFP, is exclusively absent underneath the alae gaps in mature worms. Since on its own, *cdt-2* depletion did not lead to overt heterochronic phenotypes in epidermis or gonad, it was not further studied with regard to heterochronic interactions. Taken together, my results support the notion that DRE-1/FBXO11 targets CDT-2/CDT2 across species, but they also clearly indicate that distinct DRE-1/FBXO11 substrates must accumulate to mediate the diverse developmental phenotypes of *dre-1* mutants.

Multiple lines of evidence argue that BLMP-1 constitutes a novel, and the first biochemically evidenced target of the SCF<sup>DRE-1</sup> complex in *C. elegans*. First, DRE-1 and BLMP-1 interact *in vivo* and when coexpressed in cultured cells. Second, BLMP-1::GFP and endogenous BLMP-1 levels are strongly elevated upon *dre-1* depletion, reduction of other SCF<sup>DRE-1</sup> complex components and inhibition of the proteasome. Third, although we failed to detect BLMP-1 ubiquitinated species *in vivo* and *in vitro* assays, BLMP-1 protein is substantially destabilized upon coexpression of DRE-1 in cell culture. Finally, *dre-1* and *blmp-1* show strong genetic interactions in epidermis and gonad: *blmp-1* is epistatic to *dre-1* heterochronic phenotypes in

both seam cell differentiation and gonadal migration, strongly suggesting that *blmp-1* acts downstream of *blmp-1* in a unified pathway. Interestingly, this genetic interaction also further extends to the life history traits of dauer formation and longevity. These data are in accord with my finding that *blmp-1* overexpression exacerbates *dre-1* mutant phenotypes, indicating that *dre-1* developmental alterations largely arise from increased BLMP-1 activity. Taken together, my findings demonstrate that BLMP-1 is specifically targeted for degradation by the SCF<sup>DRE-1</sup> complex.

## 3.2 The DRE-1/BLMP-1 Module Coordinates *C. elegans* Life

### History

DRE-1 and BLMP-1 work as a module to regulate several aspects of *C. elegans* life history (Figure 33). In particular, my studies establish *dre-1/blmp-1* as key regulators of epidermal and gonadal developmental timing. Our previous work demonstrated that *dre-1* loss of function induces precocious seam cell fusion and synthetic retarded gonadal migration defects. Here, I discovered *blmp-1* depletion to efficiently suppress both phenotypes. On its own, *blmp-1* mutation leads to phenotypes opposite to *dre-1*, namely retarded terminal differentiation of the seam cells (e.g. poor alae formation) on the one hand and precocious migration of gonadal dtcs on the other hand. The obtained phenotypes nicely correlate with BLMP-1::GFP levels in the corresponding tissues. While BLMP-1::GFP levels are shut down in the dtc in a *dre-1* dependent manner right before the dorsal gonadal turn, they transiently peak at the time of the seam cell fusion event in the epidermis. These findings suggest that high BLMP-1 levels in the gonad prevent its full maturation, whereas hypodermal BLMP-1 triggers epidermal terminal differentiation (Figure 33). Thus *blmp-1*, similar to its mammalian counterpart, mediates terminal differentiation in some tissues, but also controls intermediate stages of differentiation in others, presumably by regulating distinct transcriptional targets.

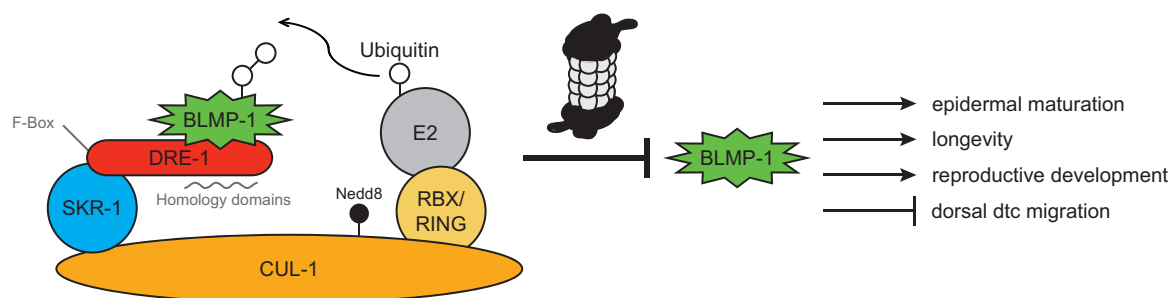


**Figure 33: DRE-1/BLMP-1 Coordinate *C. elegans* Developmental Timing and Other Life History Traits**

Model of DRE-1/BLMP-1 function in *C. elegans*: The SCF<sup>DRE-1</sup> E3-ubiquitin ligase complex controls BLMP-1 protein abundance via proteasomal degradation. Thereby *dre-1*-dependent BLMP-1 regulation not only times epidermal maturation and dorsal gonadal migration, but also affects other life history traits such as entry into dauer diapause and adult longevity.

Importantly, *blmp-1* genetically interacts with multiple heterochronic loci that govern the larval-to-adult transition. *blmp-1* loss of function enhances retarded (*let-7*, *mab-10/NAB*) and suppresses precocious (*lin-41/Trim71*, *lin-42/Period*, *hbl-1/Hunchback*, *sop-2/PcG-like*) heterochronic mutants for phenotypes in the epidermal seam cells. Similarly also *dre-1* was shown to act at the larval-to-adult transition, enhancing impenetrant *hbl-1* and *lin-41* precocious phenotypes and partially suppressing *let-7* retarded terminal seam differentiation (Fielenbach et al., 2007). Altogether, these data indicate that *dre-1/blmp-1* could work in parallel to both *hbl-1* and *lin-41*, acting downstream of *let-7* (Figure 34). Furthermore *lin-29* was shown to be epistatic to *dre-1* (Fielenbach et al., 2007), suggesting that the *dre-1/blmp-1* module acts upstream or parallel to *lin-29* (Figure 34). The fact that *lin-29* expression was found to be preceded in only a minor fraction of *dre-1* mutants (less than 10%) might argue that *dre-1* acts both through and independent of *lin-29*, maybe by regulating distinct targets (Fielenbach et al., 2007). As *blmp-1* mutation did not regulate *lin-29* expression according to our RNA-sequencing data sets, *blmp-1* might act largely parallel to *lin-29* (Figure 34).

Taken together, these genetic interactions firmly place the *dre-1/blmp-1* module in general and the new heterochronic gene *blmp-1* in particular within the heterochronic circuit controlling late larval development (Figure 34). As not all alleles used were null and ts alleles were observed at semi-permissive temperatures, further analyses are required to ultimately place *dre-1/blmp-1* within the seam cell heterochronic network. Understanding how these genetic interactions translate into molecular regulatory events should also be interesting to dissect in the future.

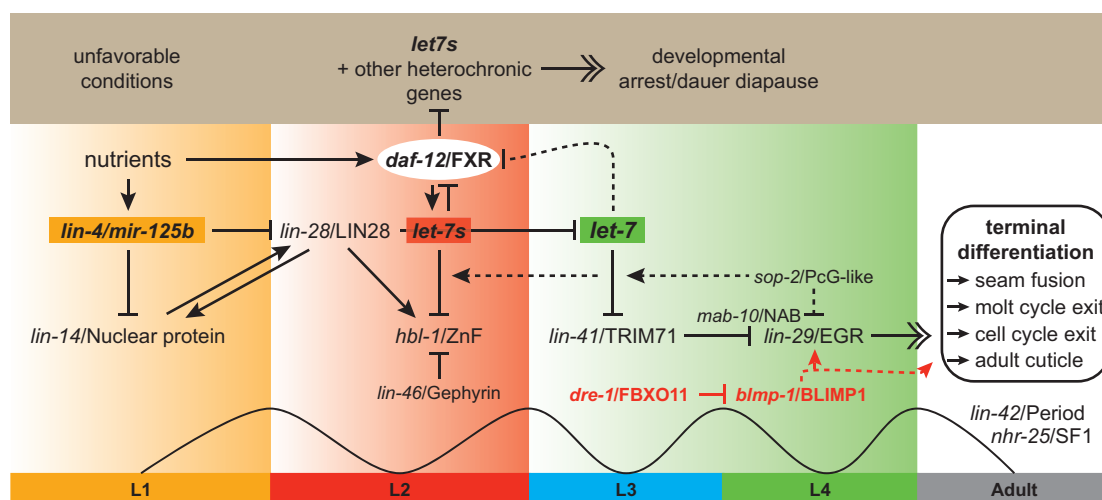


**Figure 34: *dre-1/blmp-1* Act at a Late Step in the *C. elegans* Heterochronic Seam Circuitry**

Genetic epistasis and synergy experiments place both *dre-1* and *blmp-1* at a late step in the seam cell heterochronic network. My data and previous results indicate that the *dre-1/blmp-1* module acts downstream of the *let-7* microRNA and mostly upstream of *lin-29*, but it might also have parallel functions to this key terminal maturation factor.

### 3.3 Evolutionary Conserved Functions of DRE-1/BLMP-1

Importantly, the DRE-1/BLMP-1 interaction is conserved to mammals. First, I found human BLIMP-1 to specifically coprecipitate with FBXO11 and at low levels with FBXO11's paralog FBXO10. Second, FBXO11 promotes BLIMP-1 ubiquitination *in vitro* in a manner that strongly depends on FBXO11's association to the SCF complex via its F-box domain. Third, functional FBXO11 strongly destabilizes human BLIMP-1 upon cotransfection and blockage of nascent protein synthesis in cultured cells. Conversely, shRNA mediated depletion of FBOX11 in the ARP1 multiple myeloma cell line leads to stabilization of endogenous BLIMP-1. Altogether, these data demonstrate that the interaction and degradation function of DRE-1/BLMP-1 is evolutionarily conserved (Figure 35).

Interestingly, many of *C. elegans* heterochronic genes governing seam cell development are remarkably conserved and have mammalian counterparts that regulate skin stem cell homeostasis, such as *blmp-1/BLIMP-1* itself, *daf-12/FXR/LXR/VDR*, *lin-4/mir-125b*, *let-7*, *lin-42/Period*, and others (Cianferotti et al., 2007; Horsley et al., 2006; Janich et al., 2011; Magnúsdóttir et al., 2007; Zhang et al., 2011). In particular, BLIMP-1 specifies a stem cell population in the sebaceous gland and triggers keratinocyte terminal differentiation in the epidermis, a transition from the granular to the cornified layers, which form the outer barrier toward the environment (Magnúsdóttir et al., 2007; Horsley et al., 2006). Therein, BLIMP-1 and the vitamin D receptor were shown to be downregulated by the microRNA *lin-4/mir125b*

in skin stem cells to prevent their differentiation. Together with previous reports, my data show that *C. elegans blmp-1* specifies terminal differentiation in the epidermis and that this regulation could stem from *blmp-1*-dependent transcriptional changes in molting and cuticle-related genes (Zhang et al., 2012). Moreover, dauer epistasis experiments place *blmp-1* at a late step in the dauer signaling network, in close proximity to DAF-12/FXR/LXR/VDR, thus bearing remarkable similarity to the situation in the mammalian skin. Interestingly, FBXO11 too is expressed in the skin (Hardisty-Hughes et al., 2006; Dr. Sarah Wickström, personal communication), suggesting FBXO11 might modulate BLIMP-1-dependent skin maturation by controlling its stability (Figure 35).

Although BLIMP-1 is described as a key maturation factor in mammals, our findings in the nematode might add further perspectives to BLIMP-1 function. In *C. elegans*, DRE-1/BLIMP-1 not only orchestrate developmental timing, but also affect organism-wide fates such as molting, dauer diapause, and adult longevity. Previously, *dre-1* was shown to be required for programmed death of the tail-spike cell and *blmp-1* was uncovered as regulator of the male tail tip morphogenesis (Chiorazzi et al., 2013; Nelson et al., 2011). Altogether, the rich signaling circuits governing *C. elegans* developmental timing, molting, dauer formation, longevity, and apoptosis might add novel aspects to BLIMP-1 function in mammalian stem cells and maturation. Therein, FBXO11/BLIMP-1 might not only function as switch regulating cellular differentiation, but could also be viewed as a developmental timing module that specifies distinct states of differentiation in a tissue-specific fashion.

Indeed, the notion that DRE-1/BLIMP-1 comprise a conserved functional module may have several implications in mammals (Figure 35). Among others, BLIMP-1 specifies primordial germ cell fates by repressing somatic transcriptional programs (Ohinata et al., 2005; 2009). More recently, it has been shown to not only specify pluripotent cell fates, but also to have the potential to partially reprogram somatic cells (Nagamatsu et al., 2011). Furthermore, BLIMP-1 is a key regulator of forelimb development, pharyngeal and heart morphogenesis, as well as T cell differentiation (Martins and Calame, 2008; Vincent et al., 2005). Interestingly, FBXO11 too is expressed in a variety of BLIMP-1 target tissues including the heart during morphogenesis as well as hematopoietic cells (Hardisty-Hughes et al., 2006). By inference, FBXO11 could work in tandem with BLIMP-1 in at least some of these contexts by controlling its turnover (Figure 35).

Despite its remarkable evolutionary conservation rather little is known about FBXO11 function in mammals. Its loss of function results in perinatal lethality paired with strong developmental abnormalities during facial morphogenesis in *Jeff* mutant mice (Hardisty-Hughes et al., 2006). Moreover, in mice and men *Fbxo11* mutation has been closely linked to the onset of otitis media, a chronic inflammation of the inner ear. My results indicate that aberrantly elevated BLIMP-1 levels could mediate some of these malformations, since BLIMP-1 degradation is substantially impaired upon introduction of the Q491L/*Jeff* point mutation into human *Fbxo11*. Interestingly, although not shown mechanistically yet, also CDT2 misregulation could contribute to the development of these malformations. FBXO11-dependent degradation of CDT2 stabilizes Set8, which in turn stimulates epithelial cell migration (Abbas et al., 2013a). Therefore, enhanced Set8 degradation in FBXO11 mutants might result in impaired epithelia cell migration, which has been linked to the development of cleft palates (Figure 7) (Johnston and Bronsky, 1995). Furthermore, Set8 is required to restrain TGF- $\beta$  responses by triggering pSmad2 dephosphorylation via an unknown mechanism (Abbas et al., 2013a). Likewise, FBXO11 mutant mice show increased pSmad2 levels, indicating altered TGF- $\beta$  signaling, which could stem from a lack of CDT2 degradation and thus reduced Set8 levels (Tateossian et al., 2009; Abbas et al., 2013a). These observations could directly link misregulated CDT2 to inflammatory responses (Yoshimura et al., 2010) that could to some measure contribute to the onset of chronic inner ear inflammation, whereas the function of potentially elevated BLIMP-1 or BCL6 levels in this context are yet unknown (Figure 35).

In addition to the *Jeff* mutant mice phenotypes, *Fbxo11* mutation has been found in a variety of cancers (Richter et al., 2012; Duan et al., 2012; Stransky et al., 2011; Kan et al., 2010; Yoshida et al., 2011). Recently, Duan et al. could show that FBXO11 plays a critical role in preventing tumorigenesis in the immune system by degrading BCL6 (Duan et al., 2012). FBXO11 loss results in aberrantly elevated BCL6 levels, a hallmark of many large B cell lymphomas (Basso and Dalla-Favera, 2012). In a healthy state, BCL6 maintains germinal center B cells, which constitute an intermediate step of B cell differentiation specialized for proliferation and affinity maturation (Crotty et al., 2010). Also BLIMP-1 plays a critical role during immune cell development. In contrast to its closely related Zn-finger protein BCL6, BLIMP-1 promotes terminal differentiation of B cells toward antibody-secreting cells (plasma cells) (Turner et al., 1994; Crotty et al., 2010). Thereby BCL6 and BLIMP-1 function as antagonistic self-reinforcing switch by driving cognate transcriptional programs. Also in T cells BCL6 and BLIMP-1 act antagonistically to control the memory and effector

differentiation of both helper and cytotoxic T cells (Crotty et al., 2010). In lymphocytes, BCL6 defines a cellular state of high proliferative capacity, while BLIMP-1 expressing lymphocytes exhibit low proliferative capacity and a highly active secretory machinery. Interestingly, BLIMP-1 mutation has been also linked to tumorigenesis (Hangaishi and Kurokawa, 2010): in a subclass of large B cell lymphomas (activated B cell type, ABC) BLIMP-1-controlled differentiation is frequently impaired by distinct mechanisms all ultimately preventing BLIMP-1 function (Mandelbaum et al., 2010). In contrast, elevated BLIMP-1 levels have been associated with tumorigenesis in T cell-derived tumors (Zhao et al., 2008). In sum, FBXO11 targets both BCL6 and BLIMP-1 (this work) for proteasomal degradation. However, how this proteolytic function is coordinated within healthy immune lineages and potentially impaired in tumorigenesis remains to be elucidated. One could speculate that FBXO11 adds an additional layer of regulation to the critical transcriptional coordination of lymphocyte maturation (Figure 35). Consequentially, FBXO11 dysfunction might result in a detrimental imbalance of BCL6/BLIMP-1 protein that might lead to the formation of malignant tumors. Interestingly, also FBXO10 degrades a tumor suppressor affecting the immune system, BCL2 (Chiorazzi et al., 2013), suggesting a general role for FBXO10/11 complexes in immunity and lymphoma formation. The fact that I found FBXO10 to harbor a low capability to destabilize BLIMP-1 might indicate that FBXO10 and -11 even have partially redundant functions or that they are additionally regulated by modification or spatial separation. In particular, FBXO10 is predominantly expressed in the cytoplasm, while FBXO11 is largely nuclear, supporting the latter hypothesis (Chiorazzi et al., 2013).

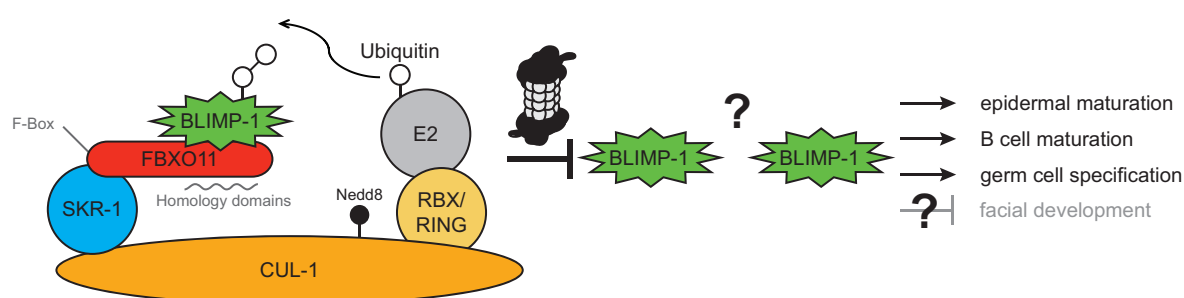


**Figure 35: FBXO11 Could Modulate BLIMP-1 Dependent Processes in Mammals by Controlling BLIMP-1 Turnover**

Model of FBXO11/BLIMP-1 function in mammals: FBXO11 triggers BLIMP-1 degradation and could by inference play a key role in BLIMP-1 dependent maturation processes such as B cell and epidermal maturation or primordial germ cell specification. Similarly, BLIMP-1 might be involved in developmental alterations associated with FBXO11 loss including facial malformations.

Taken together, I discovered BLIMP-1 as a substrate of the SCF<sup>DRE-1</sup> complex, modulating developmental timing and other life history traits in *C. elegans*. Given the remarkable degree of structural and functional conservation of these two proteins, we hypothesize that the

FBXO11/BLIMP-1 module could similarly regulate metazoan cellular fate decisions across tissues.

## **Chapter 4- SIGNIFICANCE AND**

## **FUTURE PERSPECTIVES**

## 4.1 Significance

The identification and characterization of F-box protein substrates still remains one of the biggest challenges in the field of ubiquitin-mediated proteolysis. Here, I used the model organism *C. elegans* to test *in vivo* functions of a newly identified F-box protein substrate, CDT2. Moreover, I uncovered a novel target of the F-box protein DRE-1 using a genetic approach in *C. elegans*. Importantly, I could closely link the obtained degradation function to developmental progression in epidermis and gonad, by monitoring the substrate abundance *in vivo* over time. My findings not only unraveled a novel DRE-1 substrate, but also establish *blmp-1* as a new heterochronic gene. The remarkable conservation of heterochronic gene structure and function in general, and *dre-1* as well as *blmp-1* in particular, suggest that also FBXO11/BLIMP-1 work as a global switch controlling metazoan maturation in a variety of tissues. In sum, this work furthers our understanding of post-translational control of developmental timing and might give new insights into FBXO11 function in health and disease states, thus constituting a solid basis for groundbreaking future studies.

## 4.2 Future Perspectives

Based on this work one could imagine a variety of exciting follow-up studies. In this final section I will describe several potential future directions.

### 4.2.1 Characterization of the FBXO11-Substrate Interaction Site

A central question that arises from our work is what is the biochemical nature of the FBXO11-substrate interaction site? An emerging body of evidence from Pagano's group and my study suggest that the CASH domains of FBXO11 mediate substrate binding. First, I found that FBXO11 Q491L mutation (*Jeff*) within the second CASH domain hampers BLIMP-1 binding and degradation. Second, I found a point mutation in the first CASH domain of *C. elegans* DRE-1 (*dh99*: G514S) to result in synthetic lethality upon BLIMP-1::GFP overexpression, while the *blmp-1::gfp* transgene could be recovered in the *dre-1(dh279)* (Q824STOP) allele, which lacks only the C-terminal part of the last CASH domain and the ZnF-UBR-like domain. Finally, Pagano and colleagues recently showed that specifically FBXO11 mutations within the CASH domains impair BCL6 degradation (Duan et al., 2012). Altogether, these data indicate that CASH domains of FBXO11 bind distinct substrates, but the mechanism of substrate recognition, in particular for BLIMP-1 and BCL6, remains poorly understood.

To further understand the molecular details underlying substrate recognition by FBXO11, the FBXO11-BLIMP-1 interaction site should be characterized in more detail. The use of first deletion and then point mutated versions of BLIMP-1 in coimmunoprecipitation and protein stability assays could help to identify the degron and the ubiquitinated Lys residue(s) within BLIMP-1. Studies of the CDT2-FBXO11 interaction uncovered a novel mechanism of substrate recognition, whereby substrate phosphorylation prevents its ubiquitination (Rossi et al., 2013). Similar investigations with BLIMP-1 and the first identified FBXO11 substrate BCL6 might unravel whether this ‘phospho-inhibited degron’-recognition is shared by all known FBXO11 substrates. In particular, the specific recognition of BLIMP-1 and BCL6 might be key to understand their potential regulation in the context of B cell maturation. Moreover, further molecular details on the FBXO11-substrate interaction site could unravel a specific degradation motif, that would allow identification of potential novel DRE-1/FBXO11 substrates via a bioinformatics approach, as successfully applied for SEL-10/FBXW7 (Ia Cova and Greenwald, 2012). Finally, as shown for CDT2, such a specific degradation motif might further inform about enzymes involved in post-translational modification prior to ubiquitination such as kinases or phosphatases (Rossi et al., 2013).

#### 4.2.2 Investigation of Upstream Regulators

Another key question is what are the critical upstream regulators of BLIMP-1 protein stability? In particular my findings in *C. elegans* epidermis, where DRE-1 levels are rather constant while BLIMP-1 levels show a transient peak, point to other instructive components or cofactors that contribute to BLIMP-1 regulation. Their identification might further inform coordination of developmental progression across species. Interestingly mammalian BLIMP-1 has recently been shown to be sumoylated by SUMO-1 at Lys816 (Shimshon et al., 2011; Ying et al., 2012). This modification is catalyzed by the E3 SUMO-protein ligase PIAS1 and was on the one hand reported to facilitate BLIMP-1’s proteolytic degradation and on the other hand shown to enhance BLIMP-1 dependent transcriptional repression during B cell maturation (Shimshon et al., 2011; Ying et al., 2012). How and whether BLIMP-1 sumoylation affects FBXO11-dependent BLIMP-1 degradation remains to be elucidated. Notably, the affected Lys residue is not conserved in nematodes, indicating that another Lys or another yet unidentified type of BLIMP-1 modification might contribute to the regulation of BLIMP-1 function and stability in *C. elegans* (Tunyaplin et al., 2000).

Although one might gain initial hints about additional BLIMP-1 regulators from the characterization of the FBXO11-BLIMP-1 interaction site, a genetic approach in *C. elegans*

would certainly be very powerful. As already initiated in this study, one could screen phosphatase and kinase RNAi libraries for augmentation of BLMP-1::GFP levels *in vivo*, assuming phosphorylation to prevent or support substrate recognition and subsequent degradation. Alternatively, one could test a panel of kinase inhibitors for their potential to stabilize or destabilize BLMP-1/BLIMP-1 *in vivo* in *C. elegans* or in a cell-based system. This approach was successfully applied for the identification of kinases phosphorylating the FBXO11 substrate CDT2 (Rossi et al., 2013). In a more unbiased approach one could perform EMS mutagenesis in BLMP-1::GFP overexpressing worms looking for modulation of expression (Jorgensen and Mango, 2002). In general, EMS mutagenesis has certain advantages over RNAi-based screens, since it is not limited by the drawbacks associated with RNAi technology, such as targeting only coding sequences, incomplete knockdown rates resulting in many false negatives, and the inability to activate genes. However, this particular screen is difficult because of the weak BLMP-1::GFP signal, which does not allow high-throughput analysis of BLMP-1 levels and would rely on visual screens under the compound microscope. Alternatively, one could screen for the appearance of molting or gonadal migration defects as *blmp-1* overexpression provokes both defects upon additional *dre-1* depletion. Therefore one would expect to find mutations in *dre-1* and other SCF complex components, as well as unknown modulators of BLMP-1 abundance including microRNAs, which were shown to target mammalian BLIMP-1 (Thiele et al., 2012; Zhang et al., 2011). Notably, this latter approach using synthetic phenotypes as readout assumes strongly elevated BLMP-1 levels to be causative for the molting and gonadal migration defects that I observed in *blmp-1* overexpressors upon *dre-1* depletion. However, these defects could also be a result of multiple elevated DRE-1 substrates combined with BLMP-1 overexpression.

Besides BLMP-1, DRE-1 levels are also tightly controlled particularly in the dtcs where they increase during the L2-to-L4 larval stages. One could imagine *dre-1* expression being induced or a repressor action to be released by the mid-L2 stage, when DRE-1 accumulates to trigger BLMP-1 degradation. Interestingly, *dre-1* mRNA contains multiple microRNA target sites, indicating that microRNA-mediated repression might contribute to the regulation of dtc migration through *dre-1/blmp-1* (Fielenbach et al., 2007). To test this hypothesis *dre-1*- and *blmp-1::gfp* reporter lines could be studied in microRNA mutant backgrounds that potentially target *dre-1*, including *mir-2*, *mir-59*, and *mir-71* (Fielenbach et al., 2007).

### 4.2.3 Further Identification of Downstream Effectors

Because BLMP-1 is a transcriptional regulator, a natural question arising from our studies is, what are the BLMP-1-regulated targets important for maturation? Through RNA-sequencing and qRT-PCR we showed BLMP-1 to target a set of molting and cuticle-related genes in *C. elegans*, consistent with a general role in the molt cycle and the synthesis of the adult cuticle (Zhang et al., 2012). In initial RNAi knockdown experiments with some of these targets, no candidate target depletion could fully recapitulate BLMP-1 epidermal differentiation defects, indicating that we have yet to further functionally identify specific genes that mediate BLMP-1's effects. In mammals, a variety of BLIMP-1 targets have been identified across tissues. For example BLIMP-1 resides at the c-myc promoter to block its transcription, thereby preventing proliferation during B cell maturation (Lin et al., 1997). Overall, BLIMP-1 is thought to switch-off whole gene expression programs such as mature B cell programs during B cell differentiation on the one hand and somatic programs during primordial germ cell specification on the other hand (Vincent et al., 2005; Ohinata et al., 2005; Shaffer et al., 2002). However, how BLIMP-1 fulfills these highly context-specific functions remains poorly understood. In particular, germ cell development involves major epigenetic remodeling, which strongly relies on BLIMP-1 function (Surani et al., 2007). Although BLIMP-1 harbors a SET domain (a domain generally involved in Lys methylation), BLIMP-1 itself bears no intrinsic enzymatic activity (Ancelin et al., 2006; Dillon et al., 2005). Instead, it cooperates with epigenetic regulators to control transcription and epigenetic remodeling (Su et al., 2009; Ancelin et al., 2006; Yu et al., 2000; Gyory et al., 2004; Surani et al., 2007). Therefore, a distinct set of cofactors present in different tissues might allow BLIMP-1 context-specific action. Similar context-specific activities might hold for the distinct developmental fates triggered by BLMP-1 in *C. elegans*. Moreover, one could speculate that also in *C. elegans* epigenetic regulation, potentially through BLMP-1, directs developmental progression and differentiation. Thereby certain epigenetic traits might function as cellular memory reflecting the current developmental state. In this context dauer diapause signaling, including *daf-12* and now also *blmp-1*, would be of special interest as progression through the dauer diapause to a certain extent erases developmental memory, since heterochronic mutants develop normally upon passage through dauer (Liu and Ambros, 1991; Euling and Ambros, 1996).

In sum, the identification and characterization of BLMP-1 downstream effectors in the nematode could help illuminate coordination of developmental timing in *C. elegans* and also

further elucidate the complex regulation of BLIMP-1 targets during cell fate specification in mammals. To this end, RNA-sequencing and ChIP-sequencing experiments should be repeated in young adult worms, where we obtained defects in adult alae synthesis, since our data from L3 larvae, as well as existing ChIP-sequencing data from L1 larvae (Niu et al., 2011) might not fully reflect BLMP-1 targets during *C. elegans* maturation.

In particular, terminal maturation of seam cells is ultimately induced by the Zn-finger transcription factor LIN-29 (Rougvie and Ambros, 1995). Despite BLMP-1 and LIN-29 being closely related Zn-finger proteins, LIN-29 is not directly regulated by DRE-1 (this work). Instead LIN-29 was shown to bind the NAB transcriptional cofactor MAB-10 via a motif similar to the R1 domain of mammalian NAB transcription factors EGR1-3 (Harris and Horvitz, 2011). Interestingly, *C. elegans* and also human BLMP-1/BLIMP-1 harbor an amino acid stretch very similar to the MAB-10 interaction site of LIN-29 (Figure 36). Thus BLMP-1/BLIMP-1 might cooperate with NAB transcriptional cofactors such as *mab-10* in *C. elegans*, which could be tested directly by coimmunopurification experiments.

```

EGR1: 281 TQQPSLTPLSTIKAFAT 297
LIN-29: 390 PGFNMITPLENIQRYNG 406
BLMP-1: 359 LGNFYASPLVDFKEFMR 375
BLIMP-1: 266 LYRSNISPLTSEKDLDD 282

```

**Figure 36: BLMP-1 and BLIMP-1 Show Sequence Similarity to the MAB-10 Interaction Site of LIN-29.**

Multiple sequence alignment of an amino acid stretch within the R1 domain of EGR1 with the MAB-10 interaction site of LIN-29 and related amino acid sequences within *C. elegans* BLMP-1 and human BLIMP-1.

In this context, it could also be elucidated whether BLMP-1 acts through LIN-29 or in a distinct branch to direct terminal differentiation in the epidermis, by studying LIN-29 expression in a *blmp-1* mutant background.

Besides seam cell differentiation we found *blmp-1* to direct cellular migration in *C. elegans* gonad, as its aberrant accumulation prevents dorso-ventral migratory events. The Dtc's, which lead gonad migration, are only two out of about 1000 cells of the worm, which may preclude identification of potential *blmp-1* target genes from whole worm lysates. However, previous work from the group of Prof. Joseph Culotti found transcriptional upregulation of the netrin receptor *unc-5/UNC5* to initiate the dorsal gonadal turn (Su et al., 2000), which by inference render it a potential *blmp-1* target. As initial experiments using a *unc-5::lacZ* reporter gave inconclusive results, however, *blmp-1* targets regulating dtc migration still remain elusive. Importantly, BLIMP-1 was shown to also affect cellular migration in mammals (Kurimoto et al., 2008), pointing out parallels between worms and humans and highlighting the importance of target gene analysis across species. Taken together, identification of *blmp-1* targets and cofactors might help to further understand the regulation of developmental timing, dauer

diapause, molting, and aging in *C. elegans*, and also give further insights into BLIMP-1 regulated processes in mammals.

#### 4.2.4 Explore FBXO11 and BLIMP-1 Function During Tissue Maturation

As extensively described above, *dre-1* and *blmp-1* function together to regulate developmental timing and other life history traits in *C. elegans*. Due to the remarkable degree of structural and functional conservation, one could speculate that the FBXO11/BLIMP-1 module coordinates related processes in mammals. In mice, BLIMP-1 controls B cell maturation, limb formation, skin maturation, pharyngeal and heart morphogenesis, as well as gametogenesis (Turner et al., 1994; Robertson et al., 2007; Magnúsdóttir et al., 2007). Likewise, BLIMP-1 deficient embryos die during mid-gestation and exhibit strong developmental abnormalities including brachial arch, hemorrhage and placental defects as well as complete loss of primordial germ cells (Vincent et al., 2005). In zebrafish, BLIMP-1 additionally specifies neural crest cells and drives anteroposterior axis formation, wherein similar BLIMP-1 requirements were not found in mice (Wilm and Solnica-Krezel, 2005;; Vincent et al., 2005). Surprisingly, BLMP-1 protein is not essential during *C. elegans* morphogenesis, indicating that BLIMP-1 functions and requirements expanded throughout evolution. However, the regulation of BLMP-1/BLIMP-1 protein by DRE-1/FBXO11 is highly conserved, supporting the notion that FBXO11 might govern multiple BLIMP-1-mediated differentiation processes in mammals. To directly test this hypothesis, B cell or skin stem cell differentiation could be studied upon FBXO11 depletion or overexpression using an *in vitro* system (Stocker, 1977; Karasek, 1975).

Like BLIMP-1, also FBXO11 deficiency is linked to a variety of developmental abnormalities, such as craniofacial and respiratory defects (Hardisty-Hughes et al., 2006). The etiology of craniofacial clefts is not yet fully understood, but they could arise from a failure in neural crest cell migration during embryogenesis (Chai and Maxson, 2006). Interestingly, comparable malformations have been observed in zebrafish lacking functional BLIMP-1 (Robertson et al., 2007). Although one would rather expect an inverse correlation between FBXO11 and BLIMP-1, the fact that both were already associated with craniofacial development is striking and suggests that aberrant BLIMP-1 action might contribute to FBXO11 mutant phenotypes. This hypothesis is strongly supported by my finding that introduction of the FBXO11 *Jeff* mutation to human FBXO11 almost entirely abrogates its ability to degrade human BLIMP-1. Furthermore *Blimp-1* was found to be expressed in related tissues (Chang et al., 2002). However, *in vivo* data from FBXO11 deficient mice

would be required to confirm elevation of BLIMP-1 protein. Therefore, one should first follow endogenous BLIMP-1 levels in specific tissues of *Jeff* mutant mice such as the skin or the palate shelves throughout development using a validated BLIMP-1 antibody (e.g. 3H2-E8 (Chang et al., 2002)). Additionally, one should carefully observe skin morphology, primordial germ cell specification, and B cell maturation in these mice, processes, strongly depending on BLIMP-1. However, BLIMP-1 could in some contexts be redundantly regulated *in vivo*, which would mask FBXO11-dependent regulation. Similarly, also CDT2 and BCL6 levels should be analyzed in FBXO11 deficient mice, as they could as well contribute to the malformations and the onset of chronic inner ear inflammations observed in these mice (Hardisty-Hughes et al., 2006; Hardisty et al., 2003). In particular, CDT-2 constitutes an interesting candidate as its aberrant stabilization was shown to affect cellular migration and also TGF- $\beta$  signaling, one of the key pathways mediating inflammation (Yoshimura et al., 2010). Both might directly link to craniofacial abnormalities and the onset of otitis media, respectively. So far, elevated BCL6 levels are predominantly associated with tumorigenesis, but might also contribute to *Jeff* mutant mice developmental alterations (Duan et al., 2012). To dissect the effects of the different substrates with regard to craniofacial development or inner ear inflammation, one could make use of degradation-resistant mutant versions of the three substrates, such as CDT2(T464D) (Rossi et al., 2013). Expressing them in tissue-specific contexts might recapitulate FBXO11 loss of function phenotypes, which would demonstrate a direct connection to the disease state. However, these experiments are restrained by the limited knowledge about the molecular details underlying BCL6 and BLIMP-1 degradation via FBXO11. Therefore the characterization of FBXO11-substrate interaction sites as described above also constitutes an important step toward the understanding of FBXO11 dysfunction in disease states.

#### 4.2.5 Identification of Additional DRE-1/FBXO11 Substrates

The identification of F-box protein substrates significantly contributes to our understanding of specific protein turnover in health and disease states. Although many substrates have been identified within the last 15-20 years, dozens of F-box proteins remain orphan receptors or the identified substrates only poorly explain associated phenotypes. DRE-1/FBXO11 quite recently emerged as a crucial regulator of developmental progression and tumorigenesis (Hardisty-Hughes et al., 2006; Duan et al., 2012). Since then, two substrates were described in *C. elegans*, CDT-2 and BLIMP-1, and three in mammals, CDT2, BLIMP-1, and BCL6. Interestingly, the closest *C. elegans* homolog of BCL6 also is BLIMP-1, suggesting that

mammalian BLIMP-1 and BCL6, as well as *C. elegans* BLMP-1 evolved from a common precursor.

In mice, FBXO11 knockout results in perinatal lethality and in *C. elegans dre-1* null mutants arrest at the three-fold stage of embryogenesis or as L1 larvae, often displaying molting defects (Hardisty-Hughes et al., 2006; Fielenbach et al., 2007). Preliminary experiments in the nematode indicate that neither *cdt-2* nor *blmp-1* depletion can suppress this early lethality (data not shown). Thus one could speculate DRE-1 to target more than just the two substrates in the nematode, which has been demonstrated for a variety of F-box proteins in mammals (Skaar et al., 2009b). To identify additional DRE-1 targets, one could screen for suppressors of *dre-1* larval lethality using a *dre-1(hd60)* deletion mutant carrying an extrachromosomal full-length *dre-1* rescuing construct. The screen could be based on RNAi feeding libraries or EMS mutagenesis with positive hits being animals that survive despite loss of the rescuing transgene (Jorgensen and Mango, 2002; Kamath and Ahringer, 2003). As *dre-1* affects all molts, possible substrates include known molting regulators such as *nhr-23*, *nhr-25* or *lin-42*, which all oscillate with the molt cycle. My data indicate that NHR-25 protein levels are not *dre-1* dependent and also preliminary investigations of a *lin-42* full-length fusion to GFP showed no obvious *dre-1* dependence. However multiple *lin-42* isoforms exist, which would have to be tested individually to exclude their regulation by *dre-1* (Tennessen et al., 2006). Furthermore, the screen might uncover novel regulators at the interface of molting and developmental timing, as seen for *blmp-1*. Interestingly, although *blmp-1* depletion failed to suppress larval lethality, we found *blmp-1* and *dre-1* to genetically interact in molting regulation. Moreover, *Drosophila Blimp-1* was reported to be induced by 20-hydroxycdysone to repress *nhr-25/FTZ-F1*, indicating BLMP-1 might affect chronological age across molting species (Agawa et al., 2007). To this end, it could also be interesting to dissect *blmp-1*'s role within the molt cycle and to retest its ability to suppress *dre-1* larval lethality in an RNAi-sensitized background that allows RNAi function also in neuronal tissue, before setting up a genome-wide suppressor screen. Also *cdt-2* should be retested in the synthesized background, since its depletion has previously been associated with molting defects (Frاند et al., 2005).

Taken together, F-box protein substrate identification remains challenging and where applicable *C. elegans* can be used as a tool to identify and characterize conserved substrate candidates. In particular, one could investigate the about ten highly conserved F-box proteins using genetic suppressor screens in the nematode (Table 3).

#### 4.2.6 Biological Control of Developmental Timing

Pioneering work in *C. elegans* discovered a set of heterochronic genes regulating developmental timing in the nematode (Ambros and Horvitz, 1984; Chalfie et al., 1981). By now, a complex regulatory network of more than 30 players has been built mainly on genetic epistasis that includes various conserved transcriptional, translational, and post-translational regulators (Resnick et al., 2010). Thereby the time-specific activation and degradation of regulatory factors is key to proper developmental progression. My work shows that temporal control of BLMP-1 protein levels directs maturation in the epidermis and gonad. Likewise, multiple conserved heterochronic factors are under strict temporal control, but the molecular mechanisms remain largely elusive. In particular, gene products regulating both molting and developmental timing, such as LIN-42, NHR-25, or NHR-23 oscillate with the molt cycle and must therefore be induced and degraded in a strongly coordinated fashion. To identify regulators of these proteins, EMS-based mutagenesis screens could be performed with loss of the oscillatory expression pattern as primary readout. Therefore, after mutagenesis of the P0 worms expressing full-length ORF::GFP fusion constructs, a mixed population of F3 animals could be analyzed for loss of the oscillatory GFP pattern using a worm biosorter. Besides picking up mutations in general modulators of transcription and degradation one might identify novel specific regulators of these molting and developmental timing gene coordinators. In a first, more biased approach related to this study, one could also test whether the oscillation of LIN-42, NHR-25, and NHR-23 requires SCF complex mediated degradation. If so, the knockdown of one of the six *C. elegans* Cullins by RNAi should result in a stabilization of the target protein and a consequent loss of the oscillatory pattern (Kipreos, 2005; Yamanaka et al., 2002). In sum, such experiments might further inform biological control of developmental time on a molecular level. They could help to understand the interplay of developmental timing and the molting cycle, both tied to environmental cues. Due to the remarkable conservation of all players involved, one might also gain further insights into the regulation of circadian rhythms and developmental progression in mammals.

## **Chapter 5 - MATERIAL AND METHODS**

## 5.1 Nematology and Genetics

### 5.1.1 Worm Maintenance

Worms were grown on nematode growth medium (NGM: 2.5% serva agar, 0.225% bacto-peptide, 0.3% NaCl (all w/v), 1 mM CaCl<sub>2</sub> and MgSO<sub>4</sub>, 25 mM KPO<sub>4</sub>, 5 µg/ml cholesterol) seeded with *E. coli* bacteria OP50 at 20°C unless otherwise noted (Brenner, 1974). Strains used were outcrossed at least 3 times and N2 Bristol was used as wild type reference strain. Notably *daf-9(rh6)* was maintained on plates containing additional 100 nM DA in the agar to prevent constitutive dauer entry.

### 5.1.2 Genotyping - PCR

In addition to phenotypic analysis, PCR from single worm lysates using Taq polymerase followed by 1% agarose gel electrophoresis was applied for worm genotyping. Detection of *dre-1(dh99)* required digestion of the PCR fragment with BpmI (RFLP assay).

PCR reaction:

General PCR program:

95°C	5 min	
95°C	45 s	30x
≈ 60°C	30 s	
72°C	60 s/kb	
72°C	10 min	

Primers including resulting PCR products and phenotypes used for genotyping:

Genotype	Primer or Phenotype	PCR Products
<i>blmp-1(tm548)I</i>	fwd: GATGAAGCTCCGGAAGAGTG rev: GACGCCCCAGTTTGTTTTTA	wt: 1115 bp mut: 305 bp
<i>blmp-1(tm548)I</i>	dumpy	
<i>dre-1(dh99)V</i>	fwd: TCATGCGAATCCCTACTTCC rev: AAAAGCTCACCTTCCAAGCA	wt: 638 + 258 bp (BpmI digest) mut: 898 bp (BpmI digest)
<i>dre-1(dh99)V</i>	synmig on <i>daf-12</i> RNAi	
<i>dre-1(dh279)V</i>	synmig on <i>daf-12</i> RNAi	
<i>sop-2(bx91)II</i>	lethal at 25°C	
<i>hbl-1(ve18)X</i>	potruding vulva	
<i>mab-10(e1248)II</i>	mild potruding vulva, extra seam cells	

BLMP-1::GFP*	fwd: TCAACAGCAACACATGA rev: TCACCTTCACCCTCTCCACT	305 bp
--------------	---	--------

### 5.1.3 *C. elegans* Strains

**N2** (Bristol), **AA3093** *dre-1(dh99)V*, **AA3091** *blmp-1(tm548)I*, **A2601** *dre-1(dh99)V; blmp-1(tm548)I*, **SU93** *jcIs1IV [ajm-1::gfp; unc-29(+); rol-6(su1006)]*, **AA820** *dre-1(dh99)V; jcIs1IV*, **AA2557** *blmp-1(tm548)I; jcIs1IV*, **AA2666** *dre-1(dh99)V; blmp-1(tm548)I; jcIs1IV*, **AA3175** *hbl-1(ve18)X; jcIs1IV*, **AA832** *lin-42(n1089)II; jcIs1IV*, **AA3141** *sop-2(bx91)II; jcIs1IV*, **JR667** *unc-119(e2498::Tc1)III; wIs51 [scm::gfp; unc-119(+)]*, **AA2558** *blmp-1(tm548)I; wIs51*, **AA3200** *mab-10(e1248)II; wIs51*, **EM723** *sop-2(bx91)II; him-5(e1490)V*, **MT7626** *let-7(n2853ts)X*, **RG559** *hbl-1(ve18)X*, **MT2257** *lin-42(n1089)II*, **AA528** *dre-1(dh99)V; daf-12(rh61rh411)X*, **AA885** *lin-29(n546)II; daf-12(rh61rh411)X*, **AA619** *dre-1(dh99)V; lin-29(n546)II*, **CB3518** *mab-10(e1248)II; him-5(e1490)V*, **AA2734** *unc-119(ed3)III; wglIs109 [blmp-1p::ORF::gfp::3xFLAG; unc-119(+)]* (Sarov et al., 2012), **AA2602** *blmp-1(tm548)I; wglIs109 [blmp-1p::ORF::gfp::3xFLAG; unc-119(+)]*, **AA2821** *dre-1(dh279)V; wglIs109*, **OP356** *unc-119(ed3)III; wglIs356 [nhr-25::TY1::EGFP::3xFLAG; unc-119(+)]* (Sarov et al., 2012), **AA2881 and 2882** *dhIs876 [dre-1p::gfp::orf 3'UTR; coel::RFP]* (integrated *dhEx452*; two lines) (Fielenbach et al., 2007), **JA1501** *pha-1(e2123)III; weEx70 [cdt-2p::cdt-2::gfp::let858(3'UTR); pha-1(+)]* (Poulin and Ahringer, 2010), **DR1572** *daf-2(e1368)III*, **CB1372** *daf-7(e1372)III*, **AA2863** *daf-9(dh6)X*, **VT825** *dpy-20(e1282)IV; malIs113 [cki-1::gfp; dpy-20(+)]*, **AA3009** *dre-1(dh99)V; malIs113*, **AA1327** *rrf-3(pk1426)II*

Underlined strains were generated in this work by crossing or UV integration.

### 5.1.4 UV Integration

UV integration of extrachromosomal arrays was achieved by UV irradiation (0.03 Joule/cm<sup>2</sup> on Viber Lourmat BLX-254 crosslinker) of L4 larvae that carry the corresponding transgene. Irradiated worms were kept in the dark for 24 hrs and the F2 and F3 generation was analyzed for stable integrands, which were then outcrossed to WT.

### 5.1.5 RNAi Depletion and Drug Treatment

RNAi-mediated knockdown was achieved by cultivating worms on HT115(DE3) bacteria expressing dsRNA of the target gene from an IPTG-inducible promoter (Kamath et al., 2001; Timmons and Fire, 1998). To induce dsRNA expression bacteria were seeded to NGM plates containing a final concentration of 1mM IPTG and 100 µg/µl ampicillin. RNAi clones were available from the Ahringer collection (Kamath and Ahringer, 2003), except for *dre-1* RNAi, which we described previously (Fielenbach et al., 2007), and *cdt-2* RNAi, which I obtained from the Vidal library (Rual et al., 2004). All clones were verified by sequencing using T7

primer after plasmid purification (MiniPrep, Qiagen). For knockdown experiments L4 larvae or eggs were moved to the RNAi plates and analyzed 2-3 days later as indicated.

Proteasome inhibition using the drug bortezomib was achieved by transferring L3 larvae to a plate containing 100  $\mu$ M bortezomib (in DMSO) on top of the OP50 bacteria lawn, for 6 h.

### 5.1.6 Worm Synchronization

To synchronize *C. elegans* populations gravid adult worms were washed from plates using M9 buffer (0.6% Na<sub>2</sub>HPO<sub>4</sub>, 0.3% KH<sub>2</sub>PO<sub>4</sub>, 0.5% NaCl (all w/v), 1 mM MgSO<sub>4</sub>). Somatic tissues were removed by adding 1 ratio of bleach solution (0.5 M KOH, 20% (v/v) NaClO) and vigorous shaking for 10 min. Remaining eggs were washed at least 3x in M9 before counting and distribution to seeded NGM plates. Notably bleach treated worms are still unsynchronized by about 8 hrs. For more precise synchronization worms were either synchronized by short egg-lay periods or newly hatched L1 larvae were carefully washed off from plates after bleach treatment or previous washing using M9 buffer, as eggs stick to the bacteria lawn.

### 5.1.7 Microscopy and Phenotype Analysis

General handling and observation of nematodes was performed on a Leica M80 stereomicroscope. Heterochronic phenotypes were analyzed at specific larval stages as assessed by gonad morphology and vulval formation using Nomarski DIC and fluorescence microscopy on a Carl Zeiss Axio Imager Z1. Seam cell number (*scm-1::gfp* marker), seam cell fusion (*ajm-1::gfp* marker) and adult alae formation were scored each on one side of individual animals. Worms were anesthetized with 1 mM levamisole. GFP intensity in seam/hypodermal cells was leveled from 5-10 cells per animal, whereas for measurements in the dtc, one dtc per animal was analyzed. Fluorescence intensity was determined using the ImageJ software (<http://rsbweb.nih.gov/ij/>).

### 5.1.8 Dauer Assays, Laser Microsurgery and Lifespan Analysis

For dauer assays worms were synchronized by egg-lay on NGM plates lacking cholesterol seeded with OP50 bacteria or RNAi plates with HT115 bacteria. Dauer larvae were scored after 48 hrs (27°C) or 60 hrs (25°C).

Ablation of germline precursor cells was achieved by laser microsurgery as described (Gerisch et al., 2001). In brief, L1 larvae were subdued to laser microsurgery on a Carl Zeiss Axio Imager Z1 right after hatching, whereby the germ cell precursors Z2 and Z3 were

ablated with a laser beam. Worms were immediately recovered in M9 medium using a mouth pipette. Success of the laser microsurgery was assessed 2-3 days later, when mock-ablated worms fully established a functional germline and laid eggs.

Lifespan assays were performed at 20°C. Worms were synchronized by egg-lay and transferred to RNAi plates at the L4 stage. Worms undergoing internal hatching, bursting vulva or crawling off the plates were censored.

## 5.2 Molecular Biology

### 5.2.1 RNA Isolation and qRT-PCR

For qRT-PCR analysis synchronized populations of about 1000 L3 larvae, 400 L4 larvae or 200 adult worms were harvested in 200  $\mu$ l QIAzol (Qiagen). After 3-4 freeze thaw cycles ( $N_2(l)/37^\circ C$ ) Chloroform was added and the aqueous phase was used for total RNA extraction using the RNeasy Mini Kit (Qiagen) according to the manufacturer's instructions. RNA quantity and quality was determined on a NanoDrop 2000c (peqLab). cDNA was subsequently generated from 100 ng RNA using the iScript cDNA Synthesis Kit (BioRad). qRT-PCR was performed with Power SYBR Green master mix (Applied Biosystems) on a ViiA 7 Real-Time PCR System (Applied Biosystems). Four technical replicates were pipetted on a 384-well plate either manually or by use of the JANUS automated workstation (PerkinElmer). Primers were validated by determination of standard- and melting curves. Data were analyzed for comparative CT values and normalized to *ama-1*, which served as internal control.

qRT-PCR primer sequences:

Gene	Primer	Sequence (5'-3')
<i>blmp-1</i>	fwd	ATCTTCCACACCGCCATCA
	rev	TCGCACCTGACGCTGAAAC
<i>nas-36</i>	fwd	CAAATGTATGGGCAGATTGGG
	rev	GGGCACGCTTTCAAATTACAG
<i>bed-3</i>	fwd	GCATGTTGGAAAGATTTCGTGG
	rev	GGCAGCTTGTTC AATAGTTGG
<i>wrt-2</i>	fwd	TGCATACGCCGATCATATTCC
	rev	CAGTCCATCCGAAGCATTTTG
<i>ptr-8</i>	fwd	CGGCAGAAAATTCAGTCTAATCC
	rev	TCCCATTTGCTTAACTGTCTTCG

<i>col-7</i>	fwd	CGGAATTGTGGTATTTGGAGC
	rev	CATCCTGGTTTATCATTGAGTTCC
<i>col-124</i>	fwd	GACTTTCTCCACCATTGCAG
	rev	GGGATACGGTTGACTTGAGAG
<i>col-91</i>	fwd	CGAGACTATGGAACTTTTGACG
	rev	GAGCTTGACAGTCTGGAAGAG
<i>ama-1</i>	fwd	GGATGGAATGTGGGTTGAGA
	rev	CGGATTCTTGAATTCGCGC

qRT-PCR program:

50°C	2 min	activation
95°C	10 min	
95°C	15 s	40x
60°C	1 min	
95°C	15 s	melting curve
60°C	1 min	
95°C	15 s	

### 5.2.2 RNA-Sequencing and Data Analysis (in part performed by Dr. Corinna Klein)

Worms were synchronized by egg-lay ( $\approx$  200 adults, 3 hrs) and collected in M9 at the mid-L3 stage. Total RNA was extracted as described above, but RNA quality was additionally controlled on a Tape Station 2200 (Agilent Technologies). Libraries were prepared with the Illumina TruSeq RNA and DNA Sample Preparation Kit v2 and sequenced on an Illumina HiSeq 2000 sequencer at the Max Planck-Genome-Centre, Cologne. Three biological replicates per genotype with a library size in the range of 41-47 million reads were further analyzed by Dr. Corinna Klein (MPI bioinformatics facility). Sequences were trimmed at both ends with the FASTA/Q Trimmer of the FASTX-Toolkit ([http://hannonlab.cshl.edu/fastx\\_toolkit](http://hannonlab.cshl.edu/fastx_toolkit) by Hannon Lab), and then preprocessed reads were mapped to the genome with tophat2 (v2.0.7) (Kim et al., 2013) allowing only unique mapping. On average 96.1% of the reads could be aligned. Subsequently, differential gene expression analysis was performed with cuffdiff, which is part of the cufflinks package (v2.0.2) (Trapnell et al., 2010). Genes with a FPKM value  $>0.5$  in at least one of the N2 and *blmp-1* samples were considered expressed. Those with a q-value  $<0.05$  and fold change  $>\pm 1.5$  were classified as differentially expressed. I then used DAVID analysis to identify

enriched gene-ontology/biological processes (Huang et al., 2009). ReviGO was used for visualization of the resulting GO term classes and its semantic similarity (Supek et al., 2011).

### 5.2.3 Plasmid Construction and Molecular Cloning (performed by Dr. Christoph Geisen)

Plasmids were constructed as follows: cDNAs for human *FBXO11*, *FBXO10*, *FBXO5*, *PRDM1*, *C. elegans dre-1*, *blmp-1*, *lin-29* and *Discosoma sp.* DsRed1-derived mRFP (Campbell et al., 2002) were PCR amplified with specific primers from commercially available cDNA-clones (Open Biosystems/Thermo Scientific) or public repository plasmids (Addgene or Harvard PlasmID) and subcloned into plasmids derived from pcDNA3.1- (Invitrogen) carrying either a N-terminal 6xHis- or FLAG-HA-tag (RGS6xHis-pcDNA3.1- and FLAG-HA-pcDNA3.1-) and driving expression through the cytomegalovirus promoter. To generate RGS6xHis-pcDNA3.1- and FLAG-HA-pcDNA3.1- the following DNA oligonucleotides were subcloned into the *Nhe* I and *Xba* I sites of pcDNA3.1- using DNA-oligos :

RGS6xHis:

GCTAGCCACCATGAGAGGATCGCATCACCATCACCATCACGGGCCCTCTAGA;

FLAG-HA:

GCTAGCCACCATGGACTACAAAGACGATGACGATAAAGGGGGCGGTG  
GAGGTTACCCATACGATGTTCCAGATTACGCTGGTGGAGGTGGAGGTTCTAGA.

The latter was only achieved after point mutation to generate a “FLAG – 5xGly – HA – 5xGly – tag”, of FLAG- and the HA-tag. DN-Cullins were purchased from Addgene (15818-15820, (Jin et al., 2005)).

In general DH5 $\alpha$  bacteria (Invitrogen) were used for subcloning and transformed by 40 s heat shock at 42°C. Plasmids were purified using Mini-, Midi- or HiSpeed Maxi kits (Qiagen) according to the manufacturer’s instructions.

## 5.3 Biochemistry

### 5.3.1 Antibodies

The following antibodies were used in this study: BLMP-1 (rb, Novus Bio), GFP (ms, Clontech),  $\alpha$ -Tubulin (ms, Sigma), HA (rat, Roche), His (ms, Qiagen and rb, Santa Cruz),

FLAG (ms and rb, SIGMA), PCNA (ms, Invitrogen), BLIMP-1 (rb, ab59369, Abcam and ms, 3H2-E8, Novus Bio), FBXO11 (rb, NB100-59826, Novus Bio), and SKP1 (Pagano lab).

### 5.3.2 *C. elegans* Biochemistry

For western blot analysis synchronized L4 larvae were collected in M9 buffer, lysed in 2x SDS sample buffer (Biorad) and equal volumes were applied to SDS-PAGE and immunoblotting. Band intensity was quantified with Adobe Photoshop.

For immunoprecipitation (IP) assays eggs were isolated by bleach treatment. After a 3 hrs hatching-period L1 larvae were washed off with M9 buffer and transferred to RNAi plates. L3 larvae were lysed in worm IP buffer (50 mM Tris/HCl pH 7.4, 150 mM NaCl, 1 mM EDTA, 0.1% NP-40, protease and phosphatase inhibitor cocktail (Roche)) using a dounce homogenizer. Worm lysates were incubated with 40  $\mu$ l GFP-Trap agarose beads (Chromotek) for 1 hr at 4°C and washed 5x with worm washing buffer (as worm IP buffer, but 300 mM NaCl and 0.75% NP-40). Precipitants were eluted with 2x SDS sample buffer (Biorad) and analyzed by SDS-PAGE and immunoblotting.

### 5.3.3 Cell Culture and IP Experiments

HEK293T cells were maintained in Dulbecco's Modified Eagle's Medium supplemented with 10% fetal bovine serum (Gibco). Transfections were performed using Lipofectamine 2000 (Invitrogen) according to the manufacturer's instructions. For IP experiments (not prior to ubiquitination assay), cells were treated with 15  $\mu$ M MG132 or DMSO control for 4 hrs prior to harvesting. Cells were lysed 20 hrs post-transfection in lysis buffer (50 mM Tris/HCl pH 7.4, 120 mM NaCl, 0.5% NP-40, protease and phosphatase inhibitor cocktail (Roche)) and equal protein amounts (Bradford assay) were incubated with anti-FLAG-M2 resin (Sigma) for 1 hr at 4°C. Precipitated proteins were eluted by competition with 150 ng/ $\mu$ l 3xFLAG peptide (Sigma) and analyzed by SDS-PAGE and immunoblotting. To study BLIMP-1 turnover, transfected cells were treated with 100  $\mu$ g/ml cycloheximide (CHX, AppliChem) for the indicated time intervals 20 hrs post-transfection. Cells were lysed in lysis buffer and analyzed by SDS-PAGE and immunoblotting. Whole cell lysates and CHX treatment in ARP1 cells was performed by Dr. Lukas Cermak as described (Duan et al., 2012).

### 5.3.4 Gene Silencing by shRNAs (performed by Dr. Lukas Cermak)

Sequences of FBXO11 shRNAs were as follows: #1: GAGTTTACATCTTTGGTGA, #2: CAATTGTTTCGGCATAACAA. shRNA lentiviruses were produced as described (Phan et

al., 2007). ARP1 multiple myeloma cells were infected by re-suspension in virus-containing supernatants and centrifugation. 24 hrs after infection, cells were resuspended in fresh medium and selected with puromycin.

### **5.3.5 *In Vitro* Ubiquitination (performed by Dr. Lukas Cermak)**

HEK293T cells were cotransfected with His-BLIMP-1 and FLAG-FBXO11 or -FBXO11(F-box<sup>MUT</sup>) and lysed using isotonic NP-40 buffer with Turbonuclease (Accelagen). Lysates were precleared with 0.40 mm filters and FLAG-tagged complexes were isolated using anti-FLAG-M2 resin (Sigma). Complexes were eluted by competition with 3xFLAG peptide (Sigma).

*In vitro* ubiquitination assays were performed in a volume of 30  $\mu$ l containing 0.1  $\mu$ M UBE1 (Boston Biochem), 10 ng/ml Ubch3, 10 ng/ml Ubch5c, 1  $\mu$ M ubiquitin aldehyde,  $\pm 2.5 \mu$ g/ $\mu$ l ubiquitin (Sigma), and either SCF<sup>FBXO11</sup> or SCF<sup>FBXO11-Fbox-MUT</sup> complex in a ubiquitination buffer (50 mM Tris [pH 7.6], 2 mM ATP, 5 mM MgCl<sub>2</sub>, 0.6 mM DTT, okadaic acid 0.1 mM) for 45 min at 37°C.

## **5.4 Statistical Analysis**

Results are presented as mean+95%CI, SD or SEM as indicated. Statistical analyses were performed using one-way ANOVA with Tukey or Dunnett post test (ANOVA), Fisher's Exact test, unpaired *t test*, or Mantel-Cox (Log Rank) method as indicated using GraphPad Prism (GraphPad software).

## **Chapter 6 - REFERENCES**

- Abbas, T., Mueller, A. C., Shibata, E., Keaton, M., Rossi, M., and Dutta, A. (2013a). CRL1-FBXO11 promotes Cdt2 ubiquitylation and degradation and regulates Pr-Set7/Set8-mediated cellular migration. *Mol Cell* *49*, 1147–1158.
- Abbas, T., Shibata, E., Park, J., Jha, S., Karnani, N., and Dutta, A. (2010). CRL4(Cdt2) regulates cell proliferation and histone gene expression by targeting PR-Set7/Set8 for degradation. *Mol Cell* *40*, 9–21.
- Abbas, T., Sivaprasad, U., Terai, K., Amador, V., Pagano, M., and Dutta, A. (2008). PCNA-dependent regulation of p21 ubiquitylation and degradation via the CRL4Cdt2 ubiquitin ligase complex. *Genes Dev* *22*, 2496–2506.
- Abbas, T., Keaton, M., and Dutta, A. (2013b). Regulation of TGF- $\beta$  signaling, exit from the cell cycle, and cellular migration through cullin cross-regulation: SCF-FBXO11 turns off CRL4-Cdt2. *Cell Cycle* *12*, 2175–2182.
- Abbas, T., and Dutta, A. (2011). CRL4Cdt2: master coordinator of cell cycle progression and genome stability. *Cell Cycle* *10*, 241–249.
- Abbott, A. L., Alvarez-Saavedra, E., Miska, E. A., Lau, N. C., Bartel, D. P., Horvitz, H. R., and Ambros, V. (2005). The let-7 MicroRNA Family Members mir-48, mir-84, and mir-241 Function Together to Regulate Developmental Timing in *Caenorhabditis elegans*. *Dev Cell* *9*, 403–414.
- Abrahante, J. E., Miller, E. A., and Rougvie, A. E. (1998). Identification of heterochronic mutants in *Caenorhabditis elegans*. Temporal misexpression of a collagen::green fluorescent protein fusion gene. *Genetics* *149*, 1335–1351.
- Abrahante, J. E., Daul, A. L., Li, M., Volk, M. L., Tennessen, J. M., Miller, E. A., and Rougvie, A. E. (2003). The *Caenorhabditis elegans* hunchback-like gene *lin-57/hbl-1* controls developmental time and is regulated by microRNAs. *Dev Cell* *4*, 625–637.
- Agawa, Y., Sarhan, M., Kageyama, Y., Akagi, K., Takai, M., Hashiyama, K., Wada, T., Handa, H., Iwamatsu, A., Hirose, S., et al. (2007). *Drosophila* Blimp-1 is a transient transcriptional repressor that controls timing of the ecdysone-induced developmental pathway. *Mol. Cell. Biol.* *27*, 8739–8747.
- Alberch, P., Gould, S. J., OSTER, G. F., and WAKE, D. B. (1979). Size and Shape in Ontogeny and Phylogeny. *Paleobiology* *5*, 296–317.
- Albert, P. S., and Riddle, D. L. (1988). Mutants of *Caenorhabditis elegans* that form dauer-like larvae. *Dev Biol* *126*, 270–293.
- Ambros, V. (2003). MicroRNA pathways in flies and worms: growth, death, fat, stress, and timing. *Cell* *113*, 673–676.
- Ambros, V. (2011). MicroRNAs and developmental timing. *Curr. Opin. Genet. Dev.* *21*, 511–517.
- Ambros, V. (2004). The functions of animal microRNAs. *Nature* *431*, 350–355.
- Ambros, V., and Horvitz, H. R. (1984). Heterochronic mutants of the nematode *Caenorhabditis elegans*. *Science* *226*, 409–416.
- Ambros, V., and Horvitz, H. R. (1987). The *lin-14* locus of *Caenorhabditis elegans* controls the time of expression of specific postembryonic developmental events. *Genes Dev* *1*, 398–414.
- Ancelin, K., Lange, U. C., Hajkova, P., Schneider, R., Bannister, A. J., Kouzarides, T., and Surani, M. A. (2006). Blimp1 associates with Prmt5 and directs histone arginine methylation in mouse germ cells. *Nat Cell Biol* *8*, 623–630.
- Andersen, E. C., and Horvitz, H. R. (2007). Two *C. elegans* histone methyltransferases repress *lin-3* EGF transcription to inhibit vulval development. *Development* *134*, 2991–2999.
- Angelo, G., and Van Gilst, M. R. (2009). Starvation protects germline stem cells and extends reproductive longevity in *C. elegans*. *Science* *326*, 954–958.
- Antebi, A. (2013). Regulation of longevity by the reproductive system. *Exp. Gerontol.* *48*, 596–602.
- Antebi, A., Yeh, W. H., Tait, D., Hedgecock, E. M., and Riddle, D. L. (2000). *daf-12* encodes a nuclear receptor that regulates the dauer diapause and developmental age in *C. elegans*. *Genes Dev* *14*, 1512–1527.
- Antebi, A., Culotti, J. G., and Hedgecock, E. M. (1998). *daf-12* regulates developmental age and the dauer alternative in *Caenorhabditis elegans*. *Development* *125*, 1191–1205.

- Arantes-Oliveira, N., Apfeld, J., Dillin, A., and Kenyon, C. (2002). Regulation of life-span by germ-line stem cells in *Caenorhabditis elegans*. *Science* 295, 502–505.
- Arasu, P., Wightman, B., and Ruvkun, G. (1991). Temporal regulation of *lin-14* by the antagonistic action of two other heterochronic genes, *lin-4* and *lin-28*. *Genes Dev* 5, 1825–1833.
- Asahina, M., Ishihara, T., Jindra, M., Kohara, Y., Katsura, I., and Hirose, S. (2000). The conserved nuclear receptor Ftz-F1 is required for embryogenesis, moulting and reproduction in *Caenorhabditis elegans*. *Genes Cells* 5, 711–723.
- Austin, J., and Kimble, J. (1987). *glp-1* is required in the germ line for regulation of the decision between mitosis and meiosis in *C. elegans*. *Cell* 51, 589–599.
- Bachmair, A., Finley, D., and Varshavsky, A. (1986). In vivo half-life of a protein is a function of its amino-terminal residue. *Science* 234, 179–186.
- Bai, C., Sen, P., Hofmann, K., Ma, L., Goebel, M., Harper, J. W., and Elledge, S. J. (1996). SKP1 connects cell cycle regulators to the ubiquitin proteolysis machinery through a novel motif, the F-box. *Cell* 86, 263–274.
- Banerjee, D., Kwok, A., Lin, S., and Slack, F. J. (2005). Developmental timing in *C. elegans* is regulated by *kin-20* and *tim-1*, homologs of core circadian clock genes. *Dev Cell* 8, 287–295.
- Banerjee, D., and Slack, F. (2002). Control of developmental timing by small temporal RNAs: a paradigm for RNA-mediated regulation of gene expression. *Bioessays* 24, 119–129.
- Bartel, B., Wüning, I., and Varshavsky, A. (1990). The recognition component of the N-end rule pathway. *EMBO J.* 9, 3179–3189.
- Basso, K., and Dalla-Favera, R. (2012). Roles of BCL6 in normal and transformed germinal center B cells. *Immunol. Rev.* 247, 172–183.
- Baugh, L. R., and Sternberg, P. W. (2006). DAF-16/FOXO regulates transcription of *cki-1/Cip/Kip* and repression of *lin-4* during *C. elegans* L1 arrest. *Curr Biol* 16, 780–785.
- Bedford, L., Paine, S., Sheppard, P. W., Mayer, R. J., and Roelofs, J. (2010). Assembly, structure, and function of the 26S proteasome. *Trends Cell Biol.* 20, 391–401.
- Benanti, J. A., Cheung, S. K., Brady, M. C., and Toczyski, D. P. (2007). A proteomic screen reveals SCFGrr1 targets that regulate the glycolytic-gluconeogenic switch. *Nat Cell Biol* 9, 1184–1191.
- Bethke, A., Fielenbach, N., Wang, Z., Mangelsdorf, D. J., and Antebi, A. (2009). Nuclear hormone receptor regulation of microRNAs controls developmental progression. *Science* 324, 95–98.
- Birby, D. A., Link, E. M., Vowels, J. J., Tian, H., Colacurcio, P. L., and Thomas, J. H. (2000). A transmembrane guanylyl cyclase (DAF-11) and Hsp90 (DAF-21) regulate a common set of chemosensory behaviors in *caenorhabditis elegans*. *Genetics* 155, 85–104.
- Bluestone, C. D., and Klein, J. O. (2001). [CITATION][C]. Otitis Media in Infants and Children.
- Brenner, S. (1974). The genetics of *Caenorhabditis elegans*. *Genetics* 77, 71–94.
- Busino, L., Bassermann, F., Maiolica, A., Lee, C., Nolan, P. M., Godinho, S. I. H., Draetta, G. F., and Pagano, M. (2007). SCFFbx13 controls the oscillation of the circadian clock by directing the degradation of cryptochrome proteins. *Science* 316, 900–904.
- Butcher, R. A., Fujita, M., Schroeder, F. C., and Clardy, J. (2007). Small-molecule pheromones that control dauer development in *Caenorhabditis elegans*. *Nat. Chem. Biol.* 3, 420–422.
- Büssing, I., Slack, F. J., and Grosshans, H. (2008). *let-7* microRNAs in development, stem cells and cancer. *Trends Mol Med* 14, 400–409.
- Cai, Q., Sun, Y., Huang, X., Guo, C., Zhang, Y., Zhu, Z., and Zhang, H. (2008). The *Caenorhabditis elegans* PcG-like gene *sop-2* regulates the temporal and sexual specificities of cell fates. *Genetics* 178, 1445–1456.
- Campbell, R. E., Tour, O., Palmer, A. E., Steinbach, P. A., Baird, G. S., Zacharias, D. A., and Tsien, R. Y. (2002). A monomeric red fluorescent protein. *Proc Natl Acad Sci USA* 99, 7877–7882.
- Cassada, R. C., and Russell, R. L. (1975). The dauerlarva, a post-embryonic developmental variant of the nematode *Caenorhabditis elegans*. *Dev Biol* 46, 326–342.
- Caygill, E. E., and Johnston, L. A. (2008). Temporal regulation of metamorphic processes in *Drosophila* by the *let-7* and miR-125 heterochronic microRNAs. *Curr Biol* 18, 943–950.

- Centore, R. C., Havens, C. G., Manning, A. L., Li, J., Flynn, R. L., Tse, A., Jin, J., Dyson, N. J., Walter, J. C., and Zou, L. (2010). CRL4(Cdt2)-mediated destruction of the histone methyltransferase Set8 prevents premature chromatin compaction in S phase. *Mol Cell* 40, 22–33.
- Chai, Y., and Maxson, R. E. (2006). Recent advances in craniofacial morphogenesis. *Dev Dyn* 235, 2353–2375.
- Chalfie, M., Horvitz, H. R., and Sulston, J. E. (1981). Mutations that lead to reiterations in the cell lineages of *C. elegans*. *Cell* 24, 59–69.
- Chang, D. H., Cattoretti, G., and Calame, K. L. (2002). The dynamic expression pattern of B lymphocyte induced maturation protein-1 (Blimp-1) during mouse embryonic development. *Mech. Dev.* 117, 305–309.
- Chang, H., Martinez, N. J., Thornton, J. E., Hagan, J. P., Nguyen, K. D., and Gregory, R. I. (2012). Trim71 cooperates with microRNAs to repress Cdkn1a expression and promote embryonic stem cell proliferation. *Nat Commun* 3, 923.
- Chau, V., Tobias, J. W., Bachmair, A., Marriott, D., Ecker, D. J., Gonda, D. K., and Varshavsky, A. (1989). A multiubiquitin chain is confined to specific lysine in a targeted short-lived protein. *Science* 243, 1576–1583.
- Chawla, G., and Sokol, N. S. (2012). Hormonal activation of let-7-C microRNAs via EcR is required for adult *Drosophila melanogaster* morphology and function. *Development* 139, 1788–1797.
- Chen, J., Lai, F., and Niswander, L. (2012). The ubiquitin ligase mLin41 temporally promotes neural progenitor cell maintenance through FGF signaling. *Genes Dev* 26, 803–815.
- Chen, Z., Eastburn, D. J., and Han, M. (2004). The *Caenorhabditis elegans* nuclear receptor gene *nhr-25* regulates epidermal cell development. *Mol. Cell. Biol.* 24, 7345–7358.
- Chiorazzi, M., Rui, L., Yang, Y., Ceribelli, M., Tishbi, N., Maurer, C. W., Ranuncolo, S. M., Zhao, H., Xu, W., Chan, W. C., et al. (2013). Related F-box proteins control cell death in *Caenorhabditis elegans* and human lymphoma. *Proc Natl Acad Sci USA* 110, 3943–3948.
- Chisholm, A. D., and Hsiao, T. I. (2012). The *Caenorhabditis elegans* epidermis as a model skin. I: development, patterning, and growth. *Wiley Interdiscip Rev Dev Biol* 1, 861–878.
- Cianferotti, L., Cox, M., Skorija, K., and Demay, M. B. (2007). Vitamin D receptor is essential for normal keratinocyte stem cell function. *Proc Natl Acad Sci USA* 104, 9428–9433.
- Ciechanover, A., Heller, H., Elias, S., Haas, A. L., and Hershko, A. (1980). ATP-dependent conjugation of reticulocyte proteins with the polypeptide required for protein degradation. *Proc Natl Acad Sci USA* 77, 1365–1368.
- Cook, J. R., Lee, J., Yang, Z., Krause, C. D., Herth, N., Hoffmann, R., and Pestka, S. (2006). FBXO11/PRMT9, a new protein arginine methyltransferase, symmetrically dimethylates arginine residues. *Biochem Biophys Res Commun* 342, 472–481.
- Cope, G. A., and Deshaies, R. J. (2003). COP9 signalosome: a multifunctional regulator of SCF and other cullin-based ubiquitin ligases. *Cell* 114, 663–671.
- Crotty, S., Johnston, R. J., and Schoenberger, S. P. (2010). Effectors and memories: Bcl-6 and Blimp-1 in T and B lymphocyte differentiation. *Nat Immunol* 11, 114–120.
- D'Angiolella, V., Donato, V., Forrester, F. M., Jeong, Y., Pellacani, C., Kudo, Y., Saraf, A., Florens, L., Washburn, M. P., and Pagano, M. (2012). Cyclin F-mediated degradation of ribonucleotide reductase M2 controls genome integrity and DNA repair. *Cell* 149, 1023–1034.
- De Beer, G. R. (1951). Embryos and ancestors.
- Deshaies, R. J., and Joazeiro, C. A. P. (2009). RING domain E3 ubiquitin ligases. *Annu. Rev. Biochem.* 78, 399–434.
- Dikic, I., Wakatsuki, S., and Walters, K. J. (2009). Ubiquitin-binding domains - from structures to functions. *Nat Rev Mol Cell Biol* 10, 659–671.
- Dikic, I., and Dötsch, V. (2009). Ubiquitin linkages make a difference. *Nat. Struct. Mol. Biol.* 16, 1209–1210.
- Dillon, S. C., Zhang, X., Trievel, R. C., and Cheng, X. (2005). The SET-domain protein superfamily: protein lysine methyltransferases. *Genome Biol.* 6, 227.
- Ding, L., Spencer, A., Morita, K., and Han, M. (2005). The developmental timing regulator AIN-1 interacts with miRISCs and may target the argonaute protein ALG-1 to cytoplasmic P bodies in *C. elegans*. *Mol Cell* 19, 437–447.

- Ding, M., Chao, D., Wang, G., and Shen, K. (2007). Spatial regulation of an E3 ubiquitin ligase directs selective synapse elimination. *Science* 317, 947–951.
- Donzelli, M., Squatrito, M., Ganoth, D., Hershko, A., Pagano, M., and Draetta, G. F. (2002). Dual mode of degradation of Cdc25 A phosphatase. *EMBO J.* 21, 4875–4884.
- Dougan, D. A., Micevski, D., and Truscott, K. N. (2012). The N-end rule pathway: from recognition by N-recognins, to destruction by AAA+proteases. *Biochim. Biophys. Acta* 1823, 83–91.
- Dreier, L., Burbea, M., and Kaplan, J. M. (2005). LIN-23-mediated degradation of beta-catenin regulates the abundance of GLR-1 glutamate receptors in the ventral nerve cord of *C. elegans*. *Neuron* 46, 51–64.
- Drury, L. S., Perkins, G., and Diffley, J. F. (1997). The Cdc4/34/53 pathway targets Cdc6p for proteolysis in budding yeast. *EMBO J.* 16, 5966–5976.
- Duan, S. S., Cermak, L. L., Pagan, J. K. J., Rossi, M. M., Martinengo, C. C., di Celle, P. F. P., Chapuy, B. B., Shipp, M. M., Chiarle, R. R., and Pagano, M. M. (2012). FBXO11 targets BCL6 for degradation and is inactivated in diffuse large B-cell lymphomas. *Nature* 481, 90–93.
- Duchaine, T. F., Wohlschlegel, J. A., Kennedy, S., Bei, Y., Conte, D., Pang, K., Brownell, D. R., Harding, S., Mitani, S., Ruvkun, G., et al. (2006). Functional proteomics reveals the biochemical niche of *C. elegans* DCR-1 in multiple small-RNA-mediated pathways. *Cell* 124, 343–354.
- Duda, D. M., Borg, L. A., Scott, D. C., Hunt, H. W., Hammel, M., and Schulman, B. A. (2008). Structural insights into NEDD8 activation of cullin-RING ligases: conformational control of conjugation. *Cell* 134, 995–1006.
- Ecsedi, M., and Grosshans, H. (2013). LIN-41/TRIM71: emancipation of a miRNA target. *Genes Dev* 27, 581–589.
- Edwards, M. K., and Wood, W. B. (1983). Location of specific messenger RNAs in *Caenorhabditis elegans* by cytological hybridization. *Dev Biol* 97, 375–390.
- Euling, S., and Ambros, V. (1996). Reversal of cell fate determination in *Caenorhabditis elegans* vulval development. *Development* 122, 2507–2515.
- Fang, S., Lorick, K. L., Jensen, J. P., and Weissman, A. M. (2003). RING finger ubiquitin protein ligases: implications for tumorigenesis, metastasis and for molecular targets in cancer. *Semin. Cancer Biol.* 13, 5–14.
- Fay, D. S., Stanley, H. M., Han, M., and Wood, W. B. (1999). A *Caenorhabditis elegans* homologue of hunchback is required for late stages of development but not early embryonic patterning. *Dev Biol* 205, 240–253.
- Feinbaum, R., and Ambros, V. (1999). The timing of *lin-4* RNA accumulation controls the timing of postembryonic developmental events in *Caenorhabditis elegans*. *Dev Biol* 210, 87–95.
- Feldman, R. M., Correll, C. C., Kaplan, K. B., and Deshaies, R. J. (1997). A complex of Cdc4p, Skp1p, and Cdc53p/cullin catalyzes ubiquitination of the phosphorylated CDK inhibitor Sic1p. *Cell* 91, 221–230.
- Fielenbach, N., Guardavaccaro, D., Neubert, K., Chan, T., Li, D., Feng, Q., Hutter, H., Pagano, M., and Antebi, A. (2007). DRE-1: An Evolutionarily Conserved F Box Protein that Regulates *C. elegans* Developmental Age. *Dev Cell* 12, 443–455.
- Fielenbach, N., and Antebi, A. (2008). *C. elegans* dauer formation and the molecular basis of plasticity. *Genes Dev* 22, 2149–2165.
- Finley, D., Sadis, S., Monia, B. P., Boucher, P., Ecker, D. J., Crooke, S. T., and Chau, V. (1994). Inhibition of proteolysis and cell cycle progression in a multiubiquitination-deficient yeast mutant. *Mol. Cell. Biol.* 14, 5501–5509.
- Florens, L., and Washburn, M. P. (2006). Proteomic analysis by multidimensional protein identification technology. *Methods Mol. Biol.* 328, 159–175.
- Frand, A. R., Russel, S., and Ruvkun, G. (2005). Functional genomic analysis of *C. elegans* molting. *PLoS Biol.* 3, e312.
- Frescas, D., and Pagano, M. (2008). Deregulated proteolysis by the F-box proteins SKP2 and beta-TrCP: tipping the scales of cancer. *Nat. Rev. Cancer* 8, 438–449.
- Frieden, E. (1981). The Dual Role of Thyroid Hormones in Vertebrate Development and Calorigenesis. In (Boston, MA: Springer US), pp. 545–563.

- Fukuyama, M., Rougvie, A. E., and Rothman, J. H. (2006). *C. elegans* DAF-18/PTEN mediates nutrient-dependent arrest of cell cycle and growth in the germline. *Curr Biol* *16*, 773–779.
- Fukuyama, M., Gendreau, S. B., Derry, W. B., and Rothman, J. H. (2003). Essential embryonic roles of the CKI-1 cyclin-dependent kinase inhibitor in cell-cycle exit and morphogenesis in *C. elegans*. *Dev Biol* *260*, 273–286.
- Galan, J. M., and Peter, M. (1999). Ubiquitin-dependent degradation of multiple F-box proteins by an autocatalytic mechanism. *Proc Natl Acad Sci USA* *96*, 9124–9129.
- Galan, J. M., and Haguenuer-Tsapis, R. (1997). Ubiquitin lys63 is involved in ubiquitination of a yeast plasma membrane protein. *EMBO J.* *16*, 5847–5854.
- Gao, M. X., Liao, E. H., Yu, B., Wang, Y., Zhen, M., and Derry, W. B. (2008). The SCF FSN-1 ubiquitin ligase controls germline apoptosis through CEP-1/p53 in *C. elegans*. *Cell Death Differ.* *15*, 1054–1062.
- Gerisch, B., Weitzel, C., Kober-Eisermann, C., Rottiers, V., and Antebi, A. (2001). A hormonal signaling pathway influencing *C. elegans* metabolism, reproductive development, and life span. *Dev Cell* *1*, 841–851.
- Gerisch, B., and Antebi, A. (2004). Hormonal signals produced by DAF-9/cytochrome P450 regulate *C. elegans* dauer diapause in response to environmental cues. *Development* *131*, 1765–1776.
- Geuten, K., and Coenen, H. (2013). Heterochronic genes in plant evolution and development. *Front Plant Sci* *4*, 381.
- Gissendanner, C. R., Crossgrove, K., Kraus, K. A., Maina, C. V., and Sluder, A. E. (2004). Expression and function of conserved nuclear receptor genes in *Caenorhabditis elegans*. *Dev Biol* *266*, 399–416.
- Gissendanner, C. R., and Sluder, A. E. (2000). *nhr-25*, the *Caenorhabditis elegans* ortholog of *ftz-f1*, is required for epidermal and somatic gonad development. *Dev Biol* *221*, 259–272.
- Golden, J. W., and Riddle, D. L. (1984). A *Caenorhabditis elegans* dauer-inducing pheromone and an antagonistic component of the food supply. *J. Chem. Ecol.* *10*, 1265–1280.
- Goldstein, G., Scheid, M., Hammerling, U., Schlesinger, D. H., Niall, H. D., and Boyse, E. A. (1975). Isolation of a polypeptide that has lymphocyte-differentiating properties and is probably represented universally in living cells. *Proc Natl Acad Sci USA* *72*, 11–15.
- Goudeau, J., Bellemin, S., Toselli-Mollereau, E., Shamalnasab, M., Chen, Y., and Aguilaniu, H. (2011). Fatty acid desaturation links germ cell loss to longevity through NHR-80/HNF4 in *C. elegans*. *PLoS Biol.* *9*, e1000599.
- Gould, S. J. (1977). Ontogeny and phylogeny.
- Greer, E. L., Maures, T. J., Hauswirth, A. G., Green, E. M., Leeman, D. S., Maro, G. S., Han, S., Banko, M. R., Gozani, O., and Brunet, A. (2010). Members of the H3K4 trimethylation complex regulate lifespan in a germline-dependent manner in *C. elegans*. *Nature* *466*, 383–387.
- Grishok, A., Pasquinelli, A. E., Conte, D., Li, N., Parrish, S., Ha, I., Baillie, D. L., Fire, A., Ruvkun, G., and Mello, C. C. (2001). Genes and mechanisms related to RNA interference regulate expression of the small temporal RNAs that control *C. elegans* developmental timing. *Cell* *106*, 23–34.
- Grosshans, H., Johnson, T., Reinert, K. L., Gerstein, M., and Slack, F. J. (2005). The temporal patterning microRNA *let-7* regulates several transcription factors at the larval to adult transition in *C. elegans*. *Dev Cell* *8*, 321–330.
- Gyory, I., Wu, J., Fejér, G., Seto, E., and Wright, K. L. (2004). PRDI-BF1 recruits the histone H3 methyltransferase G9a in transcriptional silencing. *Nat Immunol* *5*, 299–308.
- Hada, K., Asahina, M., Hasegawa, H., Kanaho, Y., Slack, F. J., and Niwa, R. (2010). The nuclear receptor gene *nhr-25* plays multiple roles in the *Caenorhabditis elegans* heterochronic gene network to control the larva-to-adult transition. *Dev Biol* *344*, 1100–1109.
- Hallam, S. J., and Jin, Y. (1998). *lin-14* regulates the timing of synaptic remodelling in *Caenorhabditis elegans*. *Nature* *395*, 78–82.
- Hammell, C. M., Karp, X., and Ambros, V. (2009a). A feedback circuit involving *let-7*-family miRNAs and DAF-12 integrates environmental signals and developmental timing in *Caenorhabditis elegans*. *Proc Natl Acad Sci USA* *106*, 18668–18673.
- Hammell, C. M., Lubin, I., Boag, P. R., Blackwell, T. K., and Ambros, V. (2009b). *nhl-2* Modulates microRNA activity in *Caenorhabditis elegans*. *Cell* *136*, 926–938.

- Hangaishi, A., and Kurokawa, M. (2010). Blimp-1 is a tumor suppressor gene in lymphoid malignancies. *Int J Hematol* *91*, 46–53.
- Hao, B., Oehlmann, S., Sowa, M. E., Harper, J. W., and Pavletich, N. P. (2007). Structure of a Fbw7-Skp1-cyclin E complex: multisite-phosphorylated substrate recognition by SCF ubiquitin ligases. *Mol Cell* *26*, 131–143.
- Hardin, J., MacLeod, S., Grigorieva, I., Chang, R., Barlogie, B., Xiao, H., and Epstein, J. (1994). Interleukin-6 prevents dexamethasone-induced myeloma cell death. *Blood* *84*, 3063–3070.
- Hardisty, R. E., Erven, A., Logan, K., Morse, S., Guionaud, S., Sancho-Oliver, S., Hunter, A. J., Brown, S. D. M., and Steel, K. P. (2003). The deaf mouse mutant Jeff (Jf) is a single gene model of otitis media. *J. Assoc. Res. Otolaryngol.* *4*, 130–138.
- Hardisty-Hughes, R. E., Tateossian, H., Morse, S. A., Romero, M. R., Middleton, A., Tymowska-Lalanne, Z., Hunter, A. J., Cheeseman, M., and Brown, S. D. M. (2006). A mutation in the F-box gene, *Fbxo11*, causes otitis media in the Jeff mouse. *Hum. Mol. Genet.* *15*, 3273–3279.
- Harris, D. T., and Horvitz, H. R. (2011). MAB-10/NAB acts with LIN-29/EGR to regulate terminal differentiation and the transition from larva to adult in *C. elegans*. *Development* *138*, 4051–4062.
- Hayes, G. D., Frand, A. R., and Ruvkun, G. (2006). The mir-84 and let-7 paralogous microRNA genes of *Caenorhabditis elegans* direct the cessation of molting via the conserved nuclear hormone receptors NHR-23 and NHR-25. *Development* *133*, 4631–4641.
- Hedgecock, E. M., Culotti, J. G., Hall, D. H., and Stern, B. D. (1987). Genetics of cell and axon migrations in *Caenorhabditis elegans*. *Development* *100*, 365–382.
- Hershko, A., Ciechanover, A., Heller, H., Haas, A. L., and Rose, I. A. (1980). Proposed role of ATP in protein breakdown: conjugation of protein with multiple chains of the polypeptide of ATP-dependent proteolysis. *Proc Natl Acad Sci USA* *77*, 1783–1786.
- Hershko, A., and Ciechanover, A. (1998). The ubiquitin system. *Annu. Rev. Biochem.* *67*, 425–479.
- Hicke, L. (2001). Protein regulation by monoubiquitin. *Nat Rev Mol Cell Biol* *2*, 195–201.
- Hicke, L., and Dunn, R. (2003). Regulation of membrane protein transport by ubiquitin and ubiquitin-binding proteins. *Annu. Rev. Cell Dev. Biol.* *19*, 141–172
- Hochbaum, D., Zhang, Y., Stuckenholtz, C., Labhart, P., Alexiadis, V., Martin, R., Knölker, H., and Fisher, A. L. (2011). DAF-12 regulates a connected network of genes to ensure robust developmental decisions. *PLoS Genet* *7*, e1002179.
- Hong, Y., Roy, R., and Ambros, V. (1998). Developmental regulation of a cyclin-dependent kinase inhibitor controls postembryonic cell cycle progression in *Caenorhabditis elegans*. *Development* *125*, 3585–3597.
- Hoppe, T. (2005). Multiubiquitylation by E4 enzymes: 'one size' doesn't fit all. *Trends Biochem. Sci.* *30*, 183–187.
- Hoppe, T., Cassata, G., Barral, J. M., Springer, W., Hutagalung, A. H., Epstein, H. F., and Baumeister, R. (2004). Regulation of the myosin-directed chaperone UNC-45 by a novel E3/E4-multiubiquitylation complex in *C. elegans*. *Cell* *118*, 337–349.
- Hori, T., Osaka, F., Chiba, T., Miyamoto, C., Okabayashi, K., Shimbara, N., Kato, S., and Tanaka, K. (1999). Covalent modification of all members of human cullin family proteins by NEDD8. *Oncogene* *18*, 6829–6834.
- Horsley, V., O'Carroll, D., Tooze, R., Ohinata, Y., Saitou, M., Obukhanych, T., Nussenzweig, M., Tarakhovskiy, A., and Fuchs, E. (2006). Blimp1 defines a progenitor population that governs cellular input to the sebaceous gland. *Cell* *126*, 597–609.
- Hsin, H., and Kenyon, C. (1999). Signals from the reproductive system regulate the lifespan of *C. elegans*. *Nature* *399*, 362–366.
- Huang, D. W., Sherman, B. T., and Lempicki, R. A. (2009). Systematic and integrative analysis of large gene lists using DAVID bioinformatics resources. *Nat Protoc* *4*, 44–57.
- Hubbard, E. J., Wu, G., Kitajewski, J., and Greenwald, I. (1997). *sel-10*, a negative regulator of *lin-12* activity in *Caenorhabditis elegans*, encodes a member of the CDC4 family of proteins. *Genes Dev* *11*, 3182–3193.

- Janich, P., Pascual, G., Merlos-Suárez, A., Batlle, E., Ripperger, J., Albrecht, U., Cheng, H. M., Obrietan, K., Di Croce, L., and Benitah, S. A. (2011). The circadian molecular clock creates epidermal stem cell heterogeneity. *Nature* *480*, 209–214.
- Jeon, M., Gardner, H. F., Miller, E. A., Deshler, J., and Rougvie, A. E. (1999). Similarity of the *C. elegans* developmental timing protein LIN-42 to circadian rhythm proteins. *Science* *286*, 1141–1146.
- Jérôme, T., Laurie, P., Louis, B., and Pierre, C. (2007). Enjoy the Silence: The Story of let-7 MicroRNA and Cancer. *Curr. Genomics* *8*, 229–233.
- Jia, K., Albert, P. S., and Riddle, D. L. (2002). DAF-9, a cytochrome P450 regulating *C. elegans* larval development and adult longevity. *Development* *129*, 221–231.
- Jin, J., Ang, X. L., Shirogane, T., and Wade Harper, J. (2005). Identification of substrates for F-box proteins. *Meth. Enzymol.* *399*, 287–309.
- Jin, J., Cardozo, T., Lovering, R. C., Elledge, S. J., Pagano, M., and Harper, J. W. (2004). Systematic analysis and nomenclature of mammalian F-box proteins. *Genes Dev* *18*, 2573–2580.
- Johnson, S. M., Grosshans, H., Shingara, J., Byrom, M., Jarvis, R., Cheng, A., Labourier, E., Reinert, K. L., Brown, D., and Slack, F. J. (2005). RAS is regulated by the let-7 microRNA family. *Cell* *120*, 635–647.
- Johnson, T. E., Mitchell, D. H., Kline, S., Kemal, R., and Foy, J. (1984). Arresting development arrests aging in the nematode *Caenorhabditis elegans*. *Mech. Ageing Dev.* *28*, 23–40.
- Johnston, M. C., and Bronsky, P. T. (1995). Prenatal Craniofacial Development: New Insights on Normal and Abnormal Mechanisms. *Critical Reviews in Oral Biology & Medicine* *6*, 368–422.
- Johnstone, I. L., and Barry, J. D. (1996). Temporal reiteration of a precise gene expression pattern during nematode development. *EMBO J.* *15*, 3633–3639.
- Jorgensen, E. M., and Mango, S. E. (2002). The art and design of genetic screens: *caenorhabditis elegans*. *Nat Rev Genet* *3*, 356–369.
- Jørgensen, S., Eskildsen, M., Fugger, K., Hansen, L., Larsen, M. S. Y., Kousholt, A. N., Syljuåsen, R. G., Trelle, M. B., Jensen, O. N., Helin, K., et al. (2011). SET8 is degraded via PCNA-coupled CRL4(CDT2) ubiquitylation in S phase and after UV irradiation. *J. Cell Biol.* *192*, 43–54.
- Kamath, R. S., Martinez-Campos, M., Zipperlen, P., Fraser, A. G., and Ahringer, J. (2001). Effectiveness of specific RNA-mediated interference through ingested double-stranded RNA in *Caenorhabditis elegans*. *Genome Biol.* *2*, RESEARCH0002.
- Kamath, R. S., and Ahringer, J. (2003). Genome-wide RNAi screening in *Caenorhabditis elegans*. *Methods* *30*, 313–321.
- Kamura, T., Conrad, M. N., Yan, Q., Conaway, R. C., and Conaway, J. W. (1999). The Rbx1 subunit of SCF and VHL E3 ubiquitin ligase activates Rub1 modification of cullins Cdc53 and Cul2. *Genes Dev* *13*, 2928–2933.
- Kan, Z., Jaiswal, B. S., Stinson, J., Janakiraman, V., Bhatt, D., Stern, H. M., Yue, P., Haverty, P. M., Bourgon, R., Zheng, J., et al. (2010). Diverse somatic mutation patterns and pathway alterations in human cancers. *Nature* *466*, 869–873.
- Karasek, M. A. (1975). In vitro growth and maturation of epithelial cells from postembryonic skin. *J. Invest. Dermatol.* *65*, 60–66.
- Karp, X., and Ambros, V. (2012). Dauer larva quiescence alters the circuitry of microRNA pathways regulating cell fate progression in *C. elegans*. *Development* *139*, 2177–2186.
- Karp, X., Hammell, M., Ow, M. C., and Ambros, V. (2011). Effect of life history on microRNA expression during *C. elegans* development. *RNA* *17*, 639–651.
- Karp, X., and Greenwald, I. (2013). Control of cell-fate plasticity and maintenance of multipotency by DAF-16/FoxO in quiescent *Caenorhabditis elegans*. *Proc Natl Acad Sci USA* *110*, 2181–2186.
- Kasuga, H., Fukuyama, M., Kitazawa, A., Kontani, K., and Katada, T. (2013). The microRNA miR-235 couples blast-cell quiescence to the nutritional state. *Nature* *497*, 503–506.
- Kim, D., Pertea, G., Trapnell, C., Pimentel, H., Kelley, R., and Salzberg, S. L. (2013). TopHat2: accurate alignment of transcriptomes in the presence of insertions, deletions and gene fusions. *Genome Biol.* *14*, R36.
- Kim, Y., Starostina, N. G., and Kipreos, E. T. (2008). The CRL4Cdt2 ubiquitin ligase targets the degradation of p21Cip1 to control replication licensing. *Genes Dev* *22*, 2507–2519.

- Kimura, K. D., Tissenbaum, H. A., Liu, Y., and Ruvkun, G. (1997). *daf-2*, an insulin receptor-like gene that regulates longevity and diapause in *Caenorhabditis elegans*. *Science* *277*, 942–946.
- King-Jones, K., and Thummel, C. S. (2005). Nuclear receptors—a perspective from *Drosophila*. *Nat Rev Genet* *6*, 311–323.
- Kipreos, E. (2005). Ubiquitin-mediated pathways in *C. elegans*. *WormBook*, 1–24.
- Kipreos, E. T., Gohel, S. P., and Hedgecock, E. M. (2000). The *C. elegans* F-box/WD-repeat protein LIN-23 functions to limit cell division during development. *Development* *127*, 5071–5082.
- Koegl, M., Hoppe, T., Schlenker, S., Ulrich, H. D., Mayer, T. U., and Jentsch, S. (1999). A novel ubiquitination factor, E4, is involved in multiubiquitin chain assembly. *Cell* *96*, 635–644.
- Koelle, M. R., Segraves, W. A., and Hogness, D. S. (1992). DHR3: a *Drosophila* steroid receptor homolog. *Proc Natl Acad Sci USA* *89*, 6167–6171.
- Koelle, M. R., Talbot, W. S., Segraves, W. A., Bender, M. T., Cherbas, P., and Hogness, D. S. (1991). The *Drosophila* EcR gene encodes an ecdysone receptor, a new member of the steroid receptor superfamily. *Cell* *67*, 59–77.
- Koepp, D. M., Schaefer, L. K., Ye, X., Keyomarsi, K., Chu, C., Harper, J. W., and Elledge, S. J. (2001). Phosphorylation-dependent ubiquitination of cyclin E by the SCFFbw7 ubiquitin ligase. *Science* *294*, 173–177.
- Komander, D., Clague, M. J., and Urbé, S. (2009). Breaking the chains: structure and function of the deubiquitinases. *Nat Rev Mol Cell Biol* *10*, 550–563.
- Komander, D., and Rape, M. (2012). The ubiquitin code. *Annu. Rev. Biochem.* *81*, 203–229.
- Kostrouchova, M., Krause, M., Kostrouch, Z., and Rall, J. E. (1998). CHR3: a *Caenorhabditis elegans* orphan nuclear hormone receptor required for proper epidermal development and molting. *Development* *125*, 1617–1626.
- Kostrouchova, M., Krause, M., Kostrouch, Z., and Rall, J. E. (2001). Nuclear hormone receptor CHR3 is a critical regulator of all four larval molts of the nematode *Caenorhabditis elegans*. *Proc Natl Acad Sci USA* *98*, 7360–7365.
- Kouns, N. A., Nakielna, J., Behensky, F., Krause, M. W., Kostrouch, Z., and Kostrouchova, M. (2011). NHR-23 dependent collagen and hedgehog-related genes required for molting. *Biochem Biophys Res Commun* *413*, 515–520.
- Kömüves, L. G., Schmuth, M., Fowler, A. J., Elias, P. M., Hanley, K., Man, M., Moser, A. H., Lobaccaro, J. A., Williams, M. L., Mangelsdorf, D. J., et al. (2002). Oxysterol stimulation of epidermal differentiation is mediated by liver X receptor-beta in murine epidermis. *J. Invest. Dermatol.* *118*, 25–34.
- Kurimoto, K., Yabuta, Y., Ohinata, Y., Shigeta, M., Yamanaka, K., and Saitou, M. (2008). Complex genome-wide transcription dynamics orchestrated by Blimp1 for the specification of the germ cell lineage in mice. *Genes Dev* *22*, 1617–1635.
- Kwon, Y. T., Reiss, Y., Fried, V. A., Hershko, A., Yoon, J. K., Gonda, D. K., Sangan, P., Copeland, N. G., Jenkins, N. A., and Varshavsky, A. (1998). The mouse and human genes encoding the recognition component of the N-end rule pathway. *Proc Natl Acad Sci USA* *95*, 7898–7903.
- la Cova, de, C., and Greenwald, I. (2012). SEL-10/Fbw7-dependent negative feedback regulation of LIN-45/Braf signaling in *C. elegans* via a conserved phosphodegron. *Genes Dev* *26*, 2524–2535.
- Lapierre, L. R., Gelino, S., Meléndez, A., and Hansen, M. (2011). Autophagy and lipid metabolism coordinately modulate life span in germline-less *C. elegans*. *Curr Biol* *21*, 1507–1514.
- Latres, E., Chiaur, D. S., and Pagano, M. (1999). The human F box protein beta-Trcp associates with the Cull1/Skp1 complex and regulates the stability of beta-catenin. *Oncogene* *18*, 849–854.
- Lee, R. C., Feinbaum, R. L., and Ambros, V. (1993). The *C. elegans* heterochronic gene *lin-4* encodes small RNAs with antisense complementarity to *lin-14*. *Cell* *75*, 843–854.
- Lehrbach, N. J., Armisen, J., Lightfoot, H. L., Murfitt, K. J., Bugaut, A., Balasubramanian, S., and Miska, E. A. (2009). LIN-28 and the poly(U) polymerase PUP-2 regulate let-7 microRNA processing in *Caenorhabditis elegans*. *Nat. Struct. Mol. Biol.* *16*, 1016–1020.
- Li, Y., Gazdoui, S., Pan, Z., and Fuchs, S. Y. (2004). Stability of homologue of Slimb F-box protein is regulated by availability of its substrate. *J Biol Chem* *279*, 11074–11080.

- Liao, E. H., Hung, W., Abrams, B., and Zhen, M. (2004). An SCF-like ubiquitin ligase complex that controls presynaptic differentiation. *Nature* *430*, 345–350.
- Lin, S., Johnson, S. M., Abraham, M., Vella, M. C., Pasquinelli, A., Gamberi, C., Gottlieb, E., and Slack, F. J. (2003). The *C. elegans* hunchback homolog, *hbl-1*, controls temporal patterning and is a probable microRNA target. *Dev Cell* *4*, 639–650.
- Lin, Y., Wong, K., and Calame, K. (1997). Repression of *c-myc* transcription by Blimp-1, an inducer of terminal B cell differentiation. *Science* *276*, 596–599.
- Liu, J., Furukawa, M., Matsumoto, T., and Xiong, Y. (2002). NEDD8 modification of CUL1 dissociates p120(CAND1), an inhibitor of CUL1-SKP1 binding and SCF ligases. *Mol Cell* *10*, 1511–1518.
- Liu, Z., Kirch, S., and Ambros, V. (1995). The *Caenorhabditis elegans* heterochronic gene pathway controls stage-specific transcription of collagen genes. *Development* *121*, 2471–2478.
- Liu, Z., and Ambros, V. (1991). Alternative temporal control systems for hypodermal cell differentiation in *Caenorhabditis elegans*. *Nature* *350*, 162–165.
- Loedige, I., Gaidatzis, D., Sack, R., Meister, G., and Filipowicz, W. (2013). The mammalian TRIM-NHL protein TRIM71/LIN-41 is a repressor of mRNA function. *Nucleic Acids Res* *41*, 518–532.
- Ludewig, A. H., Kober-Eisermann, C., Weitzel, C., Bethke, A., Neubert, K., Gerisch, B., Hutter, H., and Antebi, A. (2004). A novel nuclear receptor/coregulator complex controls *C. elegans* lipid metabolism, larval development, and aging. *Genes Dev* *18*, 2120–2133.
- Magnúsdóttir, E., Kalachikov, S., Mizukoshi, K., Savitsky, D., Ishida-Yamamoto, A., Panteleyev, A. A., and Calame, K. (2007). Epidermal terminal differentiation depends on B lymphocyte-induced maturation protein-1. *Proc Natl Acad Sci USA* *104*, 14988–14993.
- Mandelbaum, J., Bhagat, G., Tang, H., Mo, T., Brahmachary, M., Shen, Q., Chadburn, A., Rajewsky, K., Tarakhovskiy, A., Pasqualucci, L., et al. (2010). BLIMP1 is a tumor suppressor gene frequently disrupted in activated B cell-like diffuse large B cell lymphoma. *Cancer Cell* *18*, 568–579.
- Margottin, F., Bour, S. P., Durand, H., Selig, L., Benichou, S., Richard, V., Thomas, D., Strebel, K., and Benarous, R. (1998). A novel human WD protein, h-beta TrCp, that interacts with HIV-1 Vpu connects CD4 to the ER degradation pathway through an F-box motif. *Mol Cell* *1*, 565–574.
- Martins, G., and Calame, K. (2008). Regulation and functions of Blimp-1 in T and B lymphocytes. *Annu Rev Immunol* *26*, 133–169.
- Mathias, N., Johnson, S. L., Winey, M., Adams, A. E., Goetsch, L., Pringle, J. R., Byers, B., and Goebel, M. G. (1996). Cdc53p acts in concert with Cdc4p and Cdc34p to control the G1-to-S-phase transition and identifies a conserved family of proteins. *Mol. Cell. Biol.* *16*, 6634–6643.
- Mehta, N., Loria, P. M., and Hobert, O. (2004). A genetic screen for neurite outgrowth mutants in *Caenorhabditis elegans* reveals a new function for the F-box ubiquitin ligase component LIN-23. *Genetics* *166*, 1253–1267.
- Monsalve, G. C., Van Buskirk, C., and Frand, A. R. (2011). LIN-42/PERIOD controls cyclical and developmental progression of *C. elegans* molts. *Curr Biol* *21*, 2033–2045.
- Morita, K., and Han, M. (2006). Multiple mechanisms are involved in regulating the expression of the developmental timing regulator *lin-28* in *Caenorhabditis elegans*. *EMBO J.* *25*, 5794–5804.
- Moss, E. G. (2007). Heterochronic genes and the nature of developmental time. *Curr Biol* *17*, R425–34.
- Moss, E. G., Lee, R. C., and Ambros, V. (1997). The cold shock domain protein LIN-28 controls developmental timing in *C. elegans* and is regulated by the *lin-4* RNA. *Cell* *88*, 637–646.
- Motola, D. L., Cummins, C. L., Rottiers, V., Sharma, K. K., Li, T., Li, Y., Suino-Powell, K., Xu, H. E., Auchus, R. J., Antebi, A., et al. (2006). Identification of ligands for DAF-12 that govern dauer formation and reproduction in *C. elegans*. *Cell* *124*, 1209–1223.
- Murray, M. J., Saini, H. K., Siegler, C. A., Hanning, J. E., Barker, E. M., van Dongen, S., Ward, D. M., Raby, K. L., Groves, I. J., Scarpini, C. G., et al. (2013). LIN28 Expression in malignant germ cell tumors downregulates *let-7* and increases oncogene levels. *Cancer Res.* *73*, 4872–4884.
- Nagamatsu, G., Kosaka, T., Kawasumi, M., Kinoshita, T., Takubo, K., Akiyama, H., Sudo, T., Kobayashi, T., Oya, M., and Suda, T. (2011). A germ cell-specific gene, *Prmt5*, works in somatic cell reprogramming. *J Biol Chem* *286*, 10641–10648.

- Nam, Y., Chen, C., Gregory, R. I., Chou, J. J., and Sliz, P. (2011). Molecular basis for interaction of let-7 microRNAs with Lin28. *Cell* *147*, 1080–1091.
- Nayak, S., Santiago, F. E., Jin, H., Lin, D., Schedl, T., and Kipreos, E. T. (2002). The *Caenorhabditis elegans* Skp1-related gene family: diverse functions in cell proliferation, morphogenesis, and meiosis. *Curr Biol* *12*, 277–287.
- Nelson, M. D., Zhou, E., Kiontke, K., Fradin, H., Maldonado, G., Martin, D., Shah, K., and Fitch, D. H. A. (2011). A Bow-Tie Genetic Architecture for Morphogenesis Suggested by a Genome-Wide RNAi Screen in *Caenorhabditis elegans*. *PLoS Genet* *7*, e1002010.
- Niu, W., Lu, Z. J., Zhong, M., Sarov, M., Murray, J. I., Brdlik, C. M., Janette, J., Chen, C., Alves, P., Preston, E., et al. (2011). Diverse transcription factor binding features revealed by genome-wide ChIP-seq in *C. elegans*. *Genome Res* *21*, 245–254.
- Niwa, R., Zhou, F., Li, C., and Slack, F. J. (2008). The expression of the Alzheimer's amyloid precursor protein-like gene is regulated by developmental timing microRNAs and their targets in *Caenorhabditis elegans*. *Dev Biol* *315*, 418–425.
- Ohinata, Y., Ohta, H., Shigeta, M., Yamanaka, K., Wakayama, T., and Saitou, M. (2009). A signaling principle for the specification of the germ cell lineage in mice. *Cell* *137*, 571–584.
- Ohinata, Y., Payer, B., O'Carroll, D., Ancelin, K., Ono, Y., Sano, M., Barton, S. C., Obukhanych, T., Nussenzweig, M., Tarakhovskiy, A., et al. (2005). *Blimp1* is a critical determinant of the germ cell lineage in mice. *Nature* *436*, 207–213.
- Olsen, P. H., and Ambros, V. (1999). The *lin-4* regulatory RNA controls developmental timing in *Caenorhabditis elegans* by blocking LIN-14 protein synthesis after the initiation of translation. *Dev Biol* *216*, 671–680.
- Ong, K. K., Elks, C. E., Li, S., Zhao, J. H., Luan, J., Andersen, L. B., Bingham, S. A., Brage, S., Smith, G. D., Ekelund, U., et al. (2009). Genetic variation in LIN28B is associated with the timing of puberty. *Nat. Genet.* *41*, 729–733.
- Pan, Z., Kentsis, A., Dias, D. C., Yamoah, K., and Wu, K. (2004). Nedd8 on cullin: building an expressway to protein destruction. *Oncogene* *23*, 1985–1997.
- Park, S. W., Lee, S., Sohn, Y. B., Cho, S. Y., Kim, S., Kim, S. J., Kim, C. H., Ko, A., Paik, K., Kim, J., et al. (2012). LIN28B polymorphisms are associated with central precocious puberty and early puberty in girls. *Korean J Pediatr* *55*, 388–392.
- Pasquinelli, A. E., Reinhart, B. J., Slack, F., Martindale, M. Q., Kuroda, M. I., Maller, B., Hayward, D. C., Ball, E. E., Degan, B., Müller, P., et al. (2000). Conservation of the sequence and temporal expression of let-7 heterochronic regulatory RNA. *Nature* *408*, 86–89.
- Passmore, L. A., and Barford, D. (2004). Getting into position: the catalytic mechanisms of protein ubiquitylation. *Biochem. J.* *379*, 513–525.
- Pepper, A. S., McCane, J. E., Kemper, K., Yeung, D. A., Lee, R. C., Ambros, V., and Moss, E. G. (2004). The *C. elegans* heterochronic gene *lin-46* affects developmental timing at two larval stages and encodes a relative of the scaffolding protein gephyrin. *Development* *131*, 2049–2059.
- Peschiaroli, A., Scialpi, F., Bernassola, F., Pagano, M., and Melino, G. (2009). The F-box protein FBXO45 promotes the proteasome-dependent degradation of p73. *Oncogene* *28*, 3157–3166.
- Peschiaroli, A., Dorrello, N. V., Guardavaccaro, D., Venere, M., Halazonetis, T., Sherman, N. E., and Pagano, M. (2006). SCFbetaTrCP-mediated degradation of Claspin regulates recovery from the DNA replication checkpoint response. *Mol Cell* *23*, 319–329.
- Petroski, M. D., and Deshaies, R. J. (2005). Function and regulation of cullin-RING ubiquitin ligases. *Nat Rev Mol Cell Biol* *6*, 9–20.
- Phan, R. T., Saito, M., Kitagawa, Y., Means, A. R., and Dalla-Favera, R. (2007). Genotoxic stress regulates expression of the proto-oncogene *Bcl6* in germinal center B cells. *Nat Immunol* *8*, 1132–1139.
- Pickart, C. M., and Fushman, D. (2004). Polyubiquitin chains: polymeric protein signals. *Curr Opin Chem Biol* *8*, 610–616.

- Pierce, N. W., Lee, J. E., Liu, X., Sweredoski, M. J., Graham, R. L. J., Larimore, E. A., Rome, M., Zheng, N., Clurman, B. E., Hess, S., et al. (2013). Cnd1 promotes assembly of new SCF complexes through dynamic exchange of F box proteins. *Cell* *153*, 206–215.
- Pillai, R. S., Bhattacharyya, S. N., and Filipowicz, W. (2007). Repression of protein synthesis by miRNAs: how many mechanisms? *Trends Cell Biol.* *17*, 118–126.
- Piskounova, E., Polytaichou, C., Thornton, J. E., LaPierre, R. J., Pothoulakis, C., Hagan, J. P., Iliopoulos, D., and Gregory, R. I. (2011). Lin28A and Lin28B Inhibit let-7 MicroRNA Biogenesis by Distinct Mechanisms. *Cell* *147*, 1066–1079.
- Poulin, G. B., and Ahringer, J. (2010). The *Caenorhabditis elegans* CDT-2 ubiquitin ligase is required for attenuation of EGFR signalling in vulva precursor cells. *BMC Dev Biol* *10*, 109.
- Ravid, T., and Hochstrasser, M. (2008). Diversity of degradation signals in the ubiquitin-proteasome system. *Nat Rev Mol Cell Biol* *9*, 679–690.
- Reinhart, B. J., Slack, F. J., Basson, M., Pasquinelli, A. E., Bettinger, J. C., Rougvie, A. E., Horvitz, H. R., and Ruvkun, G. (2000). The 21-nucleotide let-7 RNA regulates developmental timing in *Caenorhabditis elegans*. *Nature* *403*, 901–906.
- Ren, H., and Zhang, H. (2010). Wnt signaling controls temporal identities of seam cells in *Caenorhabditis elegans*. *Dev Biol* *345*, 144–155.
- Ren, P., Lim, C. S., Johnsen, R., Albert, P. S., Pilgrim, D., and Riddle, D. L. (1996). Control of *C. elegans* larval development by neuronal expression of a TGF-beta homolog. *Science* *274*, 1389–1391.
- Resnick, T. D., McCulloch, K. A., and Rougvie, A. E. (2010). miRNAs give worms the time of their lives: small RNAs and temporal control in *Caenorhabditis elegans*. *Dev Dyn* *239*, 1477–1489.
- Richter, J., Schlesner, M., Hoffmann, S., Kreuz, M., Leich, E., Burkhardt, B., Rosolowski, M., Ammerpohl, O., Wagener, R., Bernhart, S. H., et al. (2012). Recurrent mutation of the ID3 gene in Burkitt lymphoma identified by integrated genome, exome and transcriptome sequencing. *Nat. Genet.* *44*, 1316–1320.
- Riddiford, L. M. (1993). Hormone receptors and the regulation of insect metamorphosis. *Receptor* *3*, 203–209.
- Riddiford, L. M., Cherbas, P., and Truman, J. W. (2000). Ecdysone receptors and their biological actions. *Vitam. Horm.* *60*, 1–73.
- Riddiford, L. M., Hiruma, K., Zhou, X., and Nelson, C. A. (2003). Insights into the molecular basis of the hormonal control of molting and metamorphosis from *Manduca sexta* and *Drosophila melanogaster*. *Insect Biochem. Mol. Biol.* *33*, 1327–1338.
- Riddle, D. L., Swanson, M. M., and Albert, P. S. (1981). Interacting genes in nematode dauer larva formation. *Nature* *290*, 668–671.
- Robertson, E. J., Charatsi, I., Joyner, C. J., Koonce, C. H., Morgan, M., Islam, A., Paterson, C., Lejsek, E., Arnold, S. J., Kallies, A., et al. (2007). Blimp1 regulates development of the posterior forelimb, caudal pharyngeal arches, heart and sensory vibrissae in mice. *Development* *134*, 4335–4345.
- Rossi, M., Duan, S., Jeong, Y., Horn, M., Saraf, A., Florens, L., Washburn, M. P., Antebi, A., and Pagano, M. (2013). Regulation of the CRL4(Cdt2) ubiquitin ligase and cell-cycle exit by the SCF(Fbxo11) ubiquitin ligase. *Mol Cell* *49*, 1159–1166.
- Rottiers, V., Motola, D. L., Gerisch, B., Cummins, C. L., Nishiwaki, K., Mangelsdorf, D. J., and Antebi, A. (2006). Hormonal control of *C. elegans* dauer formation and life span by a Rieske-like oxygenase. *Dev Cell* *10*, 473–482.
- Rougvie, A. E. (2001). Control of developmental timing in animals. *Nat Rev Genet* *2*, 690–701.
- Rougvie, A. E., and Ambros, V. (1995). The heterochronic gene *lin-29* encodes a zinc finger protein that controls a terminal differentiation event in *Caenorhabditis elegans*. *Development* *121*, 2491–2500.
- Rougvie, A. E., and Moss, E. G. (2013). Developmental transitions in *C. elegans* larval stages. *Curr. Top. Dev. Biol.* *105*, 153–180.
- Rual, J., Ceron, J., Koreth, J., Hao, T., Nicot, A., Hirozane-Kishikawa, T., Vandenhaute, J., Orkin, S. H., Hill, D. E., van den Heuvel, S., et al. (2004). Toward improving *Caenorhabditis elegans* phenome mapping with an ORFeome-based RNAi library. *Genome Res* *14*, 2162–2168.
- Russell, E. S. (1916). *Russell: Form and function* (1982 Reprint) - Google Scholar.

- Ruvkun, G., and Giusto, J. (1989). The *Caenorhabditis elegans* heterochronic gene *lin-14* encodes a nuclear protein that forms a temporal developmental switch. *Nature* *338*, 313–319.
- Rybak, A., Fuchs, H., Smirnova, L., Brandt, C., Pohl, E. E., Nitsch, R., and Wulczyn, F. G. (2008). A feedback loop comprising *lin-28* and *let-7* controls pre-*let-7* maturation during neural stem-cell commitment. *Nat Cell Biol* *10*, 987–993.
- Rybak, A., Fuchs, H., Hadian, K., Smirnova, L., Wulczyn, E. A., Michel, G., Nitsch, R., Krappmann, D., and Wulczyn, F. G. (2009). The *let-7* target gene mouse *lin-41* is a stem cell specific E3 ubiquitin ligase for the miRNA pathway protein Ago2. *Nat Cell Biol* *11*, 1411–1420.
- Rye, M. S., Wiertsema, S. P., Scaman, E. S. H., Oommen, J., Sun, W., Francis, R. W., Ang, W., Pennell, C. E., Burgner, D., Richmond, P., et al. (2011). FBXO11, a regulator of the TGF $\beta$  pathway, is associated with severe otitis media in Western Australian children. *Genes Immun.* *12*, 352–359.
- Samuelson, A. V., Carr, C. E., and Ruvkun, G. (2007). Gene activities that mediate increased life span of *C. elegans* insulin-like signaling mutants. *Genes Dev* *21*, 2976–2994.
- Sarikas, A., Hartmann, T., and Pan, Z. (2011). The cullin protein family. *Genome Biol.* *12*, 220.
- Sarov, M., Murray, J. I., Schanze, K., Pozniakovski, A., Niu, W., Angermann, K., Hasse, S., Rupprecht, M., Vinis, E., Tinney, M., et al. (2012). A Genome-Scale Resource for In Vivo Tag-Based Protein Function Exploration in *C. elegans*. *Cell* *150*, 855–866.
- Saunders, D. S., Henrich, V. C., and Gilbert, L. I. (1989). Induction of diapause in *Drosophila melanogaster*: photoperiodic regulation and the impact of arrhythmic clock mutations on time measurement. *Proc Natl Acad Sci USA* *86*, 3748–3752.
- Scheffner, M., Nuber, U., and Huibregtse, J. M. (1995). Protein ubiquitination involving an E1-E2-E3 enzyme ubiquitin thioester cascade. *Nature* *373*, 81–83.
- Schoenheimer, R. (1942). Google Scholar. *Annu. Rev. Biochem.*
- Segade, F., Daly, K. A., Allred, D., Hicks, P. J., Cox, M., Brown, M., Hardisty-Hughes, R. E., Brown, S. D. M., Rich, S. S., and Bowden, D. W. (2006). Association of the FBXO11 gene with chronic otitis media with effusion and recurrent otitis media: the Minnesota COME/ROM Family Study. *Arch. Otolaryngol. Head Neck Surg.* *132*, 729–733.
- Seggerson, K., Tang, L., and Moss, E. G. (2002). Two genetic circuits repress the *Caenorhabditis elegans* heterochronic gene *lin-28* after translation initiation. *Dev Biol* *243*, 215–225.
- Segref, A., Torres, S., and Hoppe, T. (2011). A Screenable in vivo Assay to Study Proteostasis Networks in *Caenorhabditis elegans*. *Genetics*.
- Segref, A., and Hoppe, T. (2009). Think locally: control of ubiquitin-dependent protein degradation in neurons. *EMBO Rep* *10*, 44–50.
- Sempere, L. F., Freemantle, S., Pitha-Rowe, I., Moss, E., Dmitrovsky, E., and Ambros, V. (2004). Expression profiling of mammalian microRNAs uncovers a subset of brain-expressed microRNAs with possible roles in murine and human neuronal differentiation. *Genome Biol.* *5*, R13.
- Shaffer, A. L., Lin, K. I., Kuo, T. C., Yu, X., and Hurt, E. M. (2002). Blimp-1 orchestrates plasma cell differentiation by extinguishing the mature B cell gene expression program. *Immunity*.
- Shapiro-Shelef, M., Lin, K., McHeyzer-Williams, L. J., Liao, J., McHeyzer-Williams, M. G., and Calame, K. (2003). Blimp-1 is required for the formation of immunoglobulin secreting plasma cells and pre-plasma memory B cells. *Immunity* *19*, 607–620.
- Shaye, D. D., and Greenwald, I. (2011). OrthoList: a compendium of *C. elegans* genes with human orthologs. *PLoS ONE* *6*, e20085.
- Shimshon, L., Michaeli, A., Hadar, R., Nutt, S. L., David, Y., Navon, A., Waisman, A., and Tirosh, B. (2011). SUMOylation of Blimp-1 promotes its proteasomal degradation. *FEBS Lett.* *585*, 2405–2409.
- Shirogane, T., Jin, J., Ang, X. L., and Harper, J. W. (2005). SCF $\beta$ -TRCP controls clock-dependent transcription via casein kinase 1-dependent degradation of the mammalian period-1 (Per1) protein. *J Biol Chem* *280*, 26863–26872.
- Shyh-Chang, N., Zhu, H., Yvanka de Soysa, T., Shinoda, G., Seligson, M. T., Tsanov, K. M., Nguyen, L., Asara, J. M., Cantley, L. C., and Daley, G. Q. (2013). *Lin28* enhances tissue repair by reprogramming cellular metabolism. *Cell* *155*, 778–792.

- Silhánková, M., Jindra, M., and Asahina, M. (2005). Nuclear receptor NHR-25 is required for cell-shape dynamics during epidermal differentiation in *Caenorhabditis elegans*. *J. Cell. Sci.* *118*, 223–232.
- Simmer, F., Tijsterman, M., Parrish, S., Koushika, S. P., Nonet, M. L., Fire, A., Ahringer, J., and Plasterk, R. H. A. (2002). Loss of the putative RNA-directed RNA polymerase RRF-3 makes *C. elegans* hypersensitive to RNAi. *Curr Biol* *12*, 1317–1319.
- Singh, R. N., and Sulston, J. E. (1978). Some observations on moulting in *Caenorhabditis elegans*. *Nematologica*.
- Skaar, J. R., Pagan, J. K., and Pagano, M. (2013). Mechanisms and function of substrate recruitment by F-box proteins. *Nat Rev Mol Cell Biol* *14*, 369–381.
- Skaar, J. R., Pagan, J. K., and Pagano, M. (2009a). SnapShot: F box proteins I. *Cell* *137*, 1160–1160.e1.
- Skaar, J. R., D'Angiolella, V., Pagan, J. K., and Pagano, M. (2009b). SnapShot: F Box Proteins II. *Cell* *137*, 1358–1358.e1.
- Skowyra, D., Craig, K. L., Tyers, M., Elledge, S. J., and Harper, J. W. (1997). F-box proteins are receptors that recruit phosphorylated substrates to the SCF ubiquitin-ligase complex. *Cell* *91*, 209–219.
- Slack, F. J., Basson, M., Liu, Z., Ambros, V., Horvitz, H. R., and Ruvkun, G. (2000). The *lin-41* RBCC gene acts in the *C. elegans* heterochronic pathway between the *let-7* regulatory RNA and the *LIN-29* transcription factor. *Mol Cell* *5*, 659–669.
- Smith, K. K. (2001). Heterochrony revisited: the evolution of developmental sequences. *Biological Journal of the Linnean Society*.
- Smith, K. K. (2002). Sequence heterochrony and the evolution of development. *J. Morphol.* *252*, 82–97.
- Smith, K. K. (2003). Time's arrow: heterochrony and the evolution of development. *Int. J. Dev. Biol.* *47*, 613–621.
- Sokol, N. S. (2012). Small temporal RNAs in animal development. *Curr. Opin. Genet. Dev.* *22*, 368–373.
- Sokol, N. S., Xu, P., Jan, Y., and Ambros, V. (2008). *Drosophila* *let-7* microRNA is required for remodeling of the neuromusculature during metamorphosis. *Genes Dev* *22*, 1591–1596.
- Stocker, J. W. (1977). Functional maturation of B cells in vitro. *Immunology* *32*, 275–281.
- Spence, J., Sadis, S., Haas, A. L., and Finley, D. (1995). A ubiquitin mutant with specific defects in DNA repair and multiubiquitination. *Mol. Cell. Biol.* *15*, 1265–1273.
- Stransky, N., Egloff, A. M., Tward, A. D., Kostic, A. D., Cibulskis, K., Sivachenko, A., Kryukov, G. V., Lawrence, M. S., Sougnez, C., McKenna, A., et al. (2011). The mutational landscape of head and neck squamous cell carcinoma. *Science* *333*, 1157–1160.
- Su, M., Merz, D. C., Killeen, M. T., Zhou, Y., Zheng, H., Kramer, J. M., Hedgecock, E. M., and Culotti, J. G. (2000). Regulation of the *UNC-5* netrin receptor initiates the first reorientation of migrating distal tip cells in *Caenorhabditis elegans*. *Development* *127*, 585–594.
- Su, S., Ying, H., Chiu, Y., Lin, F., Chen, M., and Lin, K. (2009). Involvement of histone demethylase LSD1 in Blimp-1-mediated gene repression during plasma cell differentiation. *Mol. Cell. Biol.* *29*, 1421–1431.
- Sulston, J. E., Schierenberg, E., White, J. G., and Thomson, J. N. (1983). The embryonic cell lineage of the nematode *Caenorhabditis elegans*. *Dev Biol* *100*, 64–119.
- Sulston, J. E., and Horvitz, H. R. (1977). Post-embryonic cell lineages of the nematode, *Caenorhabditis elegans*. *Dev Biol* *56*, 110–156.
- Sun, Y., Hu, Z., Goeb, Y., and Dreier, L. (2013). The F-box protein MEC-15 (FBXW9) promotes synaptic transmission in GABAergic motor neurons in *C. elegans*. *PLoS ONE* *8*, e59132.
- Sundaram, M., and Greenwald, I. (1993). Suppressors of a *lin-12* hypomorph define genes that interact with both *lin-12* and *glp-1* in *Caenorhabditis elegans*. *Genetics* *135*, 765–783.
- Supek, F., Bošnjak, M., Škunca, N., and Šmuc, T. (2011). REVIGO summarizes and visualizes long lists of gene ontology terms. *PLoS ONE* *6*, e21800.
- Surani, M. A., Hayashi, K., and Hajkova, P. (2007). Genetic and epigenetic regulators of pluripotency. *Cell* *128*, 747–762.

- Sze, J. Y., Victor, M., Loer, C., Shi, Y., and Ruvkun, G. (2000). Food and metabolic signalling defects in a *Caenorhabditis elegans* serotonin-synthesis mutant. *Nature* *403*, 560–564.
- Takamizawa, J., Konishi, H., Yanagisawa, K., Tomida, S., Osada, H., Endoh, H., Harano, T., Yatabe, Y., Nagino, M., Nimura, Y., et al. (2004). Reduced expression of the let-7 microRNAs in human lung cancers in association with shortened postoperative survival. *Cancer Res.* *64*, 3753–3756.
- Tasaki, T., Mulder, L. C. F., Iwamatsu, A., Lee, M. J., Davydov, I. V., Varshavsky, A., Muesing, M., and Kwon, Y. T. (2005). A family of mammalian E3 ubiquitin ligases that contain the UBR box motif and recognize N-degrons. *Mol. Cell. Biol.* *25*, 7120–7136.
- Tatar, M., and Yin, C. (2001). Slow aging during insect reproductive diapause: why butterflies, grasshoppers and flies are like worms. *Exp. Gerontol.* *36*, 723–738.
- Tateossian, H., Hardisty-Hughes, R. E., Morse, S., Romero, M. R., Hilton, H., Dean, C., and Brown, S. D. (2009). Regulation of TGF-beta signalling by Fbxo11, the gene mutated in the Jeff otitis media mouse mutant. *Pathogenetics* *2*, 5.
- Tennessen, J. M., Gardner, H. F., Volk, M. L., and Rougvie, A. E. (2006). Novel heterochronic functions of the *Caenorhabditis elegans* period-related protein LIN-42. *Dev Biol* *289*, 30–43.
- Tennessen, J. M., Opperman, K. J., and Rougvie, A. E. (2010). The *C. elegans* developmental timing protein LIN-42 regulates diapause in response to environmental cues. *Development* *137*, 3501–3511.
- Terai, K., Abbas, T., Jazaeri, A. A., and Dutta, A. (2010). CRL4(Cdt2) E3 ubiquitin ligase monoubiquitinates PCNA to promote translesion DNA synthesis. *Mol Cell* *37*, 143–149.
- Thiele, S., Wittmann, J., Jäck, H., and Pahl, A. (2012). miR-9 enhances IL-2 production in activated human CD4(+) T cells by repressing Blimp-1. *Eur J Immunol*.
- Thomas, D., Kuras, L., Barbey, R., Cherest, H., Blaiseau, P. L., and Surdin-Kerjan, Y. (1995). Met30p, a yeast transcriptional inhibitor that responds to S-adenosylmethionine, is an essential protein with WD40 repeats. *Mol. Cell. Biol.* *15*, 6526–6534.
- Thomas, J. H. (2006). Adaptive evolution in two large families of ubiquitin-ligase adapters in nematodes and plants. *Genome Res* *16*, 1017–1030.
- Thomson, J. M., Newman, M., Parker, J. S., Morin-Kensicki, E. M., Wright, T., and Hammond, S. M. (2006). Extensive post-transcriptional regulation of microRNAs and its implications for cancer. *Genes Dev* *20*, 2202–2207.
- Thornton, J. E., and Gregory, R. I. (2012). How does Lin28 let-7 control development and disease? *Trends Cell Biol.* *22*, 474–482.
- Thrower, J. S., Hoffman, L., Rechsteiner, M., and Pickart, C. M. (2000). Recognition of the polyubiquitin proteolytic signal. *EMBO J.* *19*, 94–102.
- Thummel, C. S. (1996). Flies on steroids—*Drosophila* metamorphosis and the mechanisms of steroid hormone action. *Trends Genet.* *12*, 306–310.
- Timmons, L., and Fire, A. (1998). Specific interference by ingested dsRNA. *Nature* *395*, 854.
- Trapnell, C., Williams, B. A., Pertea, G., Mortazavi, A., Kwan, G., van Baren, M. J., Salzberg, S. L., Wold, B. J., and Pachter, L. (2010). Transcript assembly and quantification by RNA-Seq reveals unannotated transcripts and isoform switching during cell differentiation. *Nat. Biotechnol.* *28*, 511–515.
- Tsunematsu, R., Nakayama, K., Oike, Y., Nishiyama, M., Ishida, N., Hatakeyama, S., Bessho, Y., Kageyama, R., Suda, T., and Nakayama, K. I. (2004). Mouse Fbw7/Sel-10/Cdc4 is required for notch degradation during vascular development. *J Biol Chem* *279*, 9417–9423.
- Tunyaplin, C., Shapiro, M. A., and Calame, K. L. (2000). Characterization of the B lymphocyte-induced maturation protein-1 (Blimp-1) gene, mRNA isoforms and basal promoter. *Nucleic Acids Res* *28*, 4846–4855.
- Turner, C. A., Mack, D. H., and Davis, M. M. (1994). Blimp-1, a novel zinc finger-containing protein that can drive the maturation of B lymphocytes into immunoglobulin-secreting cells. *Cell* *77*, 297–306.
- Turner, M. J., Jiao, A. L., and Slack, F. J. (2014). Autoregulation of lin-4 microRNA transcription by RNA activation (RNAa) in *C. elegans*. *Cell Cycle* *13*.
- Vadla, B., Kemper, K., Alaimo, J., Heine, C., and Moss, E. G. (2012). lin-28 controls the succession of cell fate choices via two distinct activities. *PLoS Genet* *8*, e1002588.

- Van Wynsberghe, P. M., Kai, Z. S., Massirer, K. B., Burton, V. H., Yeo, G. W., and Pasquinelli, A. E. (2011). LIN-28 co-transcriptionally binds primary let-7 to regulate miRNA maturation in *Caenorhabditis elegans*. *Nat. Struct. Mol. Biol.* *18*, 302–308.
- Vella, M. C., Choi, E., Lin, S., Reinert, K., and Slack, F. J. (2004). The *C. elegans* microRNA let-7 binds to imperfect let-7 complementary sites from the lin-41 3'UTR. *Genes Dev* *18*, 132–137.
- Vertegaal, A. C. O. (2007). Small ubiquitin-related modifiers in chains. *Biochem Soc Trans* *35*, 1422–1423.
- Vincent, S. D., Dunn, N. R., Sciammas, R., Shapiro-Shalef, M., Davis, M. M., Calame, K., Bikoff, E. K., and Robertson, E. J. (2005). The zinc finger transcriptional repressor Blimp1/Prdm1 is dispensable for early axis formation but is required for specification of primordial germ cells in the mouse. *Development* *132*, 1315–1325.
- Viswanathan, S. R., Daley, G. Q., and Gregory, R. I. (2008). Selective blockade of microRNA processing by Lin28. *Science* *320*, 97–100.
- Welcker, M., and Clurman, B. E. (2008). FBW7 ubiquitin ligase: a tumour suppressor at the crossroads of cell division, growth and differentiation. *Nat. Rev. Cancer* *8*, 83–93.
- White, J. (1988). 4 The Anatomy. Cold Spring Harbor Monograph Archive *17*, 81–122.
- Wightman, B., Bürglin, T. R., Gatto, J., Arasu, P., and Ruvkun, G. (1991). Negative regulatory sequences in the lin-14 3'-untranslated region are necessary to generate a temporal switch during *Caenorhabditis elegans* development. *Genes Dev* *5*, 1813–1824.
- Wightman, B., Ha, I., and Ruvkun, G. (1993). Posttranscriptional regulation of the heterochronic gene lin-14 by lin-4 mediates temporal pattern formation in *C. elegans*. *Cell* *75*, 855–862.
- Wilkinson, K. D. (2005). The discovery of ubiquitin-dependent proteolysis. *Proc Natl Acad Sci USA* *102*, 15280–15282.
- Willems, A. R., Lanker, S., Patton, E. E., Craig, K. L., Nason, T. F., Mathias, N., Kobayashi, R., Wittenberg, C., and Tyers, M. (1996). Cdc53 targets phosphorylated G1 cyclins for degradation by the ubiquitin proteolytic pathway. *Cell* *86*, 453–463.
- Wilm, T. P., and Solnica-Krezel, L. (2005). Essential roles of a zebrafish prdm1/blimp1 homolog in embryo patterning and organogenesis. *Development* *132*, 393–404.
- Wood, W. B. (1988). *The Nematode Caenorhabditis elegans*. paperback.
- Wójcik, C., and DeMartino, G. N. (2003). Intracellular localization of proteasomes. *Int. J. Biochem. Cell Biol.* *35*, 579–589.
- Wu, G., Xu, G., Schulman, B. A., Jeffrey, P. D., Harper, J. W., and Pavletich, N. P. (2003). Structure of a beta-TrCP1-Skp1-beta-catenin complex: destruction motif binding and lysine specificity of the SCF(beta-TrCP1) ubiquitin ligase. *Mol Cell* *11*, 1445–1456.
- Wu, L., and Belasco, J. G. (2005). Micro-RNA regulation of the mammalian lin-28 gene during neuronal differentiation of embryonal carcinoma cells. *Mol. Cell. Biol.* *25*, 9198–9208.
- Wulczyn, F. G., Smirnova, L., Rybak, A., Brandt, C., Kwidzinski, E., Ninnemann, O., Strehle, M., Seiler, A., Schumacher, S., and Nitsch, R. (2007). Post-transcriptional regulation of the let-7 microRNA during neural cell specification. *FASEB J.* *21*, 415–426.
- Xia, D., Huang, X., and Zhang, H. (2009). The temporally regulated transcription factor sel-7 controls developmental timing in *C. elegans*. *Dev Biol* *332*, 246–257.
- Xie, Z., Komuves, L., Yu, Q., Elalieh, H., Ng, D. C., Leary, C., Chang, S., Crumrine, D., Yoshizawa, T., Kato, S., et al. (2002). Lack of the vitamin D receptor is associated with reduced epidermal differentiation and hair follicle growth. *J. Invest. Dermatol.* *118*, 11–16.
- Yamanaka, A., Yada, M., Imaki, H., Koga, M., Ohshima, Y., and Nakayama, K. (2002). Multiple Skp1-related proteins in *Caenorhabditis elegans*: diverse patterns of interaction with Cullins and F-box proteins. *Curr Biol* *12*, 267–275.
- Yen, H. S., and Elledge, S. J. (2008). Identification of SCF ubiquitin ligase substrates by global protein stability profiling. *Science* *322*, 923–929.
- Ying, H., Su, S., Hsu, P., Chang, C., Lin, I., Tseng, Y., Tsai, M., Shih, H., and Lin, K. (2012). SUMOylation of Blimp-1 is critical for plasma cell differentiation. *EMBO Rep.*

- Yoo, S., Mohawk, J. A., Siepkka, S. M., Shan, Y., Huh, S. K., Hong, H., Kornblum, I., Kumar, V., Koike, N., Xu, M., et al. (2013). Competing E3 ubiquitin ligases govern circadian periodicity by degradation of CRY in nucleus and cytoplasm. *Cell* *152*, 1091–1105.
- Yoshida, K., Sanada, M., Shiraiishi, Y., Nowak, D., Nagata, Y., Yamamoto, R., Sato, Y., Sato-Otsubo, A., Kon, A., Nagasaki, M., et al. (2011). Frequent pathway mutations of splicing machinery in myelodysplasia. *Nature* *478*, 64–69.
- Yoshimura, A., Wakabayashi, Y., and Mori, T. (2010). Cellular and molecular basis for the regulation of inflammation by TGF-beta. *J. Biochem.* *147*, 781–792.
- Yu, F., Yao, H., Zhu, P., Zhang, X., Pan, Q., Gong, C., Huang, Y., Hu, X., Su, F., Lieberman, J., et al. (2007a). *let-7* regulates self renewal and tumorigenicity of breast cancer cells. *Cell* *131*, 1109–1123.
- Yu, J., Vodyanik, M. A., Smuga-Otto, K., Antosiewicz-Bourget, J., Frane, J. L., Tian, S., Nie, J., Jonsdottir, G. A., Ruotti, V., Stewart, R., et al. (2007b). Induced pluripotent stem cell lines derived from human somatic cells. *Science* *318*, 1917–1920.
- Yu, J., Angelin-Duclos, C., Greenwood, J., Liao, J., and Calame, K. (2000). Transcriptional repression by blimp-1 (PRDI-BF1) involves recruitment of histone deacetylase. *Mol. Cell. Biol.* *20*, 2592–2603.
- Zhang, H., Azevedo, R. B. R., Lints, R., Doyle, C., Teng, Y., Haber, D., and Emmons, S. W. (2003). Global regulation of Hox gene expression in *C. elegans* by a SAM domain protein. *Dev Cell* *4*, 903–915.
- Zhang, L., Zhou, D., Li, S., and Jin, C. (2012). BLMP-1 Contributes to Collagen-related Morphogenesis in *C. elegans*. *Life Science Journal*.
- Zhang, L., Stokes, N., Polak, L., and Fuchs, E. (2011). Specific MicroRNAs are preferentially expressed by skin stem cells to balance self-renewal and early lineage commitment. *Cell Stem Cell* *8*, 294–308.
- Zhao, W., Liu, Y., Zhang, Q., Wang, L., Leboeuf, C., Zhang, Y., Ma, J., Garcia, J., Song, Y., Li, J., et al. (2008). PRDM1 is involved in chemoresistance of T-cell lymphoma and down-regulated by the proteasome inhibitor. *Blood* *111*, 3867–3871.
- Zheng, J., Yang, X., Harrell, J. M., Ryzhikov, S., Shim, E. H., Lykke-Andersen, K., Wei, N., Sun, H., Kobayashi, R., and Zhang, H. (2002). CAND1 binds to unneddylated CUL1 and regulates the formation of SCF ubiquitin E3 ligase complex. *Mol Cell* *10*, 1519–1526.
- Zhou, J., Ng, S., and Chng, W. (2013). LIN28/LIN28B: an emerging oncogenic driver in cancer stem cells. *Int. J. Biochem. Cell Biol.* *45*, 973–978.
- Zhu, H., Shah, S., Shyh-Chang, N., Shinoda, G., Einhorn, W. S., Viswanathan, S. R., Takeuchi, A., Grasemann, C., Rinn, J. L., Lopez, M. F., et al. (2010). Lin28a transgenic mice manifest size and puberty phenotypes identified in human genetic association studies. *Nat. Genet.* *42*, 626–630.

## **Chapter 7 - APPENDIX**

**Table A1: Genes Regulated in *blmp-1(tm548)* mutant Animals vs. WT Controls**

Fold change represents mean of three biological replicates from RNA-sequencing experiments of mid-L3 larvae.

Upregulated in <i>blmp-1</i> vs. WT				Downregulated in <i>blmp-1</i> vs. WT			
Gene ID	Gene	Fold change	q_value	Gene ID	Gene	Fold change	q_value
K09C8.3	<i>nas-10</i>	110,81	1,02E-07	cTel54X.1	<i>fbxa-6</i>	245,31	6,03E-06
Y39A3B.7		84,15	7,69E-04	T09D3.8		35,40	1,08E-07
F59A6.10		58,87	3,71E-05	C24F3.6	<i>col-124</i>	17,59	0,00E+00
ZK84.7	<i>ins-20</i>	38,28	6,37E-05	F15E11.12	<i>pud-4</i>	13,75	9,50E-04
F12A10.7		36,23	3,94E-04	K02E2.8		13,18	0,00E+00
C37A5.8	<i>fipr-24</i>	31,34	5,23E-03	F45D11.14		11,83	7,33E-08
F32G8.3		29,64	2,96E-02	F38A5.5	<i>nspb-3</i>	11,14	1,97E-04
C37A5.2	<i>fipr-22</i>	29,51	3,22E-04	F15E11.15	<i>pud-3</i>	10,60	5,13E-06
Y102A5C.34	<i>grd-17</i>	26,02	1,13E-02	B0034.7		9,91	5,09E-05
F22B3.7		16,52	1,21E-04	K02E2.2	<i>grd-11</i>	9,14	1,61E-13
C27B7.9		15,17	8,54E-13	C04G6.2		8,65	0,00E+00
T10B9.4	<i>cyp-13A8</i>	13,09	2,21E-06	F45D11.15		8,60	4,11E-07
C37A5.4	<i>fipr-23</i>	12,18	6,01E-03	F45D11.16		8,05	3,47E-07
F53B6.8	<i>fipr-26</i>	11,46	3,12E-02	Y5H2A.4		8,04	2,56E-06
Y68A4A.13		11,26	8,21E-03	F38A5.12	<i>nspb-2</i>	7,61	2,77E-05
F53H2.2	<i>cnc-7</i>	11,06	5,50E-07	F07E5.7		7,10	9,75E-07
F08E10.7	<i>scl-24</i>	10,90	3,81E-02	F14D7.2		6,95	4,25E-02
F07G11.9	<i>imd-4</i>	10,89	1,94E-05	K09C4.1		6,50	0,00E+00
C49G7.7		10,23	2,50E-02	F59D8.1	<i>vit-3</i>	6,45	0,00E+00
R13D7.11	<i>cnc-9</i>	9,14	2,49E-02	H02K04.1	<i>clec-229</i>	6,27	3,88E-10
R09B5.9	<i>cnc-4</i>	8,65	0,00E+00	F59D8.2	<i>vit-4</i>	6,21	0,00E+00
B0284.1		7,95	1,74E-07	Y5H2A.3	<i>abu-4</i>	6,06	1,62E-06
R04D3.1	<i>cyp-14A4</i>	7,13	2,57E-07	C04G6.13		5,93	6,72E-03
C08E8.3		6,97	1,51E-02	F17B5.6		5,33	4,30E-03
F33H12.7		6,75	2,49E-07	R12E2.6		5,32	1,77E-02
C45G7.3	<i>ilys-3</i>	6,19	4,55E-05	H06A10.1		5,32	7,33E-08
B0284.2		5,92	3,81E-02	K10C2.8		5,14	2,49E-02
D1065.3		5,89	8,02E-03	C04F6.1	<i>vit-5</i>	5,11	0,00E+00
ZK783.5		5,80	2,20E-02	R09D1.11		5,02	1,56E-04
C30B5.6		5,71	0,00E+00	C30H6.5		5,02	0,00E+00
C49G7.1		5,69	3,29E-04	F23F1.2		4,96	4,62E-13
B0205.14		5,61	1,30E-06	F56C3.9		4,83	1,51E-06
F14D7.7		5,57	4,80E-03	H10E21.2		4,78	3,02E-03
R09B5.3	<i>cnc-2</i>	5,55	3,77E-08	E02H4.4		4,59	7,98E-04
Y46C8AL.2	<i>clec-174</i>	5,39	3,15E-04	F11D5.5		4,56	4,16E-02
W09G12.8		5,31	7,17E-03	C54C8.4		4,49	2,91E-07
Y38E10A.28		5,23	2,33E-02	C27D9.2		4,47	1,75E-02
T24E12.5		5,21	5,52E-09	F36D1.8		4,32	3,45E-02

C04A11.5		5,21	2,07E-02	T02B5.1		4,24	1,03E-08
F28G4.1	<i>cyp-37B1</i>	5,06	3,86E-03	C01F1.5		4,23	0,00E+00
ZC513.14		5,05	2,43E-02	T19H5.6		4,21	2,00E-02
C33G8.3		5,03	3,97E-03	Y51H4A.9	<i>col-137</i>	4,12	2,85E-03
F13D12.3		4,98	0,00E+00	K03H9.3		4,07	9,84E-04
Y41G9A.10		4,92	6,90E-12	K09F5.2	<i>vit-1</i>	4,05	0,00E+00
F46C5.1		4,91	3,87E-03	W02B8.6	<i>mltn-5</i>	4,03	2,32E-04
F53G12.7	<i>col-45</i>	4,85	4,93E-02	F11D5.7		4,01	5,48E-05
C03G6.13	<i>tag-293</i>	4,79	6,32E-04	T14G12.6		3,97	1,06E-02
C25F9.11	<i>C25F9.11</i>	4,77	3,73E-05	Y62H9A.3		3,96	1,09E-02
T15B7.5	<i>col-141</i>	4,75	0,00E+00	C29F3.2	<i>wrt-8</i>	3,94	0,00E+00
Y44E3B.2	<i>tyr-5</i>	4,59	1,10E-02	R09D1.6		3,92	2,78E-04
ZC239.1		4,58	1,61E-13	F22E5.8		3,88	1,07E-02
F12A10.1		4,57	1,09E-04	F59A1.9	<i>fbxa-193</i>	3,85	1,18E-02
EEED8.12		4,54	5,23E-04	Y102A5C.16	<i>clec-239</i>	3,83	4,49E-04
F15B9.1	<i>far-3</i>	4,44	1,15E-07	F11A5.8	<i>oac-15</i>	3,80	2,31E-03
F35E2.5		4,36	2,41E-02	F47B7.4		3,77	3,83E-04
F09C6.2	<i>fbxa-44</i>	4,35	1,78E-02	F31D4.6	<i>try-4</i>	3,77	2,71E-05
F09E10.11	<i>tts-1</i>	4,35	1,01E-09	T22G5.6	<i>lbp-8</i>	3,59	1,42E-02
C24B9.9	<i>dod-3</i>	4,33	1,09E-03	R05A10.6		3,51	2,32E-04
F22B7.9		4,26	2,04E-11	Y37A1B.13	<i>tor-2</i>	3,48	1,27E-02
C39B5.3	<i>fbxa-62</i>	4,23	2,62E-02	F38H12.3	<i>nhr-181</i>	3,42	4,58E-04
W09G12.7		4,22	1,59E-07	R11G11.14	<i>lipl-3</i>	3,42	1,71E-02
R05H10.1		4,21	8,54E-11	F38A1.14	<i>clec-169</i>	3,40	3,09E-07
C15A11.7		4,21	0,00E+00	C54D1.2	<i>clec-86</i>	3,36	2,65E-03
F14D7.10		4,20	1,69E-02	F56G4.1	<i>oac-34</i>	3,35	7,74E-07
F55A12.6		4,17	1,53E-04	T09B4.7		3,33	2,10E-04
K01A6.7		4,06	8,88E-03	F28G4.2		3,29	1,78E-02
B0393.4		4,06	7,62E-06	R09D1.8		3,29	2,24E-02
F43G9.6	<i>fer-1</i>	3,98	1,83E-08	F56H1.1	<i>che-14</i>	3,25	0,00E+00
T28A11.3		3,97	1,44E-02	T03D3.1	<i>ugt-53</i>	3,24	2,18E-05
C01G10.17		3,96	3,87E-03	Y62H9A.4		3,22	2,49E-02
T21C9.8	<i>ttr-23</i>	3,80	1,41E-05	R52.9	<i>math-37</i>	3,20	3,74E-02
F57A8.8	<i>fipr-13</i>	3,78	3,94E-02	K09C4.5		3,18	1,15E-09
E03H4.10	<i>clec-17</i>	3,71	4,57E-08	B0507.8		3,13	2,45E-02
C33G8.2		3,70	4,28E-10	M01B2.8		3,11	1,29E-02
R08F11.3	<i>cyp-33C8</i>	3,69	0,00E+00	Y67A10A.1	<i>oac-56</i>	3,09	3,62E-03
R02C2.7		3,68	3,29E-03	F52E10.5	<i>ifa-3</i>	3,08	6,83E-03
C25F9.7	<i>srw-86</i>	3,62	4,91E-02	K02B9.1	<i>meg-1</i>	3,08	1,60E-02
Y43C5A.3		3,61	3,05E-08	ZK813.1		3,08	7,98E-03
C06B3.6		3,60	1,51E-06	B0507.10		3,07	5,11E-03
ZK970.7		3,56	0,00E+00	F59F3.5	<i>ver-4</i>	3,07	5,24E-06
T28A11.19		3,53	1,95E-02	ZK617.2	<i>lips-6</i>	3,02	0,00E+00

C45B2.8		3,49	2,96E-05	Y57G11B.5		3,01	2,45E-03
Y69A2AR.12		3,49	3,49E-02	F52F10.4	<i>oac-32</i>	2,99	2,32E-04
C17B7.10		3,47	9,76E-05	F10F2.3	<i>lips-3</i>	2,97	6,66E-08
F21F3.3		3,41	3,98E-02	K01D12.8		2,97	2,63E-06
C50C3.2		3,41	2,77E-05	Y45F10D.14		2,96	8,88E-03
C01G5.4		3,41	1,18E-02	ZK666.6	<i>clec-60</i>	2,95	1,06E-02
T06E4.5		3,40	8,84E-03	F47F6.3	<i>oac-30</i>	2,94	7,76E-09
C17H1.7		3,40	2,70E-04	F58G4.6	<i>str-146</i>	2,92	2,38E-02
Y37H2A.14		3,31	1,37E-12	F36H1.11		2,90	1,91E-02
F48G7.8		3,30	2,83E-03	C25A8.4		2,88	3,90E-03
R06B10.1		3,28	1,24E-03	C28H8.5		2,84	1,11E-08
C13D9.8	<i>ncx-9</i>	3,27	4,08E-02	W06D12.1	<i>cutl-4</i>	2,83	5,81E-04
F26D11.6		3,27	3,22E-02	K11G9.2		2,82	1,48E-05
H20J04.1		3,23	4,13E-02	ZK813.3		2,82	2,10E-02
C17B7.5		3,23	2,93E-04	F41A4.1	<i>cutl-28</i>	2,82	5,18E-09
Y65B4BR.1		3,23	1,61E-02	T09F5.9	<i>clec-47</i>	2,80	2,07E-10
F02C12.5	<i>cyp-13B1</i>	3,20	3,89E-07	T23F4.4	<i>nas-27</i>	2,79	1,84E-07
Y39B6A.25		3,19	2,52E-02	C54C8.2		2,79	1,48E-05
Y45F10D.6		3,19	3,44E-05	C29F3.5	<i>clec-230</i>	2,78	2,06E-09
C25F9.12		3,18	4,77E-02	F11H8.3	<i>col-8</i>	2,75	3,15E-08
C01G10.5		3,16	1,43E-02	Y19D10B.7		2,72	1,21E-06
ZC168.2		3,15	1,85E-02	R04B3.1		2,70	5,33E-03
C07E3.4		3,09	2,38E-02	C35A5.5		2,69	1,92E-03
ZK484.7		3,09	2,52E-02	F15E11.13		2,69	1,29E-06
C33F10.8		3,08	3,66E-02	F38A5.14	<i>nspb-1</i>	2,68	2,13E-02
C38D9.2		3,08	2,08E-03	ZK1025.6	<i>nhr-244</i>	2,67	6,81E-03
C49G7.5	<i>irg-2</i>	3,07	3,66E-02	F55G11.2		2,65	8,73E-08
R10D12.9	<i>swt-6</i>	3,06	3,15E-02	H13N06.6	<i>tbh-1</i>	2,64	9,96E-03
C09C7.1	<i>zig-4</i>	3,06	1,18E-10	Y11D7A.11	<i>col-120</i>	2,63	2,75E-04
C26F1.2	<i>cyp-32A1</i>	3,03	6,90E-12	Y102A5C.17	<i>clec-238</i>	2,62	4,57E-03
K04F1.9		3,02	1,70E-03	F15E11.14		2,59	1,62E-06
K01A6.8		3,02	3,05E-02	Y62H9A.6		2,59	5,41E-03
T26H5.9		3,01	7,53E-05	W02B12.13		2,56	7,34E-03
C01G10.4		3,01	2,45E-02	F55B11.2		2,55	2,14E-02
R08F11.4		2,99	2,84E-04	F15E11.1		2,55	1,62E-06
C06G4.5	<i>npr-17</i>	2,96	7,96E-03	C44B12.1	<i>perm-2</i>	2,52	3,90E-04
C38D4.7		2,94	1,60E-02	K11H12.11		2,50	2,88E-02
F37A4.5		2,94	4,27E-04	R10H1.5	<i>nas-23</i>	2,49	1,65E-10
F11E6.11		2,94	2,85E-03	C23H4.3		2,48	1,47E-08
C45G7.2	<i>ilys-2</i>	2,92	3,17E-02	F08H9.5	<i>clec-227</i>	2,48	7,94E-03
F54B8.3	<i>fbxa-69</i>	2,92	1,95E-02	C41H7.7	<i>clec-3</i>	2,47	8,39E-05
T10B9.2	<i>cyp-13A5</i>	2,92	2,14E-04	W08G11.1		2,47	6,94E-05
F25H5.8		2,92	3,79E-03	K07H8.6	<i>vit-6</i>	2,45	8,12E-09

Y5H2B.5	<i>cyp-32B1</i>	2,90	2,52E-04	F09C8.1		2,44	8,42E-03
ZK896.1		2,88	2,16E-03	C44B7.5		2,43	3,88E-02
F59E11.7		2,87	6,17E-05	F28G4.4		2,43	6,03E-03
F01G10.5		2,87	1,84E-02	Y46G5A.36		2,38	4,43E-03
C17B7.3		2,85	2,30E-02	C29F3.6	<i>srx-58</i>	2,37	1,34E-02
Y41C4A.2	<i>faah-6</i>	2,85	8,62E-03	Y34F4.2		2,37	1,20E-02
F01D4.8		2,83	2,12E-04	F52E4.6	<i>wrt-2</i>	2,37	3,86E-06
Y43F8C.1	<i>nlp-25</i>	2,83	1,65E-04	T09H2.1	<i>cyp-34A4</i>	2,36	4,72E-02
B0547.3	<i>srd-14</i>	2,80	2,09E-03	F21G4.3		2,35	3,44E-02
F17E9.11	<i>lys-10</i>	2,80	1,04E-02	C39D10.7		2,34	1,62E-06
C44B7.6		2,76	8,54E-08	ZK899.4	<i>tba-8</i>	2,33	9,45E-07
Y80D3A.7	<i>ptr-22</i>	2,75	6,55E-04	C15A11.5	<i>col-7</i>	2,31	2,29E-03
K12B6.8		2,74	5,83E-03	C02F5.14		2,31	5,36E-04
T27F6.8		2,73	1,16E-08	C42D4.13		2,31	2,82E-02
F20D1.5	<i>arl-7</i>	2,73	6,92E-03	F25H8.6	<i>bed-3</i>	2,31	7,40E-13
F21C10.11		2,73	4,35E-02	C04F5.7	<i>ugt-63</i>	2,30	1,48E-05
C50F7.5		2,71	1,62E-06	B0331.2		2,30	6,03E-03
C34F11.8		2,70	2,26E-02	F38E11.1	<i>hsp-12.3</i>	2,26	3,28E-02
C24G7.4		2,68	1,16E-04	F40F12.4	<i>mam-7</i>	2,26	2,83E-02
C37H5.9	<i>nas-9</i>	2,67	5,83E-10	F49C5.12		2,24	2,00E-02
K04E7.3	<i>nas-33</i>	2,64	9,73E-06	R09H10.7		2,23	2,65E-02
Y105C5A.8		2,64	9,83E-07	K11E4.2		2,23	1,13E-04
F35F10.7		2,63	3,88E-02	F49E12.1		2,20	1,70E-02
C05E11.4	<i>amt-1</i>	2,62	7,54E-03	F13B12.4		2,20	1,74E-07
Y71H2AM.16	<i>pho-9</i>	2,62	1,47E-07	ZC455.4	<i>ugt-6</i>	2,19	3,03E-08
F43C9.1		2,62	2,14E-06	Y46G5A.22		2,19	4,29E-02
Y58A7A.4		2,61	1,56E-08	Y62H9A.5		2,18	3,63E-02
C08E8.4		2,59	2,14E-04	T25G12.7	<i>dhs-30</i>	2,17	2,38E-06
M176.9		2,59	3,57E-02	F58B3.3	<i>lys-6</i>	2,17	2,52E-04
F35F10.1		2,56	2,61E-05	C27C7.3	<i>nhr-74</i>	2,16	7,53E-05
T22H9.3	<i>wago-10</i>	2,56	1,45E-03	T19H12.1	<i>ugt-9</i>	2,16	6,41E-04
T01B11.4	<i>ant-1.4</i>	2,56	1,08E-03	ZK1193.1	<i>col-19</i>	2,15	4,56E-07
C47A10.1	<i>pgp-9</i>	2,55	0,00E+00	C17C3.12	<i>acdh-2</i>	2,14	2,32E-04
F35E12.5		2,55	3,81E-11	K08H10.6		2,14	3,69E-04
C10C5.2		2,52	1,22E-03	T21D11.1		2,14	1,58E-03
F46F2.5		2,50	5,22E-06	C15A11.6	<i>col-62</i>	2,13	8,05E-03
F57H12.5		2,50	1,57E-02	ZK678.5	<i>wrt-4</i>	2,12	9,31E-12
C33A12.19		2,50	1,06E-02	C32H11.6		2,12	1,10E-02
F48F5.2		2,48	1,33E-02	F41E6.14	<i>oac-29</i>	2,11	1,77E-08
Y113G7C.1		2,47	2,32E-04	D1054.11		2,11	4,15E-03
T10H4.11	<i>cyp-34A2</i>	2,46	3,75E-05	F54C9.8	<i>puf-5</i>	2,09	3,94E-04
Y58A7A.5		2,46	1,51E-02	C26C6.3	<i>nas-36</i>	2,09	3,79E-10
C25H3.10		2,44	3,15E-04	C44B12.5	<i>perm-4</i>	2,09	2,35E-04

ZK75.1	<i>ins-4</i>	2,40	6,46E-03	F47B8.5		2,08	9,67E-03
M162.5		2,40	1,60E-04	Y37E11B.7		2,06	1,16E-02
K09D9.1		2,38	2,50E-02	K10C2.3		2,06	3,92E-05
C31B8.8		2,37	1,67E-10	ZK1055.4		2,05	1,23E-02
K01H12.2	<i>ant-1.3</i>	2,37	4,94E-03	C32H11.12	<i>dod-24</i>	2,04	7,89E-07
C27D8.2		2,36	6,92E-03	R05G6.9		2,02	1,87E-03
B0564.3		2,34	1,40E-03	F49E12.9		2,02	1,35E-05
F54D10.2	<i>fbxa-24</i>	2,34	1,26E-02	C52B11.3	<i>dop-4</i>	2,02	8,88E-03
W01F3.2		2,34	1,61E-07	F15H10.8		2,01	1,97E-03
Y8A9A.2		2,33	6,09E-04	R12C12.10		2,01	1,19E-02
C23H4.8		2,33	2,05E-02	E04F6.15		2,00	5,90E-03
R13D7.7	<i>gst-41</i>	2,32	1,45E-02	Y40H7A.10		2,00	1,69E-02
K08B4.3	<i>ugt-19</i>	2,30	4,49E-12	ZC513.2		1,97	2,09E-02
Y49G5A.1		2,29	1,51E-02	C04F1.1		1,96	2,75E-03
C54D10.10		2,29	2,29E-05	C41A3.1		1,96	1,32E-03
C16E9.1		2,28	1,20E-05	F38A3.1	<i>col-81</i>	1,95	4,03E-06
R11G11.7	<i>pqn-60</i>	2,27	1,07E-02	Y54G2A.10		1,95	1,45E-03
F35E8.8	<i>gst-38</i>	2,27	4,64E-04	T22D1.11		1,95	1,97E-03
Y39A1A.19	<i>fmo-3</i>	2,25	1,72E-11	C09B8.4		1,95	1,50E-02
F14F7.3	<i>cyp-13A12</i>	2,25	5,38E-04	B0511.11		1,95	1,81E-02
F23C8.7		2,25	4,96E-03	Y38A10A.2		1,95	2,76E-07
C55C3.3		2,22	8,07E-03	ZC250.3	<i>nstp-3</i>	1,94	4,97E-04
T13A10.11	<i>sams-5</i>	2,19	3,69E-02	F49E12.12		1,94	7,53E-05
Y58A7A.3		2,19	1,97E-09	ZK829.3		1,93	2,27E-03
B0213.17	<i>nlp-34</i>	2,19	7,24E-04	F55F3.4		1,92	1,75E-04
Y95B8A.6		2,19	4,77E-08	D1054.10		1,92	4,91E-02
Y48G8AL.11	<i>haf-6</i>	2,19	2,90E-05	F58B3.2	<i>lys-5</i>	1,91	7,94E-03
F40H3.2		2,17	1,26E-03	C36A4.1	<i>cyp-25A1</i>	1,91	4,55E-02
Y119D3B.18	<i>fbxa-91</i>	2,17	1,03E-02	K01A2.11	<i>cbn-1</i>	1,90	6,56E-04
Y36E3A.2		2,17	2,41E-02	Y37A1A.2		1,90	6,29E-03
Y119D3B.20	<i>fbxa-92</i>	2,16	1,79E-02	F17C11.3	<i>col-153</i>	1,89	1,87E-05
W08E12.2		2,16	1,46E-05	K08B12.1		1,89	2,38E-02
T19C3.9	<i>ttr-7</i>	2,16	3,43E-04	T05E7.1		1,88	9,68E-06
Y51A2D.5	<i>hmit-1.2</i>	2,14	2,69E-07	Y53F4B.25		1,87	6,17E-05
B0205.13		2,13	5,70E-05	ZC513.1		1,87	2,68E-02
B0213.3	<i>nlp-28</i>	2,12	3,64E-02	F08H9.8	<i>clec-54</i>	1,87	2,23E-02
C49G7.10		2,11	2,41E-03	ZC449.2		1,86	9,83E-03
F20G2.5		2,11	3,81E-02	T06D8.10		1,86	3,63E-08
T28D6.2	<i>tba-7</i>	2,10	1,71E-05	T02B5.3		1,85	8,86E-04
F26G1.2		2,09	3,81E-02	F17B5.1		1,85	1,55E-02
Y54F10BM.3		2,09	1,32E-02	C42D8.2	<i>vit-2</i>	1,85	7,93E-09
Y95B8A.12		2,08	7,39E-03	K07C6.5	<i>cyp-35A5</i>	1,84	4,15E-03
T05A7.1		2,07	2,71E-05	F09G8.5		1,84	2,23E-02

T23F1.6	<i>pqn-71</i>	2,05	4,55E-05	C32H11.11		1,84	7,59E-03
K08D8.4		2,05	3,30E-04	C34F6.3	<i>col-179</i>	1,84	4,57E-03
Y41G9A.5		2,05	3,94E-04	F32D1.11		1,83	6,20E-03
B0228.1		2,03	2,16E-03	E03G2.4	<i>col-186</i>	1,83	1,58E-03
T28B8.1		2,02	2,88E-03	E01G6.3		1,83	4,19E-03
K07C5.7	<i>tll-15</i>	2,02	6,72E-05	Y42A5A.2	<i>lact-8</i>	1,83	9,14E-05
C40H1.1	<i>cpb-1</i>	1,99	1,34E-06	T07G12.3		1,82	3,47E-04
T01D3.3		1,97	4,15E-03	Y69A2AR.5	<i>daao-1</i>	1,82	4,16E-02
W03D2.1	<i>pqn-75</i>	1,96	3,39E-03	C17H12.8		1,82	2,39E-06
C45B2.1		1,93	1,57E-02	Y71F9B.9		1,82	1,28E-02
C45E1.4		1,93	8,84E-03	F25E5.2		1,81	4,21E-02
F25E5.8		1,93	9,79E-04	C32H11.8		1,80	1,25E-02
Y69H2.10		1,93	1,22E-02	C01H6.1	<i>col-61</i>	1,80	1,12E-02
F44G3.2		1,92	2,86E-03	F45G2.5	<i>bli-5</i>	1,79	1,95E-02
ZK507.4	<i>dos-1</i>	1,92	4,16E-02	F10A3.4		1,78	9,40E-04
T25B9.7	<i>ugt-54</i>	1,91	2,65E-02	F38A1.5	<i>clcc-166</i>	1,77	3,25E-03
F49B2.6		1,91	1,21E-04	Y34B4A.10		1,77	6,18E-06
B0238.12		1,90	1,32E-02	Y4C6B.6		1,77	3,14E-05
K02E7.6		1,89	1,08E-03	F18F11.4		1,77	6,66E-04
C53B7.3		1,89	2,03E-03	F08A8.2		1,76	7,24E-08
F35B12.3		1,89	4,42E-02	F52D1.3	<i>abu-12</i>	1,75	1,30E-07
B0213.4	<i>nlp-29</i>	1,89	3,21E-04	F18C5.5		1,75	1,59E-03
T20D4.12		1,88	8,68E-04	K02D3.2		1,74	6,67E-03
F55G11.5	<i>dod-22</i>	1,88	3,64E-02	F39D8.4	<i>nas-13</i>	1,73	2,38E-02
T01B11.5	<i>str-176</i>	1,86	2,16E-03	Y42H9B.1	<i>col-115</i>	1,72	2,28E-02
F57C12.1	<i>nas-38</i>	1,86	1,29E-09	ZK1025.4		1,72	1,81E-02
F44F4.4	<i>ptr-8</i>	1,85	1,65E-08	Y46G5A.29		1,72	9,54E-06
Y54G2A.11		1,85	7,03E-06	M18.1	<i>col-129</i>	1,72	1,24E-04
Y54G11A.4		1,85	6,06E-03	F22E5.1		1,71	1,20E-02
F54D1.4	<i>nhr-7</i>	1,85	8,48E-03	K07G5.1	<i>crml-1</i>	1,70	3,16E-06
C44E12.1		1,85	1,18E-03	B0399.2	<i>oac-1</i>	1,69	5,43E-04
T19H12.10	<i>ugt-11</i>	1,84	4,44E-02	C46H11.2		1,69	1,01E-03
C31H2.4		1,83	2,11E-03	M03B6.3		1,69	1,65E-02
B0303.7		1,83	2,40E-06	C06B3.3	<i>cyp-35C1</i>	1,69	5,45E-05
C23H4.6		1,83	4,73E-02	H23N18.3	<i>ugt-8</i>	1,68	7,14E-03
K02G10.7	<i>aqp-8</i>	1,82	1,62E-06	F54B11.11		1,68	1,67E-03
C09F9.7		1,82	3,37E-02	ZC13.4	<i>mab-7</i>	1,68	8,80E-05
E02H1.7	<i>nhr-19</i>	1,81	7,47E-03	Y38C1AB.1		1,68	1,24E-02
R01E6.4	<i>acr-12</i>	1,81	6,07E-03	T19D7.3	<i>lpr-7</i>	1,68	3,68E-04
C54D1.1	<i>pgp-10</i>	1,81	8,80E-05	F46B3.5	<i>grd-2</i>	1,67	2,27E-04
F01E11.1	<i>ugt-57</i>	1,80	1,68E-03	F18A11.2		1,67	3,49E-03
ZC123.4		1,79	3,86E-02	R11A5.7	<i>suro-1</i>	1,67	7,88E-04
F16F9.2	<i>dpy-6</i>	1,79	6,80E-08	F26G1.6		1,67	7,22E-03

F47B7.7		1,79	4,69E-03	M02G9.2		1,66	3,93E-03
C25D7.3	<i>sdc-3</i>	1,79	2,28E-07	F58G1.5	<i>lips-9</i>	1,66	8,02E-04
B0222.5		1,78	7,57E-05	M01E10.2	<i>dpy-1</i>	1,66	3,08E-05
T28H10.2		1,78	3,59E-03	F38A1.1	<i>clec-170</i>	1,66	1,58E-03
R03A10.5		1,78	2,90E-03	Y18D10A.7	<i>ptr-17</i>	1,65	1,04E-02
B0310.2		1,78	3,87E-03	T15B7.3	<i>col-143</i>	1,65	2,09E-02
F47E1.2		1,78	6,67E-03	C02D5.1	<i>acdh-6</i>	1,65	2,41E-03
Y19D10A.9	<i>clec-209</i>	1,76	2,10E-03	F49C12.7		1,65	3,44E-02
R11F4.1		1,76	1,77E-06	C13C12.2		1,65	2,28E-03
Y44A6C.1		1,76	1,39E-02	B0365.9		1,65	2,00E-02
ZC373.7	<i>col-176</i>	1,75	2,54E-06	T22B7.7		1,64	2,09E-02
T12B3.2		1,74	3,35E-03	C12D5.9		1,64	4,91E-02
T02B11.4		1,74	1,63E-02	C05E7.2		1,63	7,99E-04
F14F9.4		1,73	1,16E-02	W07A12.7	<i>rhy-1</i>	1,63	1,06E-02
F10G2.3	<i>clec-7</i>	1,73	4,91E-02	F09G8.6	<i>col-91</i>	1,63	9,83E-05
M7.3	<i>bcc-1</i>	1,73	6,55E-04	F55G11.8		1,62	2,19E-02
C14F11.5	<i>hsp-43</i>	1,72	2,47E-03	Y11D7A.5		1,62	3,52E-02
F56A4.2		1,71	3,87E-03	T03G6.1		1,62	4,64E-04
T08A9.11	<i>ttr-59</i>	1,70	2,78E-03	D1014.5		1,62	8,09E-04
C13E3.1		1,70	1,04E-02	T16G1.2		1,61	1,22E-02
T20B3.1		1,70	2,12E-04	C07A12.5	<i>spr-3</i>	1,61	3,65E-02
F21C10.8	<i>pqn-31</i>	1,69	2,36E-03	K01B6.3		1,61	3,35E-02
T10E9.4		1,68	2,96E-02	F19H8.4	<i>mltn-9</i>	1,61	3,26E-04
T28F3.4		1,68	2,08E-04	ZC449.1		1,60	4,33E-03
W09D12.1		1,67	1,62E-04	C14A4.9		1,60	1,18E-02
F10D2.11	<i>ugt-41</i>	1,66	1,67E-03	R11E3.4	<i>set-15</i>	1,59	1,22E-02
C54D10.1	<i>cdr-2</i>	1,66	5,36E-04	Y18H1A.13	<i>col-46</i>	1,59	4,41E-02
B0213.5	<i>nlp-30</i>	1,66	1,25E-02	C05C9.1		1,59	3,03E-02
F47G3.1		1,65	5,42E-04	F41F3.4	<i>col-139</i>	1,59	1,96E-03
F14H12.3		1,64	1,10E-02	W04G3.3	<i>lpr-4</i>	1,58	2,10E-04
Y66D12A.12	<i>ztf-29</i>	1,63	6,72E-03	T05H4.7		1,58	3,17E-02
Y69A2AR.32		1,63	3,81E-02	F12F6.9	<i>col-128</i>	1,58	1,39E-02
Y113G7B.14		1,63	1,25E-02	F11G11.11	<i>col-20</i>	1,58	4,49E-03
T03F6.4		1,62	1,70E-02	T18H9.1	<i>grd-6</i>	1,58	5,70E-05
F42A8.1		1,62	4,77E-02	F01D5.10		1,58	1,10E-02
Y54E10A.4	<i>fog-1</i>	1,62	2,64E-03	F40F9.5		1,56	4,57E-03
K08A2.5	<i>nhr-88</i>	1,61	2,44E-02	ZK377.1	<i>wrt-6</i>	1,55	7,70E-04
E04F6.6		1,60	8,38E-03	C32D5.12		1,55	4,58E-02
F48C1.1	<i>aman-3</i>	1,60	4,64E-04	T04H1.6	<i>lrx-1</i>	1,54	1,95E-02
D1005.3	<i>cebp-1</i>	1,60	1,98E-03	F55A11.7		1,54	1,18E-02
Y51H7C.13		1,60	2,45E-02	F08H9.6	<i>clec-57</i>	1,54	9,91E-03
C09F9.3	<i>glna-1</i>	1,60	3,81E-02	C34F6.2	<i>col-178</i>	1,53	1,91E-02
C25E10.5		1,60	6,51E-03	C17G1.6	<i>nas-37</i>	1,53	1,23E-03

Y69H2.3		1,60	1,27E-04	T08B1.6	<i>acs-3</i>	1,53	1,92E-02
R13A5.3	<i>ttr-32</i>	1,60	3,55E-02	F30A10.2		1,53	1,56E-02
R13A5.6	<i>ttr-8</i>	1,59	2,33E-02	Y45G12C.2	<i>gst-10</i>	1,53	9,36E-03
D1005.2		1,59	1,22E-02	C41D7.2	<i>ptr-3</i>	1,53	4,94E-03
C07A9.9		1,59	3,46E-02	T17H7.7		1,53	1,06E-03
F55G11.4		1,59	8,84E-03	F07H5.8		1,52	1,63E-02
Y75B8A.3		1,59	2,67E-03	Y113G7B.12		1,52	1,00E-03
Y73F8A.21	<i>nhr-5</i>	1,58	3,67E-02				
ZC410.1	<i>nhr-11</i>	1,58	3,98E-02				
Y48G1BL.2	<i>atm-1</i>	1,58	9,91E-03				
F22F7.7		1,57	3,35E-02				
C05D11.7		1,56	1,28E-02				
F26D12.1	<i>fkh-7</i>	1,55	1,35E-02				
B0285.9	<i>ckb-2</i>	1,55	2,46E-03				
F08F3.7	<i>cyp-14A5</i>	1,55	1,59E-03				
T26H2.9	<i>nhr-79</i>	1,55	2,28E-02				
C30F2.3		1,55	1,88E-02				
F31F7.1		1,55	1,48E-02				
Y70G10A.3		1,55	1,69E-03				
Y49E10.4		1,54	1,47E-02				
F57H12.6		1,54	9,56E-03				
T04A11.4		1,53	2,78E-02				
F47A4.5		1,53	1,08E-03				
Y48G9A.4	<i>fri-1</i>	1,53	5,85E-04				
F58E6.1	<i>sta-2</i>	1,53	3,46E-02				
C02C2.1	<i>tyr-1</i>	1,51	1,08E-03				
F18E9.3		1,51	1,19E-03				
Y73F4A.2		1,51	4,87E-02				
T15B7.4	<i>col-142</i>	1,50	2,18E-03				

## Contributions

I independently conducted all experiments described in this thesis, except for:

Dauer assays (Figure 17A and 17B) and parts of the qRT-PCR (Figure 28B), which were performed together with Dr. Ben Becker (Antebi lab); lifespan analysis (Figure 18) was performed together with Dr. Shuhei Nakamura (Antebi lab); Dr. Corinna Klein (MPI Age bioinformatic department) helped with the RNA-sequencing data analysis (Figure 28A); Caroline Hoppe (Antebi lab) performed the screen for BLMP-1 upstream regulators (Table 4); Dr. Lukas Cermak (Pagano lab) performed the *in vitro* ubiquitination assay (Figure 29C) and the BLIMP-1 stability assay in ARP1 multiple myeloma cells (Figure 32). Dr. Christoph Geisen (Antebi lab) cloned the expression constructs for binding and degradation assays in HEK293T cells.

Thanks again to these people for contributing to my work.

## Erklärung

Ich versichere, dass ich die von mir vorgelegte Dissertation selbstständig angefertigt, die benutzten Quellen und Hilfsmittel vollständig angegeben und die Stellen der Arbeit - einschließlich Tabellen, Karten und Abbildungen -, die anderen Werken im Wortlaut oder dem Sinn nach entnommen sind, in jedem Einzelfall als Entlehnung kenntlich gemacht habe; dass diese Dissertation noch keiner anderen Fakultät oder Universität zur Prüfung vorgelegen hat; dass sie - abgesehen von unten angegebenen Teilpublikationen - noch nicht veröffentlicht worden ist sowie, dass ich eine solche Veröffentlichung vor Abschluss des Promotionsverfahrens nicht vornehmen werde. Die Bestimmungen dieser Promotionsordnung sind mir bekannt. Die von mir vorgelegte Dissertation ist von von Prof. Dr. Adam Antebi betreut worden.

Köln, Mai 2014

Moritz Horn

Teile dieser Arbeit wurden bereits veröffentlicht:

**Horn M**, Geisen C, Cermak L, Becker B, Nakamura S, Klein C, Pagano M and Antebi A (2014). *Dev Cell* 28, 697-710.

*DRE-1/FBXO11 Dependent Degradation of BLMP-1/BLIMP-1 Governs C. elegans Developmental Timing and Maturation*

Rossi M, Duan S, Jeong Y-T, **Horn M**, Saraf A, Florens L, Washburn MP, Antebi A, and Pagano M. (2013). *Mol Cell* 49, 1159–1166.

*Regulation of the CRL4(Cdt2) ubiquitin ligase and cell-cycle exit by the SCF(Fbxo11) ubiquitin ligase*

# Curriculum Vitae

## Persönliche Angaben

---

### Moritz Horn

\*13. September 1985 in Düren, Deutschland  
verheiratet  
Zum Kirchenpättchen 36,  
52355 Düren, Deutschland  
Moritz.Horn@web.de

## Ausbildung

---

- Seit Oktober 2010 **Doktorant** am Max Planck Institut für Biologie des Alterns in Köln, Deutschland, in der Arbeitsgruppe von Prof. Dr. Adam Antebi. Voraussichtliche Promotion im Juni 2014. Titel der Dissertation: *Coordination of Developmental Timing and Maturation by the F-box Protein DRE-1/FBXO11*
- Okt. 2005 – Juni 2010 **Studium der Biochemie** an der Eberhard Karls Universität in Tübingen, Deutschland
- Nov. 2009 – Juni 2010 **Diplomarbeit** am Institut für experimentelle und klinische Pharmakologie und Toxikologie der Universität Tübingen, Tübingen, Deutschland, in der Arbeitsgruppe von Prof. Dr. M. Schwarz.  
Titel der Diplomarbeit: *Analysis of aberrant  $\beta$ -catenin activation on proliferation and apoptosis of mouse hepatoma cells*
- Juli 1996 – Juli 2005 Städtisches Gymnasium am Wirteltor in Düren, Deutschland  
Abschluss: *Allgemeine Hochschulreife*

## Veröffentlichungen

---

- Horn M**, Geisen C, Cermak L, Becker B, Nakamura S, Klein C, Pagano M and Antebi A (2014). Dev Cell 28, 697-710  
DRE-1/FBXO11 Dependent Degradation of BLMP-1/BLIMP-1 Governs *C. elegans* Developmental Timing and Maturation
- Rossi M, Duan S, Jeong Y-T, **Horn M**, Saraf A, Florens L, Washburn MP, Antebi A, and Pagano M. (2013). Mol Cell 49, 1159–1166.  
Regulation of the CRL4(Cdt2) ubiquitin ligase and cell-cycle exit by the SCF(Fbxo11) ubiquitin ligase
- Zeller E, Mock K, **Horn M**, Colnot S, Schwarz M, and Braeuning A. (2012). Biol. Chem. 393, 1183–1191  
Dual-specificity phosphatases are targets of the Wnt/ $\beta$ -catenin pathway and candidate mediators of  $\beta$ -catenin/Ras signaling interactions